Energy Efficient Localization Techniques for WSN Communications

by

Salar Bybordi

A dissertation submitted to
Dipartimento di Elettronica, Informazione e Bioingegneria
Politecnico di Milano
in fulfillment of the requirements for the degree of
Doctor of Philosophy in Information Technology
2015

Supervisor:
Professor Luca Reggiani

Doctoral program coordinator:
Professor Carlo Fiorini

Cycle XXVI

Dedicated to my parents

and

my dear sister **Sara**

ACKNOWLEDGEMENTS

I would like to express my sincere gratitude to my supervisor Professor Luca Reggiani. There is no doubt for me that without his precious guidelines, dealing with common difficulties for a beginning PhD student was not possible and this dissertation could not be completed. I feel myself honored to have the opportunity to experience PhD research under his advisory. Beside the precious scientific topics that I have learned from him, I have gained outstanding lessons for my future research career and personal life during these years.

My special thanks goes to examiners of my thesis for their fruitful comments on my dissertation.

Last but not the least, I would like to thank my dear parents and my sister for their continuous support during these years.

TABLE OF CONTENTS

LIST OF FIGURES

Figure

LIST OF ABBREVIATIONS

APDP Average Power Delay Profile

APA Adaptive Power Allocation

AOA Angle of Arrival

CIR Channel Impulse Response

DL Downlink

EKF Extended Kalman Filter

FIM Fisher Information Matrix

FCC Federal Communications Commission

FP Fingerprinting

KF Kalman Filter

IF Intermediate Frequency

LD Location Dependent

LS Least Squares

MPCs Multipath Components

MSE Mean Square Error

ML Maximum Likelihood

NLoS Non Line of Sight

PA Power Allocation

PCRB Posterior Cramer Rao Bound

RII Ranging Information Intensity

RMSE Root Mean Square Error

RSS Received Signal Strength

SNR Signal to Noise Ratio

SPEB Squared Position Error Bound

TOA Time of Arrival

TDOA Time Difference of Arrival

TWR Two Way Ranging

UL Uplink

UPA Uniform Power Allocation

UWB Ultra-wide Band

WLS Weighted Least Squares

WSN Wireless Sensor Network

VSA Virtual Surveillance Area

ABSTRACT

This research considers energy efficient algorithms in the context of Wireless Sensor Network (WSN) localization. In this dissertation, the term localization refers to the concepts of static localization or fingerprinting for a single shot estimation of a target position and tracking of target positions over different time instants. Considered localization scenarios cover both active and passive localization. In active localization, the target participates in the estimation process of inter-node ranging information while in passive scenarios the target does not participate in the estimation process. The general trend in the design of localization algorithms is towards achieving more accurate position estimate. Additionally, algorithms should respect energy efficiency constraints due to the limited battery life in WSN nodes. The contribution of this thesis mainly focuses on the investigation and the proposal of localization algorithms which should achieve these two crucial design objectives:

- accuracy improvement;
- energy efficiency.

As already mentioned, according to these design objectives the thesis considers algorithms which exploits both active and passive localization scenarios.

The first section of the thesis deals with the investigation of energy efficient localization algorithms in which passive localization plays a crucial role. The first part developed for passive scenarios is devoted to the theoretical analysis of a hybrid tracking algorithm composed of active and passive steps. The analysis of this scheme, based on the Posterior Cramer Rao Bound (PCRB), confirms that mixing active and

passive cases can be an effective tool towards energy efficiency. The second part of the investigation related to passive scenarios deals with the energy efficiency issue inspired by two perspectives. A hybrid tracking algorithm composed of Extended Kalman Filter (EKF) based tracking and Fingerprinting (FP) is proposed in order to tackle conventional problems related to the implementation of either tracking or fingerprinting separately. One of the common drawbacks of FP is the large data size and the consequent large search space as a result of either vastness of surveillance area or finer grid resolution in FP grid map; this usually limits the application of FP to small environments or scenarios with largely spaced grid points, leading to poor localization performance. The hybrid algorithm developed here enables FP to be applied in larger environments or environments with finer space grids. The second aspect of the scheme deals with the critical concern related to tracking more than one passive target. When targets move close to each other, the correct discrimination among measures, resulting from occurred ambiguity in paths clusters scattered by different targets, turns out to be a challenging task. The final phase of this analysis is devoted to considering a TOA-based ranging technique called **soft** ranging and its potential characteristics for providing more accurate ranging measures by means of feeding a kind of a-priori information. This solution provides EKF update steps with more precise ranging measures leading to a better localization performance. Simulation results validate a zero-energy tracking algorithm in which the mobile target does not consume energy.

The second section of the thesis deals with energy efficient algorithms for active localization scenarios. Accordingly, transmit power allocation among the beacons (i.e. the reference points for the localization) is an effective tool toward this objective. In the section we present a pervasive literature review on existing Power Allocation (PA) schemes and, in particular, of the optimal ones, based on the minimization of a localization error bound (SPEB), function of the transmission power from each

beacon. Then, two new sub-optimal algorithms are investigated. The former is based on the definition of a parameter called uncertainty area, which is a convex function of transmission power in the pair-wise selection of beacons. Numerical results confirm a notable performance advantage of localization with PA schemes w.r.t to the case of uniform power allocation among beacons specially in target locations in the vicinity of beacons. The latter proposed algorithm is based on the fact that the optimal SPEB based PA approach does not show any advantage when performance (i.e. Mean Square Error (MSE)) of the ranging estimator achieves a floor corresponding to a certain threshold in the received Signal to Noise Ratio (SNR). This corresponds to the behaviour of a practical ranging estimator where achieving higher ranging accuracy is not possible by increasing transmission power over a certain threshold because of phenomena like the limits imposed by the maximum sampling rate and by the computational load available in sensors. Consequently, this sub-optimal, simplified PA algorithm is based on the distribution of transmit powers of beacons with the SNR above the threshold to beacons with the SNR below the threshold, realizing a type of simple Adaptive Power Allocation (APA) directly based on the measured SNRs. Simulation results confirm that such a simple strategy can be effective in medium-low SNR regions, even w.r.t. more sophisticated optimization procedures.

CHAPTER I

Introduction

As a matter of fact, position information is clearly an indispensable element for monitoring and tracking applications. In other words, numerous applications in the context of wireless sensor networks (WSNs) require position information for improving their effectiveness or they rely completely on position information (e.g. assume an application in the context of fire detection in an environment without having position information by the sensing nodes). Global Positioning System (GPS) is already a response or, in some cases, a promising candidate for providing pervasive and precise localization estimates [57]. However, GPS signals face a considerable attenuation in environments with strong blockage like indoor environments. In addition, the position estimation accuracy resulting from application of GPS is not generally sufficient in indoor environments with smaller dimensions. Moreover, the implementation of GPS in sensor nodes from an energy efficiency point of view is not feasible. Consequently, there is an increasing research trend toward the evaluation of position by deploying a local and possibly ad-hoc network being able to exploit specific local algorithms. Wireless sensor networks (WSN) are important part of this research and development trend [12].

A WSN is a network in which actions of sensing, processing and sharing sensed data is possible by taking advantage of inexpensive nodes [18]. Considering the facts

that WSN are applied in environments in which the locations of nodes are hard to reach and installed nodes are usually battery powered devices, we can surely state that the impact of low-power consumption in network design is of vital concern. Equivalently, novel localization algorithms should satisfy this demand of energy-efficiency. Moreover, these design lines intervene in a general trend which is toward the design of localization algorithms being able to provide more precise location information.

Ultra-wide Band (UWB) technology is counted as a propitious candidate for WSN requirements in the context of wireless localization. A distinguishing feature of UWB, and particularly impulse radio (IR) UWB, arises from its embedded nature, i.e. the application of very short pulses (few nano seconds), leading to a very large bandwidth. This characteristic is remarkable from several points of view. It enables wireless communication with low transmission power spread over a large bandwidth leading to an increased penetration capability in materials due to the presence of low frequency content, low probability of interference with other existing wireless technologies in the occupied frequency spectrum, license free transmission respecting frequency mask imposed on the working frequency region and other features pervasively described in Sec. 2.2.

As previously mentioned, due to an increased penetration capability of UWB signals in materials, the UWB signal can achieve a connection even in the presence of physical obstructions. This issue plays a key role in the performance of time based ranging techniques. In the earliest studies on UWB, these wireless systems were carrier-less, with a bandwidth from few kHz to several GHz, making simple receiver structures possible and avoiding the conventional intermediate frequency stage and related issues.

1.1 Objectives of the thesis

The localization scenarios considered in the thesis cover active scenarios, in which target actively participates in inter-node distance dependent parameter estimation as well as passive scenarios, in which the reflected (or scattered) signal information from the target is exploited in the estimation of location dependent parameters.

In this thesis, the term localization refers to a more general family of technologies and algorithms w.r.t. conventional approaches. Here localization is referred as any of the different approaches used to acquire position information: these approaches include static localization, fingerprinting (FP) techniques and tracking strategies. These different approaches will be also combined in hybrid ways for taking advantage of all the positive aspects of each solution. Static localization and FP are obviously associated to the estimation of a position in a single shot procedure. Static localization is usually composed of two steps:

- ranging,
- positioning.

In ranging, location-dependant (LD) ranging measures are estimated depending on the type of localization scenario. Then, position of target is finally estimated using positioning techniques. FP also pursues a procedure like the one in static localization with the difference that distance dependent parameters are measured over a radio map (also called grid) and saved in an off-line phase. Subsequently, target position is estimated according to pattern matching techniques between ongoing measured distance dependent parameters and those stored in the data base. Unlike the one shot nature of static localization and FP, tracking strategies aim to estimate position of a target along a trajectory, over different time steps. All of these three categories are investigated extensively in Sec. 2.3.2.

As mentioned before, due to the fact that WSN nodes are battery-enabled devices, energy efficiency of localization algorithm will directly influence lifetime of a sensor node and consequently performance of the whole network. On the other hand, providing more accurate estimation of position is an inevitable part of localization algorithm design. The main contribution of this thesis is along these two important issues.

1.2 Thesis outline and original contributions

Chapter II presents an extensive description of conventional Location Dependent (LD) measures and their application to position estimation in the context of static localization, FP and tracking. Conventional LD measures are Angle of Arrival (AOA), Received Signal Strength (RSS), Time of Arrival (TOA) and Time Difference of Arrival (TDOA). Then, a brief review of usual static localization techniques, including Least Squares (LS) approaches, is reported. In particular the chapter resumes an explanation of the FP approach; finally, the discussion ends with an explanation of commonly used tracking strategies and, in particular, of those based on Extended Kalman filters (EKF).

Chapter III provides a detailed review of existing lower bounds on MSE performance of static localization and EKF based tracking. The lower bound on MSE performance of static localization, also denoted as Squared Position Error Bound (SPEB), is based on classical Cramer-Rao bound (CRB) analysis for an unbiased estimate of vector parameters. The reader can find a pervasive review of different aspects of SPEB. Then discussion continues with a similar analysis for investigating the existing lower bound on MSE performance of discrete time non-linear filtering problem, called Posterior CRB (PCRB), with a special emphasis on iterative computation of this lower bound. It is concluded that, when filtering equations are linearized around a working point, like in the procedure involved in EKF (explained in Sec. 2.3.2.3),

the inverse of the recursively computed a posteriori Fisher Information matrix (FIM) coincides with the predicted a posteriori covariance matrix in EKF.

The main contributions of this thesis are reported in chapters IV and V. Chapter IV investigates two novel energy-efficient algorithms for passive localization scenarios. The first one is dedicated to analytical analysis of MSE performance related to a tracking strategy composed of active and passive steps. The difference between these two steps corresponds to the type of ranging measures applied for evaluating the computational elements of EKF-based tracking. The evaluation of the algorithm leads to the fact that using this hybrid tracking strategy can provide a considerable energy efficiency advantage at the cost of a reasonable loss in the performance. The second part of the investigations for passive scenarios deals with the energy efficiency issue from two other aspects. A hybrid tracking algorithm composed of EKF-based tracking and FP is proposed in order to tackle conventional problems related to implementation of either tracking or fingerprinting separately. In fact one of the common drawbacks of FP is the large data size and the consequent large search space as a result of either vastness of surveillance area or finer grid resolution in FP grid map, which limits the application of FP to small environments or scenarios with largely spaced grid points leading to poor localization performance. This hybrid algorithm enables FP to be applied in larger environments or environments with finer space grids. The second aspect of the scheme deals with the critical concern when tracking more than one passive target, i.e. to make the correct discrimination among measures as a result of occurred ambiguity in paths clusters scattered by different targets especially when targets are moving close to each other. The final phase of this analysis is dedicated to considering the application of a TOA-based ranging technique called **soft** and its potential characteristics for providing more accurate ranging measures by means of feeding a kind of a priori information. This issue provides EKF update steps with more precise ranging measures leading to a better localization performance.

Simulation results validate a zero-energy tracking algorithm in which target does not consume energy. The results of this chapter are published in **A** and **E**.

Chapter V considers two new localization algorithms with increased accuracy for active localization scenarios. To this end, appropriate PA among beacons is an effective tool for implementing localization with increased accuracy. Before proceeding to the proposed algorithms, there is a brief review on existing optimal PA strategies investigated in the literature. Subsequently, the first algorithm is based on a parameter called uncertainty area, which is defined w.r.t interaction of beacons in a pair-wise selection procedure. The proposed parameter is a convex function of beacons' transmission power. A general selection strategy among multiply allocated transmission powers for each beacon completes the algorithm structure. Simulation results are focused on the performance evaluation of the proposed algorithm and its comparison with the performance of static localization with optimal PA and without PA (i.e. Uniform Power Allocation (UPA)). Simulation results confirm a promising performance improvement by the application of the proposed PA algorithm for considered localization scenario and they also show the fact that optimal SPEB based PA does not give any advantage w.r.t UPA when the ranging estimator MSE achieves a floor as the received SNR passes a certain threshold. This behavior of ranging MSE is evident in practical ranging estimators where increasing transmission power, leading to a received SNR over a threshold SNR, does not provide any MSE performance improvement; this effect can be due to numerous causes, including maximum sampling rate and the computational load available in the sensors. This is the motivation behind the second investigated PA approach in this chapter. Consequently, this PA algorithm is based on distributing transmit power of beacons with SNR above threshold SNR to beacons with SNR below threshold SNR realizing a type of APA directly based on measured SNRs and, consequently, much simpler than other techniques. Simulation results confirm that such a simple strategy can be effective at medium-low SNR

regions, even w.r.t. more sophisticated optimization procedures. The investigated localization algorithms have been published in **B**, **C** and **D**.

1.3 List of publications

Paper A L. Reggiani and S. Bybordi, "Performance trade-offs for energy efficient localization based on EKFs," 2012 International Symposium on Wireless Communication Systems (ISWCS), August 2012.

Paper B S. Bybordi and L. Reggiani, "Algorithm for power allocation in localization processes," 2013 International Symposium on Wireless Communication Systems (ISWCS), August 2013.

Paper C S. Bybordi and L. Reggiani, "Impact of real ranging on algorithms for power allocation in localization processes," 2014 IEEE International Conference on Ultra-Wideband (ICUWB 2014), September 2014.

Paper D S. Bybordi and L. Reggiani, "A Review on suboptimal power allocation schemes for WSN localization," the 3rd International Conference on Circuits, Systems, Communications, Computers and Applications (CSCCA14), November 2014.

Paper E S. Bybordi and L. Reggiani, "Hybrid fingerprinting-EKF based tracking schemes for indoor passive localization," International Journal of Distributed Sensor Networks, vol. 2014, pp. 1-11, 2014.

CHAPTER II

Localization fundamentals

2.1 Wireless sensor networks in localization scenarios

Due to recent developments in hardware electronics and communications, low-cost and low-power WSN have found great importance in diverse applications such as industrial, medical, public services and many other fields. A WSN is collection of small, cheap, low-power sensing devices which are able to sense parameters to be monitored, process and broadcast sensed information. Considering the fact that nodes are distributed over surveillance area in which nodes locations are hard to reach, they should be manufactured with low cost and they should be able to operate by wireless communication. Additionally, since they are usually battery powered devices, wireless communication protocols should respect low-power constraints [2].

Since the main source of energy consumption in a single node is constituted by communication with other nodes, there is an increasing research trend for enabling nodes to process sensed information locally and in a distributed way [2]. This fact provides the network with longer action periods and less communication load unlike traditional sensor networks where the sensed information are required to be processed in a central processor.

A sensor node is usually equipped with a sensing part, a processor, memory, a power supply, a radio and a circuit enabling the management of all these functions

[21]. Generally speaking, WSN applications can be categorized into two cases: monitoring and tracking [21]. Monitoring applications can be summarized in applications such as environmental monitoring, battlefield surveillance, telemonitoring of human physiological data, etc.

Tracking applications are concerned with tracking objects, animals, humans and vehicles. Owing to the fact that sensor nodes are devices with limited energy resource and memory, wireless communication seems to be a suitable choice for exchanging required data in the network. Also, considering the fact that sensor nodes use limited energy resources like batteries, low power consumption is a crucial part of their design.

Having accurate position information of a single node in most of WSN applications is of great importance. For example there is an increasing interest in deployment of WSN in dangerous and remote environments. Regardless of the application context, when there is not an exact knowledge about position information of WSN nodes, localization plays a key role either as an assisting feature for application or as a major goal. To be clear, assume a WSN supposed to monitor temperature inside a building. Of course, the position information of nodes can be easily accessible. However, in case of WSN application for monitoring purposes in large areas, WSN application is pointless without having position information of nodes (e.g. WSN applications for detecting fire events over a large surveillance area like a forest). The global positioning system (GPS) of course can be a propitious candidate for this purpose in some cases [57]. On the other hand, owing to the fact that GPS signals travel long distances with low power, GPS signal is weakly received in environments with strong obstruction. Therefore, GPS signal is not practical in indoor scenarios for localization purposes. On the other hand, considering the low accuracy of GPS w.r.t to the dimensions of indoor environments, application of WSN in localization problems seems to be inevitable. In order to have target position estimated, a group of nodes, called beacons, should have a-priori information about their position. Generally speaking, due to positioning

structure in WSN and taking advantage of estimated ranging measures between each couple of beacons, final target position is estimated once pair-wise range measures are ready.

Pervasively applied measurements in position estimation are time of arrivals (TOA), time difference of arrival (TDOA), received signal strengths (RSS) and angle of arrivals (AOA). Measurements are based on information obtained from the signal exchanges among nodes. Consequently, the accuracy of the position estimate is dependent on the type of measurements between different nodes. In range based localization, firstly the ranges between nodes are measured in a phase called **ranging**. Then, the target position is estimated based on these measurements in a phase called **positioning** via static localization and/or fingerprinting (FP) in a single-shot determination of target position or tracking strategies using Bayesian filtering for estimating target position repeatedly over different time instants.

2.2 Ultrawide Band as a promising underlying technology

Based on the Federal Communications Commission (FCC) announcement, a signal is refereed as Ultrawide Band (UWB) which occupies a bandwidth greater than 20 percent of the center frequency or 500 MHz. Considering the fact that UWB occupies a large bandwidth, there will be possibility of interference with other existing wireless technologies. Consequently, FCC has forced some kind of limits on emission power which can have different values depending on the working frequency range [1]. Low level of transmission power spread over a large bandwidth makes UWB as a suitable choice for WSN requirements. In fact, UWB is able to coexist with other existing wireless standards in the same occupied bandwidth. In addition, UWB enabled WSNs can be deployed without any requirement for special permission for a targeted frequency spectrum occupation. Considering the license-free nature of UWB systems, there has been an increasing interest in deploying UWB in applications requiring

cheap wireless implementation. The large bandwidth, present in UWB systems, facilitates the use of low power wireless communication which is in agreement with WSN requirements. Of course, UWB signals are pervasively investigated in the literature [19, 14].

UWB technology is capable of communicating at very low energy levels, spread over a large bandwidth. Obviously, due to high bandwidth of UWB, there will be a fine resolution of Multipath Components (MPCs) at the receiver. Consequently, UWB is much more immune to multipath fading than other wireless technologies [26]. In the context of low data rate sensor applications, the large bandwidth is obtained by the usage of short pulses in the time domain which is called impulse radio UWB (IR-UWB). As a result, there will be a high temporal resolution of MPCs, which is one of the most influential factors in the accuracy of time-based ranging techniques [22]. In other words, the larger the bandwidth is, the better the accuracy will be. Just to elaborate this concept, an UWB pulse with the duration of 2 ns will result in a spatial resolution of about 60 cm. Equivalently, MPCs are commonly resolvable without any need for a complicated algorithm [42]. So UWB is surely a promising candidate for time based ranging techniques [31].

The earliest UWB systems were based on the usage of narrow, even sub nanoseconds, pulses without a need for using carrier, so realizing a carrier-less communication. The Absence of a conventional carrier eliminates the need for conventional circuitry required for the Intermediate Frequency (IF) stage. This issue makes the transceiver structure much simpler. In this thesis, according to the more recent IEEE 802.15.4a standard evolutions, we will consider narrow pulses with lower bandwidth (around 500 MHz) and modulated at carrier frequencies above 3 GHz. One of the greatest challenges in indoor positioning is the Non-Line-of-Sight (NLoS) impact: when the LoS link is highly attenuated or absent at the receiver, performance of ranging is severely deteriorated. As previously mentioned, one technique is to apply signals

with high penetration capability. Due to large bandwidth of UWB technology containing also low-frequency contents, UWB has an acceptable penetration capability in complex indoor environments. This issue means that, under certain conditions, UWB signal could pass group of materials or, equivalently, a LoS link necessarily is not a visible path between transmitter and receiver. In practice, the beacon distribution over surveillance areas should be designed for guaranteeing a LoS link between transmitting and receiving nodes as much as possible. Otherwise, the number of beacons is preferred to be increased at the gain of increasing the WSN implementation cost.

2.3 Localization

In localization scenarios based on WSNs, there are two groups of nodes. One group of nodes are the ones which have a priori information about their location coordinates. Another group is referred as targets, whose positions have to be estimated. Estimation of target position or, equivalently, localization mainly contains two phases. Firstly, inter-node distances are estimated using distance dependent features of the received signals like TOA, RSS, AOA in a phase called **ranging**. Ranging is done by WSN nodes which are mainly battery powered devices. Consequently, also complexity of ranging algorithms is of great concern and it should be kept as limited as possible.

The second phase, in which target position is estimated, is commonly referred as **positioning**. Estimations of targets' position can be realized via static localization, tracking strategies or FP [17, 43]. The first two cases are based on the acquisition of LD features from received signals, like RSS or TOA, by means of ranging and finally estimation of position using techniques as trilateration in static localization and EKF in tracking. On the other hand, FP takes advantage of LD features of received signals, exploited as unique signatures associated to the target locations. Firstly, a radio map containing stored LD parameters measured over predetermined points (grid points) is built during an off-line or training phase. Subsequently, target position is estimated

via pattern matching between ongoing measured LD parameters and those previously recorded.

2.3.1 Common ranging measures

2.3.1.1 Angle of arrival (AOA)

Ranging schemes using information related to AOA mostly take advantage of antenna arrays to estimate the direction, from which the signal is coming [35]. Antenna arrays are required at each receiving node instead of a single antenna. In fact, AOA based schemes estimate the node position by intersecting estimated information of direction related to signal arrival. This technique is usually referred as triangulation. However, some factors, such as the expensive implementation of antenna arrays, limit application of AOA based localization in indoor environments. Besides, the estimation accuracy of AOA based localization is influenced by different factors like dense multipath components in indoor environments and absence of LoS link between transmitter and receiver [30].

On the other hand, AOA based localization has the following advantages. For example the clock bias effect is not present, while this issue is of great concern in time based techniques like TOA. Also, in comparison with time based techniques, AOA based localization needs less receivers for computing the final position of target. For example, in case of a two dimensional scenario, two receivers are adequate to implement localization.

2.3.1.2 Received signal strength (RSS)

Transmitted power normally experiences an attenuation resulting from fading, channel variations and shadowing. Normally, the received power is a decreasing function of the distance between transmitter and receiver. Received signal strength (RSS) is implemented by measuring signal strength via measuring the power of the received

signal [31]. Then, the distance between transmitter and receiver is estimated according to some mathematical models describing propagation basic elements. The RSS measures are usually present in wireless chips. As a matter of fact, objects present in the scenario, like furniture, influence transmitted signal via absorption, reflection and additional attenuation components. This explains why RSS based localization cannot reach the same accuracy of the other methods, based on TOA or AOA. Important advantages and drawbacks of RSS can be summarized as follows. RSS based ranging is usually chip and easily implementable; in addition there are no rigid requirements for expensive and challenging time synchronization among nodes. However, as previously mentioned, RSS based localization accuracy is lower than other time based localization schemes [42].

In fact, performance of RSS depends on the accuracy of the defined model for propagation. A review of different models can be found in [16]. While the basic idea is to use free space propagation [33], the more realistic, commonly used model can be defined as

$$RSS = 10 \cdot log_{10}(P_r/P_0) = 10 \cdot log_{10}(P_t/P_0) + G_t + G_r - L_0 - 10\gamma log_{10}(d/d_0) + X, \tag{2.1}$$

where d is the distance between the transmitter and receiver (d_0 is a reference distance, e.g. 1 m and L_0 is the pathloss at d_0), P_t and P_r are transmitted and received powers in linear scale respectively (P_0 is the reference power, e.g. 1 mW), G_r and G_t are the antenna gains (usually equal to 0 dB in this context), γ is the path loss exponent and X is a log-normal random variable representing the shadow fading component (Gaussian in the dB scale).

2.3.1.3 Time of arrival (TOA)

Another candidate for estimating the distance between two nodes is to use the information related to time of arrival corresponding to the received signal. TOA based ranging uses the estimated information corresponding to the time of arrival of the received signal in order to obtain the distances among nodes. Of course, the distance between transmitting and receiving nodes is achievable by multiplying the estimated TOA by the speed of light. TOA estimations are commonly realized by taking advantage of correlators or matched filters at the receiving nodes [9]. As a matter of fact, TOA requires an acceptable level of time synchronization between transmitter and receiver considering its time based nature. Since UWB technology has a relatively high temporal resolution, it is a promising candidate for TOA based ranging.

TOA estimation can be implemented in one way or two way versions. In one way version, transmitting nodes transmit the signal in a synchronized scenario. The receiving nodes estimate TOA, knowing the corresponding times of transmission. In two way TOA, nodes are required to transmit and receive according to a precise protocol. The receiving node sends an acknowledgment to the transmitter and, consequently, TOA will be derived by the half of the round trip time after subtracting the processing and other offset times. The disadvantage of two way TOA is the fact that two transmissions should be done for each ranging measurements unlike one way TOA [42] .

Time difference of arrival (TDOA) alleviates the synchronization requirement of TOA. In TDOA, transmitters are only required to be synchronized. TDOA measures difference of TOA between two transmitting nodes and a receiving node [57]. Unlike TOA in which each measurement can be interpreted as a circle around transmitting node defining all possible locations of receiving node on the circle perimeter, in TODA, each measurement can be interpreted as a hyperbola showing all possible location of

receiving node considering that the two transmitting nodes are the hyperbola foci.

The performance of time based ranging techniques is strongly dependent on the availability of the direct link between transmitting and receiving node [22]. The direct link is not necessarily equal to a physical link in the sense that in NLoS scenarios, in which the direct physical link is absent or attenuated, direct link can sometime be detected despite the fact that it is attenuated by obstruction or strong attenuation.

The ranging algorithms used in this work are based on ranging techniques proposed in [20, 29]. The first one is based on using threshold techniques. In [20], authors propose a TOA estimator that selects the first correlator output peak that exceeds a fixed fraction of the strongest peak magnitude. In fact, it is a low-complexity estimator based on a threshold for detecting the first path.

The ranging technique mentioned in [29] outputs a discrete vector of likely distances with an associated approximation of the probability that these distances correspond to the estimates. This estimator can be used to increase the accuracy of distance estimates on a measurement by measurement basis, instead of assuming a fixed error variance which is the same for all measurements. This soft information is also used to provide a measure of the uncertainty of the distance estimate, i.e., an estimate of the error magnitude; in fact a large uncertainty is often associated to a NLOS measure or to a measure obtained at low Signal-to-Noise Ratio (SNR). This choice allows a realistic simulation of the algorithm, with low and high quality ranging measures.

2.3.2 Positioning

There are different classifications concerning the features of localization algorithms.

Cooperative and non-cooperative

Obviously, the larger the number of beacons is, the better the position estimate

will be. However, it is not always feasible to increase the number of beacons. One alternative can be to let targets communicate with each other to exchange some of the parameters and have a better position estimate; this is conceptually referred as cooperative positioning. A cooperative scenario considers all type of measurements including inter-target measurements and those between targets and reference nodes. On the other hand, in a non-cooperative scenario, position estimation relies just on the measurements between targets (agents) and reference nodes (beacons). Of course, it is obvious that the results of cooperation among agents will improve estimation accuracy.

Centralized and distributed

In centralized positioning, there is a central processing center in which position estimation is accomplished once the estimated ranging measures are sent to the processing center. However, in distributed positioning, as also it is evident from the name, the WSN nodes try to accomplish positioning by exchanging ranging measures among them. In centralized localization, nodes are not required to be complex from a processing point of view. However, since all of the ranging information is needed to be transmitted to a central station, there will be an increased traffic in the network.

Active and passive

In active localization, targets participate in the exchange of data in the localization procedure while in passive localization, targets do not participate in the exchange of data. In fact, the ranging measures are estimated according to information obtained from the signal reflected or scattered from the target.

2.3.2.1 Static localization

The commonly used approach in static localization is based, firstly, on the collection of distance dependent parameters of received signals (e.g. TOA) in the ranging phase. Then, the unknown position of the target is estimated using methods like multi-lateration or multi-angulation depending on the type of available ranging measures.

In the context of static localization, the position of a target can be calculated using the well-known geometrical method called lateration or angulation depending on the type of ranging parameters. Here, lateration and consequent formulation is pursued. Each ranging measure like TOA or RSS can be interpreted as a circle representing all possible locations of the target on a circle perimeter in which the beacon is the circle center. Therefore, by intersecting these circles, target position can be calculated. The minimum number of ranging measures or, equivalently, the number of beacons required for multi-lateration is 3 for $2D$ positioning. Assuming TOA as ranging measure, the nonlinear function between ranging measures and target position can be written as

$$d_i^2 = g_i(\mathbf{X}) = (x - x_i)^2 + (y - y_i)^2 \,, \tag{2.2}$$

where $\mathbf{X} = [x \;\; y]^T$ is the target coordinate, d_i is the ranging measure related to i^{th} beacon, $[x_i \;\; y_i]^T$ is the coordinate of i^{th} beacon.

However, trilateration is suitable when we have exact knowledge of ranging measures. In this case, three circles will intersect in one point which shows the position of the target. However, in practice, the ranging measures face uncertainty due to the ranging imperfect estimation process. Therefore, we will have an uncertainty area instead of a point as a result of just using multi-lateration technique. Consequently, in

practice the solution is to use statistical methods in order to minimize the estimation error (MSE).

Here, a brief review of the commonly used approaches for static localization will be presented. Position estimation based on range measurements is commonly carried out by finding minimum or maximum of an objective function. Equation (2.2) implies a nonlinear function relating the target position with range measures.

Least squares

Assuming $[x \ \ y]^T$ and $[x_i \ \ y_i]^T \ i = 1, .., N_b$ as coordinates of target and the i^{th} beacon respectively, the distance estimate can be written as

$$\widehat{d_i} = d_i + n_i = \left\| \begin{array}{c} x - x_i \\ y - y_i \end{array} \right\| + n_i, \tag{2.3}$$

where $\|.\|$ is the Euclidean norm operator, n_i is the i^{th} range measure error which can have different mean values and variances depending on the different channel conditions.

As a matter of fact, when there is no a priori knowledge about statistics of distance error, LS solution is a promising candidate. In case of having a priori knowledge about statistics of distance error, using Weighted Least Squares (WLS) approach can improve localization performance.

As previously mentioned, the final goal is to minimize $\sum_{i=1}^{N_b} \left(\widehat{d_i} - g_i(\mathbf{X})\right)^2$ which is essentially a nonlinear function of target coordinates. In order to obtain a final position estimate using least squares, nonlinear function mentioned in (2.2) can be linearized around the point $\mathbf{X}_0 = [x_0 \ \ y_0]^T$, which can be done simply by taking advantage of a Taylor's expansion [23] as

$$g_i(\mathbf{X}) = g_i(\mathbf{X}_0) + \left.\frac{\partial g_i}{\partial x}\right|_{\mathbf{X}_0} (x - x_0) + \left.\frac{\partial g_i}{\partial y}\right|_{\mathbf{X}_0} (y - y_0). \tag{2.4}$$

So the final version can be summarized as

$$\mathbf{G}(\mathbf{X}) = \mathbf{G}(\mathbf{X}_0) + \left.\mathbf{H}\right|_{\mathbf{X}_0} (\mathbf{X} - \mathbf{X}_0), \tag{2.5}$$

where

$$\mathbf{G}(\mathbf{X}) = \begin{bmatrix} g_1(\mathbf{X}) \\ \vdots \\ g_{N_b}(\mathbf{X}) \end{bmatrix}, \tag{2.6}$$

and

$$\mathbf{H} = \begin{bmatrix} \frac{\partial g_1}{\partial x} & \frac{\partial g_1}{\partial y} \\ \vdots & \vdots \\ \frac{\partial g_{N_b}}{\partial x} & \frac{\partial g_{N_b}}{\partial y} \end{bmatrix} = \begin{bmatrix} \frac{x-x_1}{\sqrt{(x-x_1)^2+(y-y_1)^2}} & \frac{y-y_1}{\sqrt{(x-x_1)^2+(y-y_1)^2}} \\ \vdots & \vdots \\ \frac{x-x_{N_b}}{\sqrt{\left(x-x_{N_b}\right)^2+\left(y-y_{N_b}\right)^2}} & \frac{y-y_{N_b}}{\sqrt{\left(x-x_{N_b}\right)^2+\left(y-y_{N_b}\right)^2}} \end{bmatrix}. \tag{2.7}$$

As previously mentioned the objective is to minimize the following cost function

$$\sum_{i=1}^{N_b} \left(\widehat{d}_i - g_i(\widehat{\mathbf{X}})\right)^2 = \left(\widehat{\mathbf{d}} - \mathbf{G}(\widehat{\mathbf{X}})\right)^T \left(\widehat{\mathbf{d}} - \mathbf{G}(\widehat{\mathbf{X}})\right). \tag{2.8}$$

If $\mathbf{H}\Big|_{\mathbf{X}_0}$ is denoted $\mathbf{H}_0$, the least square solution can be expressed [23]

$$\widehat{\mathbf{X}} = \mathbf{X}_0 + \left(\mathbf{H}_0{}^T\mathbf{H}_0\right)^{-1}\mathbf{H}_0{}^T(\widehat{\mathbf{d}} - \mathbf{G}(\mathbf{X}_0)). \tag{2.9}$$

As it can be inferred from the equation, an initial estimate of target location is required. In fact, the solution can be achieved iteratively by setting an accuracy threshold between the iteration steps or setting a max number of iterations. As mentioned previously, knowledge of the ranging error statistics will improve localization performance by using WLS technique [23], i.e.

$$\widehat{\mathbf{X}} = \mathbf{X}_0 + \left(\mathbf{H}_0{}^T\mathbf{W}\mathbf{H_0}\right)^{-1}\mathbf{H_0}{}^T\mathbf{W}(\widehat{\mathbf{d}} - \mathbf{G}(\mathbf{X}_0). \tag{2.10}$$

The weights are usually assumed proportional to the inverse of the measurement variances. When the error associated with each ranging measure is assumed to be a zero mean Gaussian random process, WLS and Maximum Likelihood (ML) estimates coincide.

Another alternative for static localization is to linearize the function mentioned in (2.2) in a different way. By subtracting one of the equations (let us assume for example the equation related to d_1) from the others, we obtain [36, 4]

$$(x_1 - x_j)x + (y_1 - y_j)y = \frac{1}{2}({x_1}^2 - {x_j}^2 + {y_1}^2 - {y_j}^2 + {d_j}^2 - {d_1}^2). \tag{2.11}$$

Consequently, we have a set of linear equations under the formulation

$$\begin{bmatrix} x_1 - x_2 & y_1 - y_2 \\ \vdots & \vdots \\ x_1 - x_{N_b} & y_1 - y_{N_b} \end{bmatrix} \begin{bmatrix} x \\ y \end{bmatrix} = \frac{1}{2} \begin{bmatrix} {x_1}^2 - {x_2}^2 + {y_1}^2 - {y_2}^2 + {d_2}^2 - {d_1}^2 \\ \vdots \\ {x_1}^2 - {x_{N_b}}^2 + {y_1}^2 - {y_{N_b}}^2 + {d_{N_b}}^2 - {d_1}^2 \end{bmatrix}. \tag{2.12}$$

Equation (2.12) is a set of linear equations and $\mathbf{A} \cdot \mathbf{X} = \mathbf{b}$ will have a closed form solution

$$\mathbf{X} = \left(\mathbf{X}^T \mathbf{A}\right)^{-1} \mathbf{X}^T \mathbf{b}. \tag{2.13}$$

We can also observe that the minimum required number of beacons is 4 [4].

2.3.2.2 Fingerprinting (FP)

Conventional localization algorithms using signal information like TOA, RSS, AOA and TDOA face a serious performance degradation in indoor environments affected by phenomena like harsh multipath and Non Line of Sight (NLoS). Taking advantage of LD features of signal, there can exist a radio map containing LD parameters measured in predetermined points called grids so that target position can be estimated using pattern matching algorithms. Fingerprinting contains two basic steps: in the first step which is an offline phase, LD parameters of signal are measured in a grid based map over the surveillance area in order to be used as a reference in the second phase of FP. This is an online phase in which target position is estimated by pattern matching between ongoing measurements of LD parameters and stored LD parameters in the offline phase.

The most common LD parameter is RSS. However, due to high temporal res-

olution of UWB signals, application of UWB Channel Impulse Response (CIR) or some of its features has been reported in the literature [48, 6, 11, 5, 58]. In [48], authors propose CIR as the LD metric during FP. For pattern matching required in FP, a parameter called channel spatial correlation is introduced. The target position is estimated by maximizing channel spatial correlation over FP grid points. However, due to imperfection in CIR estimation, a threshold is required to be set in order to consider reasonable spatial correlations in pattern matching.

In [6], CIR is used as a location dependent parameter. There is one fixed receiver recording CIR data collected from different location of a transmitter over different geometrical regions during the FP training (offline phase). Using a complex Gaussian distribution assumption for channel taps corresponding to a specific region, sample mean and covariance matrix are estimated over multiple observation of CIR over a specific area. In order to align measured CIRs, the strongest path is considered by taking the maximum absolute value. Besides, some simplifying assumptions including zero mean assumption and independent channel taps leading to a diagonal covariance matrix are considered. According to binary hypothesis testing, a probabilistic metric as a result of Gaussian assumption is built for two regions in order to map the location of transmitters. Because of the existence of more than two regions, it is introduced a pair-wise selection among regions and a consequent computation of a metric for each pair.

In [11], CIR is applied as a location dependent signature of a transmitter. More specifically, Average Power Delay Profile (APDP) of CIR is used for region decision. Their considered scenario contains one receiver in the way that receiver location is fixed and a test transmitter is located in different regions. During the training phase, multiple CIR PDP measurements are stored in a data base. However, localization accuracy can be improved by increasing the number of receivers as in the case of time dependent ranging techniques. Assuming the outcome of statically indepen-

dent Gaussian random variables for APDP of different regions and using a maximum likelihood estimator, the position of the transmitter is determined.

In [5], a sub-category of CIR features including the mean excess delay, the rms delay spread, the maximum excess delay, the total received power, the number of multipath components, the power of the first path, the arrival time of the first path of the channel are used as LD parameters. For the pattern matching part of the FP, an artificial neural network (AAN) based algorithm is proposed.

Finally [58] presents a pervasive review of existing fingerprinting techniques for both active and passive localization.

One of the simplest mapping techniques is the selection of target coordinates based on the coordinates of FP grid point leading to minimum Euclidean distance between measured LD metric and the metric related to that specific FP grid point measured during FP offline phase. For formulating the metric, let us assume that the number of LD measures be N_M. For the sake of simplicity in mathematical representation, LD metric is assumed to be scalar although an extension to the LD vector case is straightforward. During the offline phase of FP, the LD metric vector $\mathbf{M_{p_i}}$ $(N_M \times 1)$ is measured at each point of FP grid (p_i) and stored in a database. Consequently, target position is estimated based on minimizing the following Euclidean distance over grid points

$$\underset{\{p_i\}}{\text{Arg min}} \quad \|\mathbf{M} - \mathbf{M_{p_i}}\|, \tag{2.14}$$

where $\mathbf{M}$ is the LD metrics vector measured during online phase of FP.

2.3.2.3 Tracking

Frequent estimation of moving target position over time using previously estimated position information is namely called tracking. Additionally, other motion related parameters like velocity and acceleration can be tracked. One of the commonly used

tools in tracking is Kalman Filter (KF). First introduction of KF was by Rudolph Emil Kalman [40]. The distinguished feature of KF is related to repetitive estimation over evolving time steps rather than a single one-hot estimation as in the case of static localization or FP. Mainly, it is applied for state estimation of dynamical system under the assumption that the system is linear and all the errors including those in state transitions and measurements are Gaussian. In fact, the state estimation is done by taking advantage of the estimated state in the previous time step and current measurements. The details of conventional KF for dynamical systems in which both state transition and measurement functions are linear can be found in [44]. In this section, presented KF formulation is dedicated to dynamical systems with nonlinear equations (denoted as EKF) w.r.t. their application in position tracking. KF contains two main steps, i.e. prediction and update stages. In fact, the next state is predicted using a motion model. Then, the predicted state is corrected according to the new measured data.

Extended Kalman filter (EKF)

When either state transition equation or measurement equation are not linear, by linearizing them around related working points, EKF can be applied to state tracking of the system with nonlinear equations. State transition can be represented as:

$$\mathbf{x}_{k+1} = \mathbf{f}(\mathbf{x}_k) + \mathbf{w}_k, \tag{2.15}$$

where $\mathbf{x}_k$ is the state vector at time step k. The state transition noise vector is assumed to be a zero mean Gaussian random process with covariance matrix $\mathbf{Q}_k$ i.e. $\mathbf{w}_k \sim \mathcal{N}(0, \mathbf{Q}_k)$ where $\mathbf{f}$ is in general a nonlinear function showing state

transition over time.

The measurement equation can be written as

$$\mathbf{z}_k = \mathbf{h}(\mathbf{x}_k) + \mathbf{v}_k, \tag{2.16}$$

where $\mathbf{z}_k$ is the the measured data at time k, $\mathbf{h}$ is the nonlinear function showing predicted measurements based on the state x_k, $\mathbf{v}_k$ is the measurement (observation) noise assumed to be a zero mean Gaussian noise with covariance matrix $\mathbf{R}_k$ i.e. $\mathbf{v}_k \sim \mathcal{N}(0, \mathbf{R}_k)$.

EKF estimates the state vector iteratively through the following procedure:

1. computation of a-priori estimate (prediction) using previously computed a-posteriori estimate i.e.

$$\hat{\mathbf{x}}_k^- = f(\hat{\mathbf{x}}_{k-1}). \tag{2.17}$$

2. Computation of a-priori covariance matrix using previously computed a-posteriori covariance matrix and process noise covariance matrix via

$$\mathbf{P}_k{}^- = \mathbf{A}_k \mathbf{P}_{k-1} \mathbf{A}_k{}^T + \mathbf{Q}_k, \tag{2.18}$$

   where $\mathbf{A}_k = \left.\frac{\partial f}{\partial \mathbf{x}}\right|_{\hat{\mathbf{x}}_{k-1}}$

3. Computation of Kalman gain matrix

$$\mathbf{G}_k = \mathbf{P}_k{}^{-}\mathbf{H}_k{}^{T}\left[\mathbf{S}_k\right]^{-1}, \tag{2.19}$$

where $\mathbf{H}_k$ is the linearized measurement function at $\hat{\mathbf{x}}_k^-$ i.e. $\mathbf{H}_k = \left.\frac{\partial h}{\partial \mathbf{x}}\right|_{\hat{\mathbf{x}}_k^-}$ and $\mathbf{S}_k$ is the covariance matrix related to so-called innovation process $(\tilde{\mathbf{y}_k})$ which in fact is the residual between the observed measurement $(\mathbf{z}_k)$ and predicted measurement $(h(\hat{\mathbf{x}}_k^-))$ i.e. $\tilde{\mathbf{y}_k} = \mathbf{z}_k - h(\hat{\mathbf{x}}_k^-)$. Consequently, $\mathbf{S}_k$ can be written as

$$\mathbf{S}_k = \mathbf{H}_k\mathbf{P}_k{}^{-}\mathbf{H}_k{}^{T} + \mathbf{R}_k. \tag{2.20}$$

4. A priori estimate is updated to a posteriori estimate

$$\hat{\mathbf{x}}_k = \hat{\mathbf{x}}_k^- + \mathbf{G}_k\tilde{\mathbf{y}_k}. \tag{2.21}$$

5. Finally, the a posteriori covariance matrix is computed

$$\mathbf{P}_k = (\mathbf{I} - \mathbf{G}_k\mathbf{H}_k)\mathbf{P}_k{}^{-}. \tag{2.22}$$

CHAPTER III

Lower bounds on localization

3.1 The lower bound for static localization

In this Section we will develop the tools necessary for understanding and using the lower limits of the positioning error associated to a static localization process.

3.1.1 Derivation of Fisher information matrix for target position estimation

The scenario we are considering includes one moving target (with unknown position) and a set of fixed nodes with known positions (called beacons). This is done by measuring time of arrival (TOA) of communicated signal between target and each of the beacons (ranging) and solving the associated positioning problem. We assume a set of unbiased distance (TOA) estimates

$$\widehat{d_j} = d_j + e_j; j = 1, ..., N_b, \tag{3.1}$$

where $\widehat{d_j}$ and d_j are the estimated and actual distances between the target and the j^{th} beacon and $N_b \geq 3$ is the number of beacons. Distance estimates are assumed to be unbiased and subject to a Gaussian error $e_j \sim N(0, \sigma_j^2)$. The actual distance

between the target and the j^{th} beacon is

$$d_j = \sqrt{(x - x_j)^2 + (y - y_j)^2}. \tag{3.2}$$

The variables $\begin{bmatrix} x \\ y \end{bmatrix}$ and $\begin{bmatrix} x_j \\ y_j \end{bmatrix}$ are positions of the target and the j^{th} beacon in 2D coordinates respectively. The goal is to achieve a lower bound for the mean squared error (MSE) of target position estimate. MSE for a set of unbiased parameter estimates can be written as

$$E\left[(\widehat{\theta} - \theta)^T(\widehat{\theta} - \theta)\right] = tr\left\{cov(\widehat{\theta})\right\}, \tag{3.3}$$

based on Cramer Raw Bound (CRB) for a vector of parameters to be estimated $(\widehat{\theta})$. We have

$$cov(\widehat{\theta}) \geq \mathbf{J}^{-1}, \tag{3.4}$$

where $\mathbf{J}$ is the Fisher Information Matrix (FIM). This matrix can be written as

$$\mathbf{J} = \begin{bmatrix} J_{xx} & J_{xy} \\ J_{yx} & J_{yy} \end{bmatrix} \tag{3.5}$$

and each FIM element can be computed as

$$[\mathbf{J}]_{ij} = -E\left[\frac{\partial^2 L}{\partial\theta_i \partial\theta_j}\right], \tag{3.6}$$

where L is log-likelihood function which will be defined in the following. Assuming that distance measurements are statistically independent, the joint conditional probability density function can be written as

$$P(\widehat{\mathbf{d}}|x,y) = \prod_j \frac{e^{-\frac{(\widehat{d_j}-d_j)^2}{2\sigma_j^2}}}{\sqrt{2\pi\sigma_j^2}}, \tag{3.7}$$

where $\widehat{\mathbf{d}}$ is the observation vector related to N_b independent distance (TOA) measurements between the target and each of the beacons. So the log likelihood function can be written as

$$L = -\frac{1}{2}\sum_j Ln(2\pi\sigma_j^2) - \sum_j \frac{(\widehat{d_j}-d_j)^2}{2\sigma_j^2}. \tag{3.8}$$

Here, due to the similarity in the derivation of all FIM elements, we consider only J_{xx}. From Equation(3.6), we have

$$J_{xx} = -E\left[\frac{\partial^2 L}{\partial x^2}\right] \tag{3.9}$$

and the second derivative of log-likelihood function with respect to x is

$$\frac{\partial^2 L}{\partial x^2} = -\sum_j \frac{1}{2\sigma_j^2}[-2\widehat{d_j}\left((x-x_j)^2+(y-y_j)^2\right)^{-0.5} + 2\widehat{d_j}\left((x-x_j)^2+(y-y_j)^2\right)^{-1.5}(x-x_j)^2+2]. \tag{3.10}$$

Since $E\left[\widehat{d_j}\right] = \left((x-x_j)^2+(y-y_j)^2\right)^{0.5}$, by combining (3.9) and (3.10), J_{xx} is computed as

$$\begin{aligned} J_{xx} &= \sum_j \frac{1}{\sigma_j^2}\frac{(x-x_j)^2}{(x-x_j)^2+(y-y_j)^2} \\ &= \sum_j \frac{cos^2(\alpha_j)}{\sigma_j^2} \end{aligned} \tag{3.11}$$

In brief, using (3.5),(3.6) and (3.8), FIM is computed as

$$\mathbf{J} = \begin{bmatrix} \sum_j \frac{cos^2(\alpha_j)}{\sigma_j^2} & \sum_j \frac{sin(\alpha_j)cos(\alpha_j)}{\sigma_j^2} \\ \sum_j \frac{sin(\alpha_j)cos(\alpha_j)}{\sigma_j^2} & \sum_j \frac{sin^2(\alpha_j)}{\sigma_j^2} \end{bmatrix}, \tag{3.12}$$

where $sin(\alpha_j)$ and $cos(\alpha_j)$ are defined as

$$cos(\alpha_j) = \frac{x-x_j}{\sqrt{(x-x_j)^2+(y-y_j)^2}} \tag{3.13}$$

and

$$sin(\alpha_j) = \frac{y - y_j}{\sqrt{(x - x_j)^2 + (y - y_j)^2}}. \tag{3.14}$$

Coming back to (3.3), we have

$$MSE = E\left[(\widehat{x} - x)^2 + (\widehat{y} - y)^2\right] \geq tr\left\{\mathbf{J}^{-1}\right\}. \tag{3.15}$$

and therefore

$$MSE \geq \mathbf{J}_{xx}^{-1} + \mathbf{J}_{yy}^{-1} = \frac{\sum\limits_j \frac{1}{\sigma_j^2}}{\frac{1}{4} \cdot \left[\left(\sum\limits_j \frac{1}{\sigma_j^2}\right)^2 - \left(\sum\limits_j \frac{cos(2\alpha_j)}{\sigma_j^2}\right)^2 - \left(\sum\limits_j \frac{sin(2\alpha_j)}{\sigma_j^2}\right)^2\right]}. \tag{3.16}$$

Additional considerations on the MSE associated to multiple targets can be found in [8]-[53]. In (3.16), MSE of target position estimate is denoted as SPEB in [53]. There is a slightly different notation in the presentation of (3.16) in [53] in the sense that $\lambda_j = \frac{1}{\sigma_j^2}$. In the following, some observations related to the FIM eigen-analysis are briefly mentioned [53]-[54]-[52].

3.1.2 Eigen analysis of FIM

FIM is a symmetric matrix. Based on the algebraic interpretation in Sect. 3.1.1 and taking into account FIM dimension, i.e 2×2, $\mathbf{x}^T\mathbf{J}\mathbf{x} = 1$ describes a rotated ellipse in 2D. The vector $\mathbf{x}$ is a set of points in $\mathbb{R}^2$ and, therefore, FIM can be decomposed as [54]-[52]

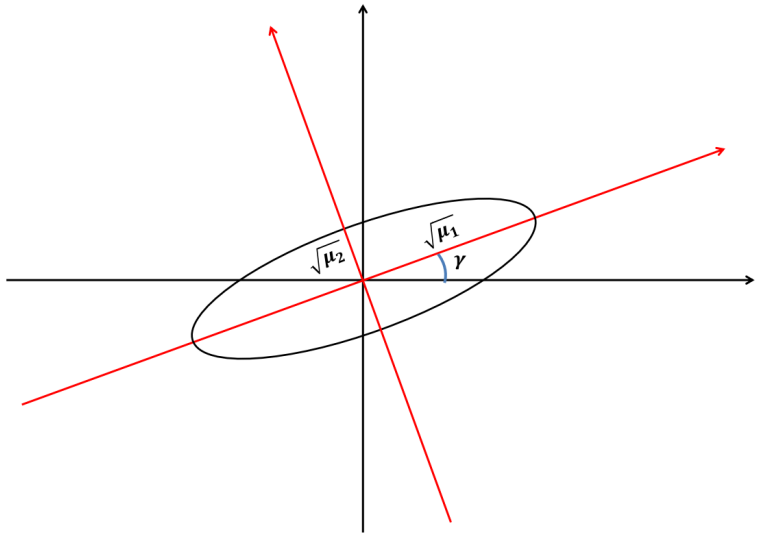

Figure 3.1: Information ellipse [54] described by semi-major and semi-minor length of $\sqrt{\mu_1}$ and $\sqrt{\mu_2}$ respectively and by the rotation angle γ

$$\mathbf{J} = \sum_j \lambda_j \mathbf{J}_r(\alpha_j) = \mathbf{U} \begin{bmatrix} \mu_1 & 0 \\ 0 & \mu_2 \end{bmatrix} \mathbf{U}^T, \tag{3.17}$$

where

$$\mathbf{J}_r(\alpha_j) = \begin{bmatrix} cos^2(\alpha_j) & sin(\alpha_j)cos(\alpha_j) \\ sin(\alpha_j)cos(\alpha_j) & sin^2(\alpha_j) \end{bmatrix}, \tag{3.18}$$

and μ_1, μ_2 are the eigenvalues of FIM. The matrix $\mathbf{U} = \begin{bmatrix} cos(\gamma) & -sin(\gamma) \\ sin(\gamma) & cos(\gamma) \end{bmatrix}$ contains the eigenvectors associated to eigenvalues μ_1 and μ_2. Let us define the information ellipse as [54]-[52]

$$\mathbf{x}^T \mathbf{J}^{-1} \mathbf{x} = 1. \tag{3.19}$$

Considering the structure of the information ellipse, we have an ellipse with major and minor axis length of $2\sqrt{\mu_1}$ and $2\sqrt{\mu_2}$ respectively. In fact, the rotation matrix $\mathbf{U}$ represents a rotation of the the old coordinates to a new coordinates system corresponding to the major and minor axes of the rotated ellipse (Fig. 3.1).

In the following, there will be a discussion about the properties of the FIM eigenstructure and its application to a localization scenario in order to achieve better localization accuracy.

3.1.2.1 FIM eigenstructure for a single beacon

In Equation (3.16), λ_j is the Ranging Information Intensity (RII) related to the j^{th} beacon [54]. The matrix $\mathbf{J}_r(\alpha_j)$ is a rank one matrix with eigenvalues $\mu_1 = 1$ and $\mu_2 = 0$ and respective eigenvectors of $\mathbf{U}_1 = \begin{bmatrix} cos(\alpha_j) \\ sin(\alpha_j) \end{bmatrix}$ and $\mathbf{U}_2 = \begin{bmatrix} -sin(\alpha_j) \\ cos(\alpha_j) \end{bmatrix}$. It should be kept in mind that the eigenvector $\mathbf{U}_2$ is in the null-space of $\mathbf{J}$.

As previously mentioned, FIM can be completely described by μ_1, μ_2 and γ, i.e. $\mathbf{J} = F(\mu_1, \mu_2, \gamma)$. For a single beacon, it can be written as $\lambda_k \mathbf{J}_r(\alpha_k) = F(\lambda_k, 0, \alpha_k)$. In fact, this formulation belongs to a degenerate ellipse (a line segment) rotated with an angle of α_k.

3.1.2.2 FIM eigenstructure for two beacons and more

For the sake of simplicity, the following FIM notation will be applied in the sequel,

$$\mathbf{J} = \begin{bmatrix} a & b \\ b & c \end{bmatrix}. \tag{3.20}$$

It is worth to elaborate the eigen-structure of FIM in (3.17). Solving the characteristic equation in order to find the eigenvalues μ_1 and μ_2, we have

$$det(\mathbf{J} - \mu_i \mathbf{I}) = 0 \; [i = 1, 2] \tag{3.21}$$

and

$$\begin{aligned} \mu_{1,2} &= \frac{a + c \pm \sqrt{(a-c)^2 + (2b)^2}}{2} \\ &= \frac{\sum\limits_j \lambda_j \pm \sqrt{\left(\sum\limits_j \lambda_j cos(2\alpha_j)\right)^2 + \left(\sum\limits_j \lambda_j sin(2\alpha_j)\right)^2}}{2}. \end{aligned} \tag{3.22}$$

It is obvious that

$$\mu_1 + \mu_2 = \sum_j \lambda_j = tr\left\{\mathbf{J}\right\}, \tag{3.23}$$

$$\mu_1 \mu_2 = \frac{\left(\sum\limits_j \lambda_j\right)^2 - \left(\sum\limits_j \lambda_j cos(2\alpha_j)\right)^2 - \left(\sum\limits_j \lambda_j sin(2\alpha_j)\right)^2}{4}. \tag{3.24}$$

and

$$\mu_1 - \mu_2 = \sqrt{(a-c)^2 + (2b)^2}$$
$$= \sqrt{\left(\sum_j \lambda_j cos(2\alpha_j)\right)^2 + \left(\sum_j \lambda_j sin(2\alpha_j)\right)^2}. \quad (3.25)$$

According to (3.16), (3.23) and (3.24), the numerator of SPEB is nothing but $\mu_1 + \mu_2$ and the denominator is $\mu_1\mu_2$. Therefore,

$$SPEB = \frac{\mu_1 + \mu_2}{\mu_1 \cdot \mu_2} = \frac{1}{\mu_1} + \frac{1}{\mu_2} = tr\left\{\begin{bmatrix} \mu_1 & 0 \\ 0 & \mu_2 \end{bmatrix}\right\}^{-1}, \quad (3.26)$$

which confirms the fact mentioned in [54] stating that SPEB is independent from the coordinate system. Equation (3.26) is an evidence of this phenomenon. Another proof using cyclic property of the trace operator is provided in [54]. This issue allows us to consider SPEB in two decoupled orthogonal directions and regardless of the coordinate system [50].

Now, let us focus on the structure of the eigenvectors. Both eigenvectors of FIM are described by γ (rotation angle of ellipse). Using (3.17), we have

$$\mathbf{U}^T\mathbf{J}\mathbf{U} = \begin{bmatrix} \mu_1 & 0 \\ 0 & \mu_2 \end{bmatrix}. \quad (3.27)$$

Simplifying the right side of (3.27), we obtain

$$\begin{bmatrix} a \cdot cos^2(\gamma) & (c-a) \cdot sin(\gamma)cos(\gamma) \\ + c \cdot sin^2(\gamma) & + b \cdot (cos^2(\gamma) \\ + 2b \cdot sin(\gamma)cos(\gamma) & - sin^2(\gamma)) \\ \\ (c-a) \cdot sin(\gamma)cos(\gamma) & a \cdot sin^2(\gamma) \\ + b \cdot (cos^2(\gamma) & + c \cdot cos^2(\gamma) \\ - sin^2(\gamma)) & - 2b \cdot sin(\gamma)cos(\gamma) \end{bmatrix} = \begin{bmatrix} \mu_1 & 0 \\ 0 & \mu_2 \end{bmatrix}. \tag{3.28}$$

By putting one of the off-diagonal elements of the right side matrix in (3.28) equal to zero, rotation angle can be computed as

$$tan(2\gamma) = \frac{2b}{a-c}. \tag{3.29}$$

Taking into account (3.25) and (3.29) (this is also shown in Fig. 3.2 in the right triangle ABC), it can be concluded that

$$sin(2\gamma) = \frac{2b}{\mu_1 - \mu_2} = \frac{\sum\limits_j \lambda_j sin(2\alpha_j)}{\mu_1 - \mu_2}, \tag{3.30}$$

and

$$cos(2\gamma) = \frac{a-c}{\mu_1 - \mu_2} = \frac{\sum\limits_j \lambda_j cos(2\alpha_j)}{\mu_1 - \mu_2}. \tag{3.31}$$

It is worth to simplify some of the trigonometric identities appearing in FIM and

SPEB formulations for later use:

$$\left(\sum_j \lambda_j cos(2\alpha_j)\right)^2 + \left(\sum_j \lambda_j sin(2\alpha_j)\right)^2 = \sum_j \lambda_j^2 + \sum_{i=1}^{N_b-1}\sum_{j=i+1}^{N_b} 2\lambda_i\lambda_j cos(2(\alpha_i - \alpha_j)). \tag{3.32}$$

$$\left(\sum_j \lambda_j\right)^2 = \sum_j \lambda_j^2 + \sum_{i=1}^{N_b-1}\sum_{j=i+1}^{N_b} 2\lambda_i\lambda_j. \tag{3.33}$$

Using the above-mentioned simplifications, (3.16) can be rewritten as

$$SPEB = \frac{2\sum_j \lambda_j}{\sum_{i=1}^{N_b-1}\sum_{j=i+1}^{N_b} \lambda_i\lambda_j(1 - cos(2(\alpha_i - \alpha_j)))}. \tag{3.34}$$

This last formulation of SPEB is the one mentioned in [50] as the objective function in order to achieve better localization performance via power allocation.

3.1.2.3 FIM structure transformation with a new beacon addition

Let us consider now the FIM structure when a new beacon is added to a set of previously present beacons in the localization scenario. This section is a summary of some related sections in [54] and [52] with some mathematical extensions and elaborations in the necessary parts.

If we assume the FIM, related to present beacons, denoted by $F(\mu_1, \mu_2, \gamma)$ and, with the new added beacon, denoted by $F(\lambda_k, 0, \alpha_k)$ which is an equivalent representation of $\lambda_k \mathbf{J}_r(\alpha_k)$, the new FIM ($\widetilde{\mathbf{J}}$) will be

$$\widetilde{\mathbf{J}} = \mathbf{J} + \lambda_k \mathbf{J}_r(\alpha_k). \tag{3.35}$$

In other words,

$$F(\widetilde{\mu_1}, \widetilde{\mu_2}, \widetilde{\gamma}) = F(\mu_1, \mu_2, \gamma) + F(\lambda_k, 0, \alpha_k) \tag{3.36}$$

and, now, $\widetilde{\mu_1}, \widetilde{\mu_2}$ and $\widetilde{\gamma}$ should be computed. Assuming that $\widetilde{\mathbf{J}}$ is written as

$$\widetilde{\mathbf{J}} = \begin{bmatrix} \widetilde{a} & \widetilde{b} \\ \widetilde{b} & \widetilde{c} \end{bmatrix} = \begin{bmatrix} a + \lambda_k cos^2(\alpha_k) & b + \lambda_k sin(\alpha_k)cos(\alpha_k) \\ b + \lambda_k sin(\alpha_k)cos(\alpha_k) & c + \lambda_k sin^2(\alpha_k) \end{bmatrix}, \tag{3.37}$$

and, according to (3.22), for the new set of eigenvalues we obtain

$$\widetilde{\mu}_{1,2} = \frac{\widetilde{a} + \widetilde{c} \pm \sqrt{(\widetilde{a} - \widetilde{c})^2 + (2\widetilde{b})^2}}{2}. \tag{3.38}$$

Considering the new elements of (3.38), the first important term to be considered is

$$\widetilde{a} + \widetilde{c} = a + c + \lambda_k \tag{3.39}$$

and the second key term is

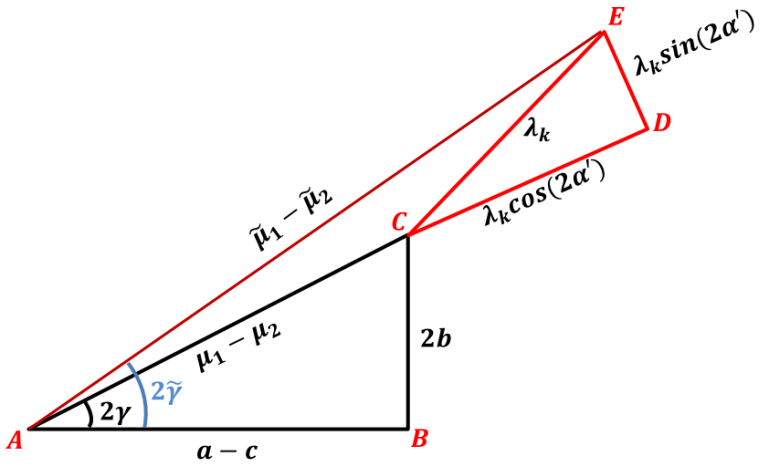

Figure 3.2: A schematic presentation of the effect due to the addition of a new beacon on the FIM structure.

$$(\widetilde{a}-\widetilde{c})^2-(2\widetilde{b})^2=(a-c+\lambda_k\cdot cos(2\alpha_k))^2+(2b+\lambda_k\cdot sin(2\alpha_k))^2$$
$$=(\mu_1-\mu_2+\lambda_k\cdot cos(2(\alpha_k-\gamma)))^2+(\lambda_k\cdot sin(2(\alpha_k-\gamma)))^2. \quad (3.40)$$

Consequently

$$\widetilde{\mu}_{1,2}=\frac{\mu_1+\mu_2+\lambda_k}{2}$$
$$\pm\frac{\sqrt{(\mu_1-\mu_2+\lambda_k\cdot cos(2(\alpha_k-\gamma)))^2+(\lambda_k\cdot sin(2(\alpha_k-\gamma)))^2}}{2}. \quad (3.41)$$

The computation of $\widetilde{\gamma}$ can be derived analytically by means of (3.29). However, it is also simple to be computed by means of the geometrical interpretation. From (3.41), it can be noticed that the addition of a new beacon causes a growth of $\lambda_k\cdot cos(2\alpha'_k)$ ($\alpha'_k=\alpha_k-\gamma$) in the direction of $\mu_1-\mu_2$ ($\mu_1-\mu_2+\lambda_k\cdot cos(2\alpha'_k)$) and a growth of $\lambda_k\cdot sin(2\alpha'_k)$ in the orthogonal direction (the right triangle ADE in Fig. (3.2)). To shed more light on this, we observe also an angular growth of $arctan(\frac{\lambda_k\cdot sin(2\alpha'_k)}{\mu_1-\mu_2+\lambda_k\cdot cos(2\alpha'_k)})$ in the previous angle 2γ leading to the new angle $2\widetilde{\gamma}$. Consequently, the new rotation

angle (after addition of a new beacon) can be computed as

$$2\widetilde{\gamma} = 2\gamma + arctan(\frac{\lambda_k \cdot sin(2\alpha'_k)}{\mu_1 - \mu_2 + \lambda_k \cdot cos(2\alpha'_k)}), \tag{3.42}$$

and therefore

$$\widetilde{\gamma} = \gamma + \frac{1}{2} \cdot arctan(\frac{\lambda_k \cdot sin(2\alpha'_k)}{\mu_1 - \mu_2 + \lambda_k \cdot cos(2\alpha'_k)}). \tag{3.43}$$

If we focus on the new formulation of SPEB, we will have

$$\begin{aligned} \tilde{SPEB} &= \frac{1}{\widetilde{\mu}_1} + \frac{1}{\widetilde{\mu}_2} \\ &= \frac{\widetilde{\mu}_1 + \widetilde{\mu}_2}{\widetilde{\mu}_1 \widetilde{\mu}_2} \\ &= \frac{\mu_1 + \mu_2 + \lambda_k}{\mu_1\mu_2 + \lambda_k(\mu_2 + (\mu_1 - \mu_2)sin^2(\alpha'_k))}. \end{aligned} \tag{3.44}$$

There are some nice theoretical conclusions resulting from the above-mentioned formulations [54, 52]. The minimum in the new SPEB formulation occurs when $\alpha_k = \gamma \pm \frac{\pi}{2}$ and is given by

$$\tilde{SPEB}_{min} = \frac{\mu_1 + \mu_2 + \lambda_k}{\mu_1(\mu_2 + \lambda_k)}. \tag{3.45}$$

In this case, the received RII from a new beacon is along the direction of the eigenvector corresponding to μ_2. On the other hand

$$\tilde{SPEB}_{max} = \frac{\mu_1 + \mu_2 + \lambda_k}{\mu_2(\mu_1 + \lambda_k)} \tag{3.46}$$

and this is the case when $\alpha_k = \gamma$, i.e. the received RII from the new added beacon is along the direction of the eigenvector corresponding to μ_1. In conclusion, a target should select the beacon which has strong intensity and a position close to the minor axis of information ellipse associated to the previously present beacons.

3.2 The Cramer Rao Bound for tracking scenarios

The conventionally referred CRB is a lower bound for MSE of a unbiased estimator that is deterministic but generally unknown. However, in tracking scenarios, our state vector is repeatedly changing and can be treated as a random variable. Consequently, a Bayesian estimator will be required and, consequently, the lower bound will depend on the evaluation of a posteriori probability density function. As in the case of classical CRB, the assumption about statistical distribution related to the noise term is of great importance in the computation of the related lower bound. This lower bound for the first time was investigated in [46] and it is also known as PCRB. However, the introduced lower bound does not have a recursive nature [32]. The works [32, 39] provide a recursive computation of the PCRB from one time step to the next.

Coming back to (2.15) and (2.16), describing dynamic nature of a nonlinear time varying system, the goal of PCRB is to find a lower bound for the covariance matrix related to the unbiased estimates of vector parameters, i.e.

$$\mathbf{P}_n = E\left\{ [\hat{\mathbf{x}}_n - \mathbf{x}_n] [\hat{\mathbf{x}}_n - \mathbf{x}_n]^T \right\} \geq {\mathbf{J}_n}^{-1}, \tag{3.47}$$

let us assume $P(\mathbf{X}_n, \mathbf{Z}_n)$ be the joint probability distribution of $\mathbf{X}_n$=$\left[\mathbf{x}_0{}^T\ \mathbf{x}_1{}^T \dots \mathbf{x}_n{}^T\right]^T$ and $\mathbf{Z}_n = \left[\mathbf{z}_0{}^T\ \mathbf{z}_1{}^T \dots \mathbf{z}_n{}^T\right]^T$ for an arbitrary n. By separating $\mathbf{X}_n$ as $\left[\mathbf{X}_{n-1}{}^T\ \mathbf{x}_n{}^T\right]^T$, Fisher information matrix $\mathbf{J}(\mathbf{X}_n)$ can be written as

$$\begin{aligned}\mathbf{J}(\mathbf{X}_n) &\triangleq \begin{bmatrix} \mathbf{A}_n & \mathbf{B}_n \\ \mathbf{B}_n{}^T & \mathbf{C}_n \end{bmatrix} \\ &= \begin{bmatrix} E\left\{-\boldsymbol{\Delta}^{\mathbf{X}_{n-1}}_{\mathbf{X}_{n-1}} \log(P(\mathbf{X}_n, \mathbf{Z}_n))\right\} & E\left\{-\boldsymbol{\Delta}^{\mathbf{x}_n}_{\mathbf{X}_{n-1}} \log(P(\mathbf{X}_n, \mathbf{Z}_n))\right\} \\ E\left\{-\boldsymbol{\Delta}^{\mathbf{X}_{n-1}}_{\mathbf{x}_n} \log(P(\mathbf{X}_n, \mathbf{Z}_n))\right\} & E\left\{-\boldsymbol{\Delta}^{\mathbf{x}_n}_{\mathbf{x}_n} \log(P(\mathbf{X}_n, \mathbf{Z}_n))\right\} \end{bmatrix},\end{aligned} \tag{3.48}$$

where $\boldsymbol{\Delta}^{\boldsymbol{\Lambda}}_{\theta}$ is defined as

$$\boldsymbol{\Delta}^{\theta}_{\boldsymbol{\Lambda}} = \nabla_{\boldsymbol{\Lambda}} \nabla_{\theta}{}^T \tag{3.49}$$

with $\nabla_\theta = [\frac{\partial}{\partial\theta_1}, \dots, \frac{\partial}{\partial\theta_r}]^T$.

Of course, we are interested in the information sub-matrix of FIM ($\mathbf{J}(\mathbf{X}_n)$) related to $\mathbf{x}_n$, i.e. $\mathbf{J}_n$ by which we will be able to define a lower bound for MSE of the unbiased estimate vector at time step n i.e. $\hat{\mathbf{x}}_n$. Using Schur's complement characteristics [32]

$$\mathbf{J}_n = \mathbf{C}_n - \mathbf{B}_n{}^T \mathbf{A}_n{}^{-1} \mathbf{B}_n. \tag{3.50}$$

As it is observable, the last equation has not a recursive nature. In [32], the authors propose the computation of $\mathbf{J}_n$ recursively via

$$\mathbf{J}_{n+1} = \mathbf{D}_n^{22} - \mathbf{D}_n^{21} \left(\mathbf{J}_n + \mathbf{D}_n^{11}\right)^{-1} \mathbf{D}_n^{12} \tag{3.51}$$

where

$$\mathbf{D}_n^{11} = E\left\{-\boldsymbol{\Delta}_{\mathbf{x}_n}^{\mathbf{x}_n} \log(P(\mathbf{x}_{n+1}|\mathbf{x}_n))\right\}, \tag{3.52}$$

$$\mathbf{D}_n^{12} = E\left\{-\boldsymbol{\Delta}_{\mathbf{x}_n}^{\mathbf{x}_{n+1}} \log(P(\mathbf{x}_{n+1}|\mathbf{x}_n))\right\}, \tag{3.53}$$

$$\mathbf{D}_n^{21} = E\left\{-\boldsymbol{\Delta}_{\mathbf{x}_{n+1}}^{\mathbf{x}_n} \log(P(\mathbf{x}_{n+1}|\mathbf{x}_n))\right\}, \tag{3.54}$$

and

$$\mathbf{D}_n^{22} = E\left\{-\boldsymbol{\Delta}_{\mathbf{x}_{n+1}}^{\mathbf{x}_{n+1}} \log(P(\mathbf{x}_{n+1}|\mathbf{x}_n))\right\} + E\left\{-\boldsymbol{\Delta}_{\mathbf{x}_{n+1}}^{\mathbf{x}_{n+1}} \log(P(\mathbf{z}_{n+1}|\mathbf{x}_{n+1}))\right\}. \tag{3.55}$$

In [39], authors investigate the closed form of (3.52)-(3.55) using the same linear system model of EKF. Final version of the recursive procedure can be computed as

$$\mathbf{J}_{n+1} = \mathbf{H}_{n+1}{}^T \mathbf{R}_{n+1}{}^{-1} \mathbf{H}_{n+1} + \left(\mathbf{Q}_n + \mathbf{A}_n \mathbf{J}_n{}^{-1} \mathbf{A}_n{}^T\right)^{-1}. \tag{3.56}$$

Let us remark that A and H are linearized process and measurement function

Table 3.1: a summary of different localization scenarios considered in this thesis

Downlink (DL)	B.tx	B.rx	T.tx	T.rx	active / passive	Alg. computation	Ranging measure
DL1	•			•	active	B,T/C,D	TOA
DL2	•			•	passive	B/C,D	TOA
DL3	•			•	relay	B/C,D	TOA
Uplink (UL)							
UL1		•	•		active	B/C,D	TOA
Two way ranging (TWR)							
TW1	•	•	•	•	active	B,T/C,D	TOA

respectively and Q, R are covariance matrices related to the process and measurement noises.

3.3 Reference scenarios

Table 3.1 presents a summary of the considered localization scenarios in this thesis. The acronyms Downlink (DL) and Uplink (UL) describe the way of communication between target and beacons, i.e. the way that they point out communication from beacon to target and vice versa respectively. The technique Two Way Ranging (TWR) has been described in Sect. 2.3.1.3. The letters B and T indicate the role of beacons and target in the localization scenario respectively. The suffices tx and rx indicate that the related entities, either at beacons or targets, act as transmitter or receiver respectively. The letters C and D reveal the centralized or distributed nature of the localization algorithm that can be applied (see also Sect. 2.3.2).

Considering the previously defined abbreviations in table 3.1, we can specify the following categories for an active localization scenario:

- Beacons act as transmitters while the target acts as receiver. Consequently,

the localization algorithm has a centralized nature and it is implemented at the target.

- The target performs as a transmitter and the beacons act as receivers. As a result, localization algorithms can be either centralized or distributed and they are implemented at the beacons.

- Both target and beacons act as transmitters and receivers in the context of TWR. Obviously, localization algorithms can have a centralized nature in one node (either target or beacons) or a distributed nature at the beacons or also with some shared tasks between target and beacons.

Subsequently, this classification can be specified for passive localization scenarios:

- The transmitted signal from one beacon, after being reflected from the target acting as a passive scatterer or a device enabled with backscattering mechanism, is received by another beacon. As a result, the localization algorithm can be implemented either in a centralized or a distributed version at the beacons.

CHAPTER IV

Energy efficient algorithms for passive localization scenarios

Reliable position information, obtained with a reasonable complexity overhead and possibly low energy consumption, is necessary for a successful operation of a WSN. This chapter investigates algorithms for passive localization scenarios respecting energy efficiency issues.

In Sec. 4.1, the PCRB revised in Sect. 3.2 is applied for analyzing theoretically the performance of the tracking systems proposed in [37] in order to achieve a trade-off between localization performance and the ratio between regenerative and non-regenerative steps. As a result, it is concluded that non-regenerative steps during tracking is an effective way for realizing interesting energy savings.

Sec 4.2 investigates two ways for improving performance of passive tracking:

1. use of a-priori information for enhancing ranging quality;

2. hybrid tracking achieved by a combination of standard EKFs and fingerprinting techniques based on different channel signatures.

In fact, due to structure of soft ranging, which can take advantage of some a-priori information about cluster parameters, the use of a-priori information can improve the

ranging measure, hence leading to a better localization performance. More importantly, the proposed hybrid tracking technique composed of a fingerprinting stage and its fusion with the measures resulting from EKFs shows a remarkable performance enhancement in all the cases with a single target. On the other hand, in the scenarios with more than one target and passive localization, performance, even if improved, remains unsatisfactory in a large percentage of cases because of the ambiguities in associating the ranging measures to the different targets especially at critical points when the targets intersecting each others' trajectory or they are too close. This fact is particularly evident since here each target acts as a passive scatterer as in a typical radar scenario and specific techniques should be adopted for limiting the impact of these ambiguities.

The possible application areas of this type of algorithm are numerous including, e.g., indoor asset localization using low-complexity amplify-and forward devices and monitoring systems. Moreover, these technologies may be used as radio infrastructures for implementing broadband location-based services in environments like railway stations, airports and industrial facilities.

4.1 Analytic evaluation of hybrid localization composed of active and passive phases

The section regards the analysis of the performance bounds of an approach for improving the trade-off between energy consumption and performance in a localization and tracking process. A set of fixed beacons is used for localizing a target that is moving in a limited environment and tracking is realized by mixing active signal transmissions, which allow using standard techniques for deriving distances and locations, as well as passive signal receptions, which exploit scattering caused by the target during signal propagation. Obviously, when the beacons exploit passive signal

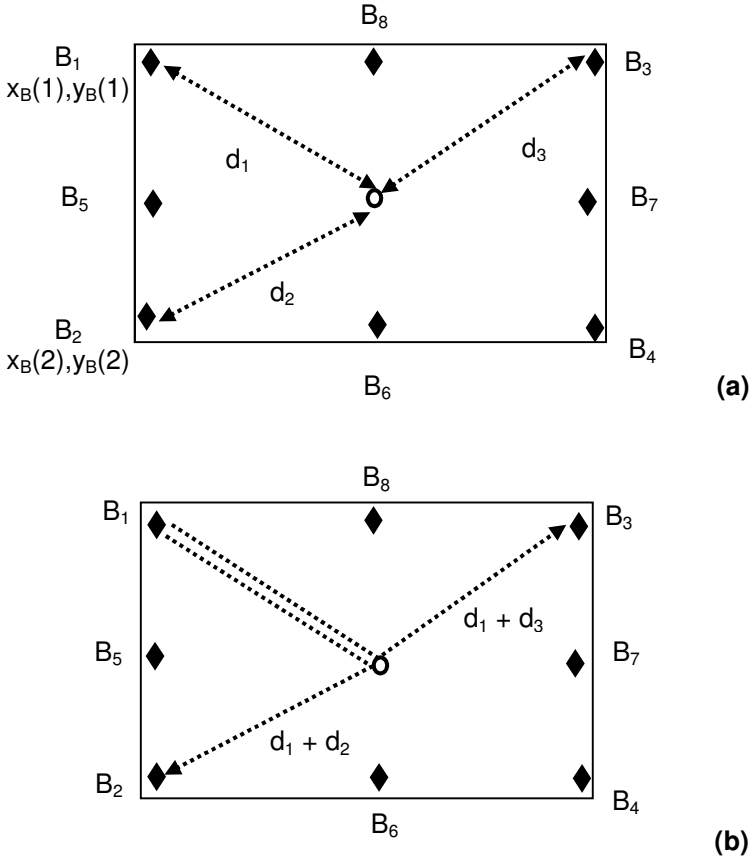

Figure 4.1: System reference scenario with positions of beacons. Combination of regenerative (a) and non-regenerative (b) measures.

reflections, the target does not consume energy, differently from the steps characterized by the active exchange of radio signals.

The principle exploited in the process is simple: the target device alternates phases in which it acts as an active transmitter with signal regeneration (namely, it transmits a specific packet to the beacons for allowing estimation of times of arrival and distances as in Fig. 4.1-a) to phases without signal regeneration in which it acts as a passive scatterer, a backscatterer or a simple relay (Fig. 4.1-b). So, when the target is in a regenerative phase, the i-th beacon estimates the direct distance d_i to the target. On the other hand, when the target is in a non-regenerative phase, each couple of beacons, i and j, is interested in the measure of the reflected or relayed path, $d_i + d_j$ (Fig. 4.1).

We analyze the performance bounds of an algorithm for tracking mobile devices that can behave alternatively as active transmitters and passive scatterers or relays with low signal amplification. The algorithm, originally proposed in [37], can be used for saving energy in small mobile devices, or sensors, extending their limited battery life. Here, we come back to the principle, used in the tracking process, i.e. alternating active and passive transmissions, and we apply PCRB for understanding analytically how effectively this principle constitutes a way for tuning the trade-off between energy consumption and localization performance.

4.1.1 An introduction to the hybrid localization algorithm

The tracking algorithm, described in [37], is composed of regenerative and non-regenerative phases. The difference between these two phases at the beacons is the following: in regenerative phases, the beacons exploit the signal, received from the target, for estimating the corresponding distance while, in the non-regenerative phases, the beacons derive measures based on the total reflected paths between each couple of beacons. The tracking algorithm combine these two types of transmissions by means of an adapted EKF.

Based on what discussed in chapter II, inverse of recursively computed FIM in PCRB computation procedure coincide with estimated a posteriori covariance matrix in EKF. Therefore, the elements required either for EKF procedure or PCRB computation will be the same. In the following, there is a brief description about computation of the aforementioned elements.

In our scenario, the mobile targets move in a delimited area with two-dimensional coordinates (x, y). The set of N_B beacons have known coordinates $(x_B(i), y_B(i))$ $(i = 1, \cdots, N_B)$. Trajectories, randomly extracted for deriving the average MSE (or Root Mean Square Error (RMSE)), respond to different models. Both equations of state transition and measurement describing dynamic nature of the system can be

derived w.r.t the scenario considered in our simulations. In fact, the equation related to state transition is based on the conventional kinematic equation for a constant acceleration object. Therefore, the state transition equation can be written as

$$\mathbf{x_{k+1}} = A_k \mathbf{x_k} + \mathbf{w_k} \tag{4.1}$$

where $\mathbf{x_k} = [x, v_x, a_x, y, v_y, a_y]^T$ is the state vector containing the coordinates, the velocity and the acceleration in both x and y directions. A_k is the state matrix and w_k is a Gaussian noise process with covariance Q_k. If T_S denotes the sampling rate of the process, the state and the covariance matrices can be expressed as [51]

$$A_k = \begin{bmatrix} 1 & T_S & 0.5T_S^2 & 0 & 0 & 0 \\ 0 & 1 & T_S & 0 & 0 & 0 \\ 0 & 0 & 1 & 0 & 0 & 0 \\ 0 & 0 & 0 & 1 & T_S & 0.5T_S^2 \\ 0 & 0 & 0 & 0 & 1 & T_S \\ 0 & 0 & 0 & 0 & 0 & 1 \end{bmatrix} \tag{4.2}$$

and

$$Q_k = \sigma_w^2 \begin{bmatrix} Q_0 & 0 \\ 0 & Q_0 \end{bmatrix} \tag{4.3}$$

with

$$Q_0 = \begin{bmatrix} 1/20T_S^5 & 1/8T_S^4 & 1/6T_S^3 \\ 1/8T_S^4 & 1/3T_S^3 & 1/2T_S^2 \\ 1/6T_S^3 & 1/2T_S^2 & T_S \end{bmatrix}. \tag{4.4}$$

The process is completed by the observation model, i.e. the relation between the observations, the vector $\mathbf{z_k}$, and the state vector and it is defined as

$$\mathbf{z_k} = h(\mathbf{x_k}) + \mathbf{v_k} \tag{4.5}$$

where $\mathbf{v_k}$ is the Gaussian noise with covariance R_k. The linearized measurement matrix H_k depends on the type of step, regenerative or non-regenerative, since the measures are different in the two phases. So, at the k-th update step, the set of measures, accumulated by the ranging phase, is passed to the EKF. In fact, the measures coming from regenerative and non-regenerative steps are subject to different update steps, implemented in the EKFs. If $\{\hat{x}_k^-, \hat{y}_k^-\}$ denotes the predicted coordinates of the target position, the linearized measurement function ($\mathbf{H}_k$) for regenerative (active) phase will be a $N_b \times 6$ matrix and its main elements can be expressed as

$$h_k(i,1) = \frac{\hat{x}_k^- - x_B(i)}{\sqrt{(\hat{x}_k^- - x_B(i))^2 + (\hat{y}_k^- - y_B(i))^2}}$$

$$h_k(i,2) = \frac{\hat{y}_k^- - y_B(i)}{\sqrt{(\hat{x}_k^- - x_B(i))^2 + (\hat{y}_k^- - y_B(i))^2}} \tag{4.6}$$

for the i^{th} beacon.

On the other hand, during non-regenrative(passive) phase, With N_B beacons, we will have $N_M = \begin{pmatrix} N_B \\ 2 \end{pmatrix}$ ranging measures. Accordingly, the linearized measurement function ($\mathbf{H}_k$) for non-regenerative (passive) phase will be a $N_M \times 6$ matrix and its main elements can be stated as

$$
\begin{aligned}
h_k(i,1) &= \frac{\hat{x}_k^- - x_B(c_{i,1})}{\sqrt{(\hat{x}_k^- - x_B(c_{i,1}))^2 + (\hat{y}_k^- - y_B(c_{i,1}))^2}} \\
&+ \frac{\hat{x}_k^- - x_B(c_{i,2})}{\sqrt{(\hat{x}_k^- - x_B(c_{i,2}))^2 + (\hat{y}_k^- - y_B(c_{i,2}))^2}} \\
h_k(i,2) &= \frac{\hat{y}_k^- - y_B(c_{i,1})}{\sqrt{(\hat{x}_k^- - x_B(c_{i,1}))^2 + (\hat{y}_k^- - y_B(c_{i,1}))^2}} \\
&+ \frac{\hat{y}_k^- - y_B(c_{i,2})}{\sqrt{(\hat{x}_k^- - x_B(c_{i,2}))^2 + (\hat{y}_k^- - y_B(c_{i,2}))^2}}
\end{aligned} \tag{4.7}
$$

for the i^{th} pair $\{c_{i,1}, c_{i,2}\}$ of beacons (Fig. 4.1). The other elements of H_k turn out to be zero in both phases of regenerative and non-regenerative.

When a beacon is not transmitting, it is monitoring the received signal and searches for the preambles of the other nodes in the network. When it finds one such preamble, it executes a ranging algorithm for estimating the distance. When the target is in a regenerative phase, it transmits a signal, e.g. a packet with a known preamble and time stamped on it, that is used by the beacons for estimating the N_B distances between the target and the beacons; if we assume that beacons can communicate with each other and cooperate, they can solve the localization problem. During this phase, the mobile target spends an energy E_A, fixed at each active step since we suppose that its transmit power P_T and the packets lengths are constant during the trajectory. When the target is in the non-regenerative phase, the beacons transmit a packet and they receive it after its interaction with the target. In this phase we may distinguish the following cases:

- the target acts as a scatterer and reflected paths are received by all the beacons. This situation may correspond to small targets which can be approximated as scattering points in the environment.

- The target exploits a backscattering mechanism into the transceiver device. In

this case, the target is associated to a device, that can generate a backscattered signal, independently from its size. This has been recently investigated for UWB technology in [47][56].

- The target acts as a relay, which amplifies the signal without regenerating it. Differently from two previously mentioned cases, this case does not correspond to a complete passive phase. Since the target transmits with a power that is equal to $A_R P_R$ where A_R is the fixed relay amplification and P_R is the power received by a beacon. Consequently, the energy spent in this phase is not zero but $E_A \cdot A_R P_R / P_T$. The relay case will not be considered in the numerical results presented in this section.

The necessity of using reflected paths (in non-regenerative phase) between two beacons instead of directly reflected paths (e.g. between each beacon and the target) depends on the fact that each beacon is generally not able to transmit and receive simultaneously; in this application, due to the indoor short distances, the duration of a packet transmission is often much longer than the propagation time. Finally we remark that

- Here, energy savings are referred only to the energy saved by the mobile target since the beacons are supposed to be fixed and without limited battery life.

- in the non regenerative phases, either the energy spent for transmitting or the energy for decoding and other computational tasks is saved at the mobile targets. So, we do not need to separate the amount of energy spent for transmitting from that spent for decoding, usually much lower.

The combination of regenerative and non-regenerative steps corresponds to a predefined pattern characterized by the fraction λ of non-regenerative steps w.r.t. the total one; so, the generic pattern has a period composed by N_{REG} regenerative and

$(1-\lambda)/\lambda \cdot N_{REG}$ non-regenerative steps. Energy savings, when the target power P_T is kept fixed, will be proportional to the factor λ.

4.1.2 Posterior Cramer-Rao Bound for EKF tracking

PCRB has been shown to be the MSE bound for an unbiased sequential Bayesian estimator and methods based on the process linearization can provide the result corresponding to the EKF implementation. Sect. 4.1.3 resumes the CRB bounds on the ranging measures that are the fundamental components of the measure covariance matrix in the PCRB and EKF processes. Then Sect. 4.1.4 presents the steps of the analysis.

4.1.3 Ranging measures covariance matrices

In order to compute the measurement covariance matrix, we use classical CRBs. For Time-of-Arrival (TOA) estimation, the CRB can be expressed as [46]

$$\sigma_{TOA}^2 \geq \frac{1}{8\pi^2 \cdot \beta^2 E_P/N_0} \tag{4.8}$$

where β is the effective bandwidth of the pulse and E_P/N_0 is the signal to noise ratio. E_P is the received energy. There are two options for E_p. The first one is the received energy of the first path. The second one is the total energy if the receiver performs an algorithm for estimating all the relevant paths. There is an average gap (in dB) between these two energies. In our case, the second option is considered. Simply, CRB for ranging distance can be obtained by the product $c^2 \cdot \sigma_{TOA}^2$ where c is the speed of light. The distance between two nodes can also be measured using the received signal strength (RSS) and the CRLB for a distance d_i using RSS can be written as [34]

$$\sigma_{RSS}^2 \geq \left(\frac{ln10}{10}\right)^2 \cdot \left(\frac{\sigma_S d_i}{\gamma}\right)^2, \tag{4.9}$$

where σ_S is the standard deviation of a zero-mean Gaussian random variable describing the log-normal shadowing effect and γ is the path loss exponent factor.

In our scenario, with N_B beacons, the measurement covariance matrix R_k in the regenerative steps is written as a diagonal $(N_B \times N_B)$ matrix with entries equal to $\{\sigma^2_{TOA}(d_1), \sigma^2_{TOA}(d_2), \cdots, \sigma^2_{TOA}(d_{N_B})\}$ while in the non-regenerative ones, with a measure for each of the N_M couple of beacons, R_k is a $(N_M \times N_M)$ diagonal matrix with entries equal to $\{\sigma^2_{TOA}(d_1+d_2), \sigma^2_{TOA}(d_1+d_3), \cdots, \sigma^2_{TOA}(d_{N_B-1}+d_{N_B})\}$. Similar entries are assumed for the RSS case (4.9). The measure variance depends on the total path distance since distance is the factor that affects E_P/N_0 in (4.8) or that appears directly in (4.9). Finally, we remark that, for the validity of the CRB, we focus on unbiased estimates, which correspond to Line-of-Sight (LoS) measures.

4.1.4 PRCB computation for hybrid EKF tracking

The key equations for deriving the Posterior CRB for recursive Bayesian estimation through the updating of the posterior Fisher information matrix have been presented in [13, 45, 32], and in [38, 39, 7] the whole procedure has been realized and applied to radar tracking systems. The estimation of the nonlinear PCRB is computed by means of a linearization that reflects exactly the Extended version of the Kalman filtering. Consequently, the procedure for computing the final localization MSE bound is similar to the EKF iterative procedure but, here, the Fisher information matrix J_k is the object of the recursion. In fact, when the process and the observation models are described by the linear equations (4.1) and (4.5), it can be shown that

$$J_{k+1} = H^T_{k+1} \cdot R^{-1}_{k+1} \cdot H_{k+1} + (Q_k + A_k \cdot J^{-1}_k \cdot A^T_k)^{-1}. \tag{4.10}$$

The estimator CRB turns out to be the covariance

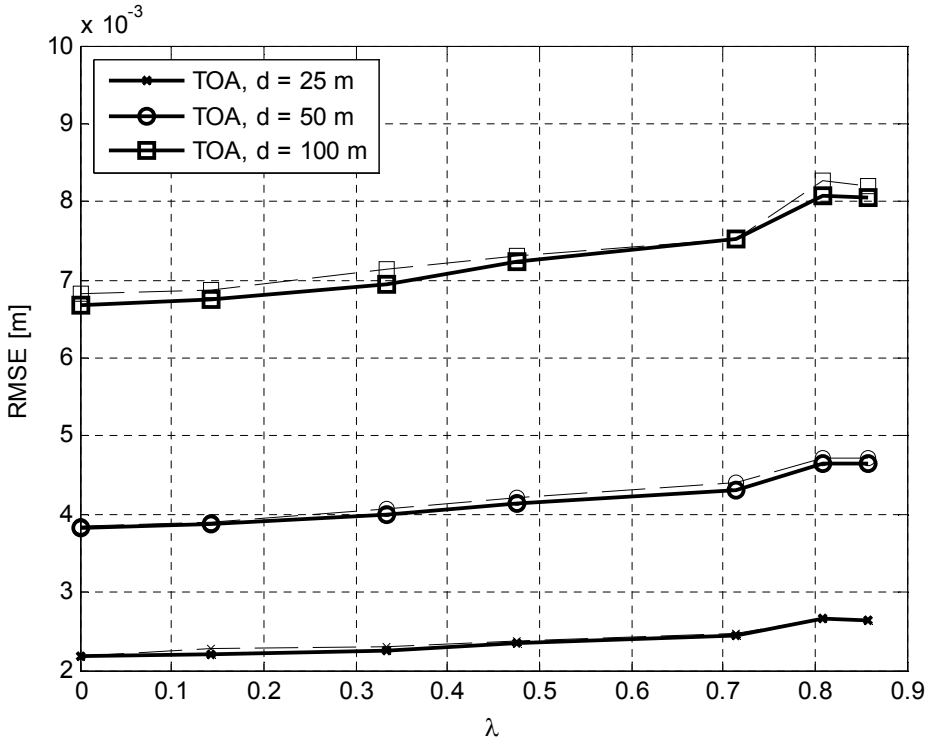

Figure 4.2: RMSE as a function of λ for TOA-based localization and different room sides d. The dashed curve are the simulations, reported here as a verification for the analytical PCRB results (continuous lines).

$$E[(\widehat{\mathbf{x}}_\mathbf{k} - \mathbf{x}_\mathbf{k}) \cdot (\widehat{\mathbf{x}}_\mathbf{k} - \mathbf{x}_\mathbf{k})^T] \geq J_k^{-1}. \tag{4.11}$$

The overall iterative procedure starts from an initial estimate

$$J_0 = E[-\nabla_{\mathbf{x_0}} \nabla_{\mathbf{x_0}}^T ln(p(\mathbf{x_0}))] = \begin{bmatrix} \sigma_I^{-2} & 0 & \cdots & 0 \\ 0 & \sigma_I^{-2} & \cdots & 0 \\ 0 & 0 & \cdots & 0 \\ 0 & 0 & \cdots & \sigma_I^{-2} \end{bmatrix} \tag{4.12}$$

where σ_I^2 is the error variance on the initial state vector and the probability density function $p(\mathbf{x_0})$ is assumed Gaussian.

4.1.5 Evaluation of PCRB

Numerical results will be focused on the relation between the localization error (i.e. the difference ϵ between estimated and correct points at each algorithm step) and the factor λ for fixed performance conditions. Performance is expressed by the position RMSE, derived by the PRCB analysis (Sect. 4.1.2), and by simulations, based on the standard EKF. The computations and simulations have been carried out in square rooms with variable side of d m and the number of beacons is fixed to the symmetric configuration $N_B = 4$ at the room corners for all figures except for Fig. 4.6 where N_B varies from 3 to 8. Both procedures achieve the RMSE estimate by averaging 100 different trajectories starting from the room center and corresponding to the constant acceleration model perturbed by the Gaussian noise process with covariance (4.3) and $\sigma_w = 0.4\ m/s^2$ for both x and y coordinates. Simulated trajectories have $20 - 100$ time samples according to the room side d, and a sample interval $T_S = 0.5$ s for a total observation time equal to $30 \cdot d/25$ s (scaled w.r.t. the room side). The measurement data are generated by adding the measurement noise, assumed to be a white random variable with zero mean and standard deviation given by the CRBs for ranging measures resumed in Sect. 4.1.3. The initial estimation of the target position is subject to a Gaussian error with $\sigma_I = 0.1$ m for TOA and 1 m for RSS. Here only passive non-regenerative steps are considered (i.e. no relays are used).

The physical parameters of the transmission are taken from the UWB technology. The standard pulse has a reference bandwidth of 512 MHz and the propagation exponent changes from a favorable value $\gamma = 1.63$ (according to residential LoS UWB channel model) to a more severe $\gamma = 4$. Each receiver noise figure is fixed to 7 dB and each node (beacon or target) has a transmission spectral power density equal to $-41.3 + \Delta E_T$ dBm/MHz where ΔE_T can vary in order to compare the systems at the same RMSE and obtain a fair comparison among the energy saving options (in terms of λ).

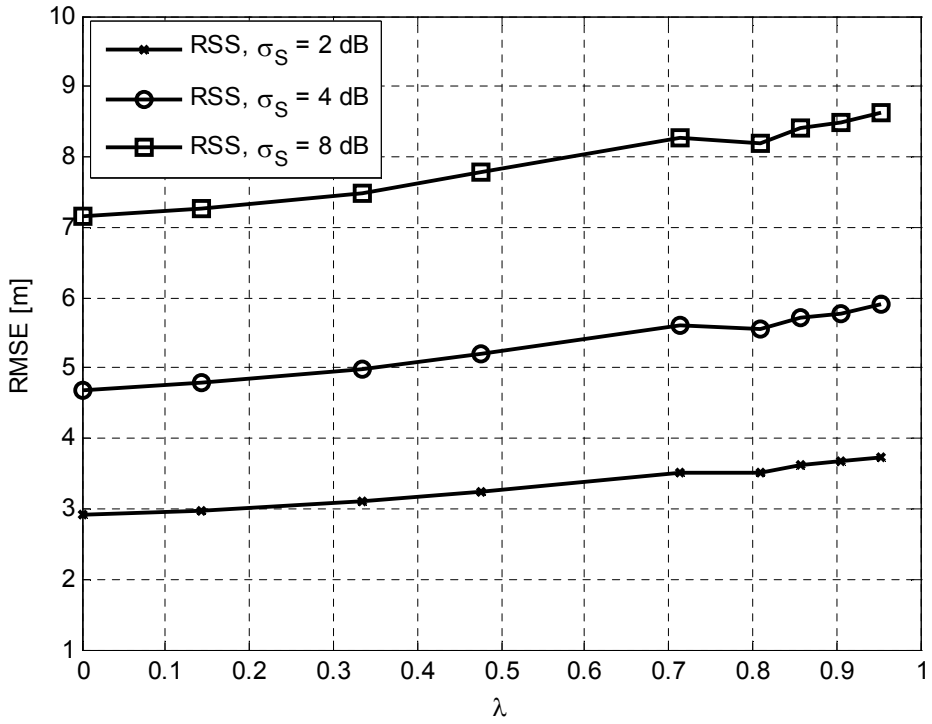

Figure 4.3: RMSE as a function of λ for RSS-based localization and different shadowing root mean squares σ_S ($d = 25$ m)

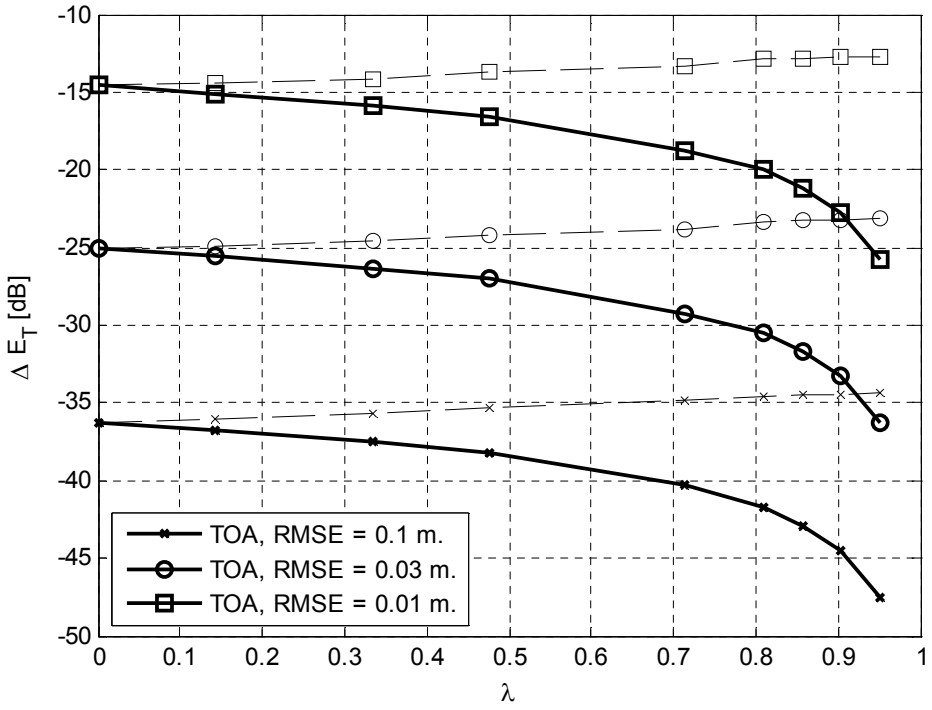

Figure 4.4: Total energy savings as a function of λ for TOA-based localization (bold lines). Dashed lines are the increase of energy in the regenerative steps for keeping the output RMSE fixed. $B_W = 512$ MHz, $d = 25$ m.

The channel path loss parameters and the transmit power spectral density are used for computing the CRB of the ranging measures according to (4.8): in fact the signal-to-noise ratio depends on the transmitted power, on the distance and on the corresponding path loss.

The numerical results are divided into two groups, the first category (Figs. 4.2-4.3) reporting the RMSE as a function of λ for several parameter selections in order to see the impact of non-regenerative step on performance and also for comparing analytical with simulative results, and the second category (Figs. 4.4-4.6) reporting the transmit target energy reduction ΔE_T that can be achieved by fixing the output RMSE as a function of λ. In Figs. 4.2-4.3, we can observe the RMSE for TOA and RSS based localization systems respectively for different d and channel parameters and the curves reveal a slight RMSE increase as λ approaches 1. In the plots, $\lambda = 0$, or absence of non-regenerative steps, can be considered as the reference performance point.

Figs. 4.4-4.6 reveal the amount of energy savings realized by the different regenerative and non-regenerative patterns keeping the RMSE and hence the output performance fixed in order to realize a more significant comparison. The factor ΔE_T [dB] is the reduction of the target transmitted energy that takes into account two contributions: the increase of energy spent during the regenerative steps for compensating the performance reduction due to the λ increase and the decrease of energy obtained from the fraction of non-regenerative steps, proportional to λ.

The main result of this analysis is that the hybrid technique turns out to be effective in the extension of the energy savings as λ increases without loss in the output performance, as can be seen in Fig. 4.4 for different target RMSE. This kind of energy gap turns out to be present for all the variations of the main parameters used in the reference scenario: the room side d and the signal bandwidth B_W (Fig. 4.5) affect the signal attenuation and the TOA resolution respectively, the number

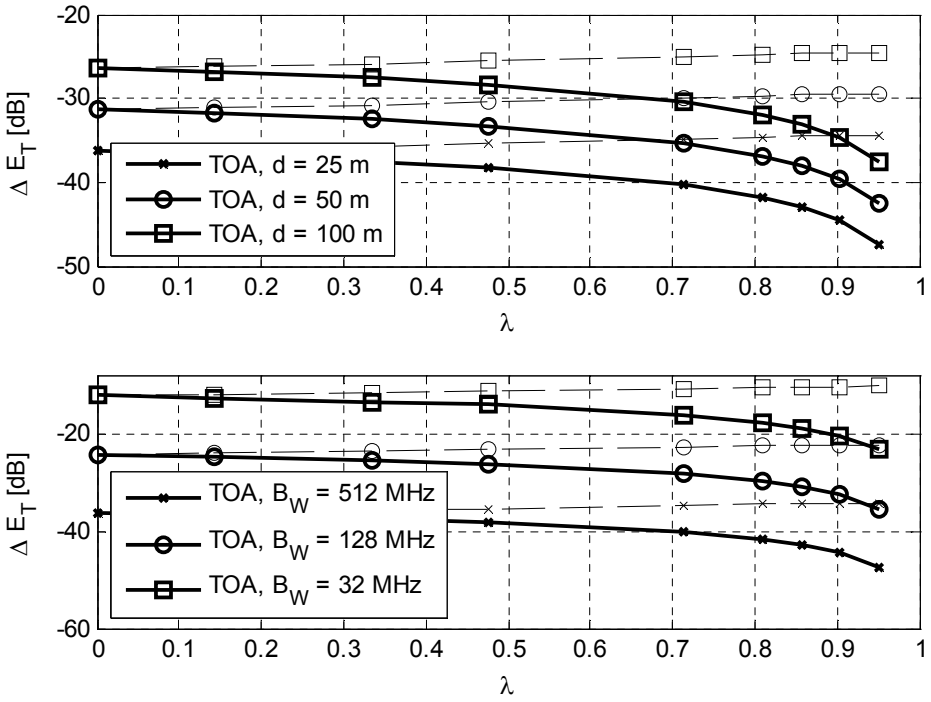

Figure 4.5: Total energy savings as a function of λ for TOA-based localization (bold lines) and different B_W or d. Dashed lines are the increase of energy in the regenerative steps for keeping the output RMSE fixed. $RMSE = 0.1$ m, $B_W = 512$ MHz (top), $d = 25$ m (bottom).

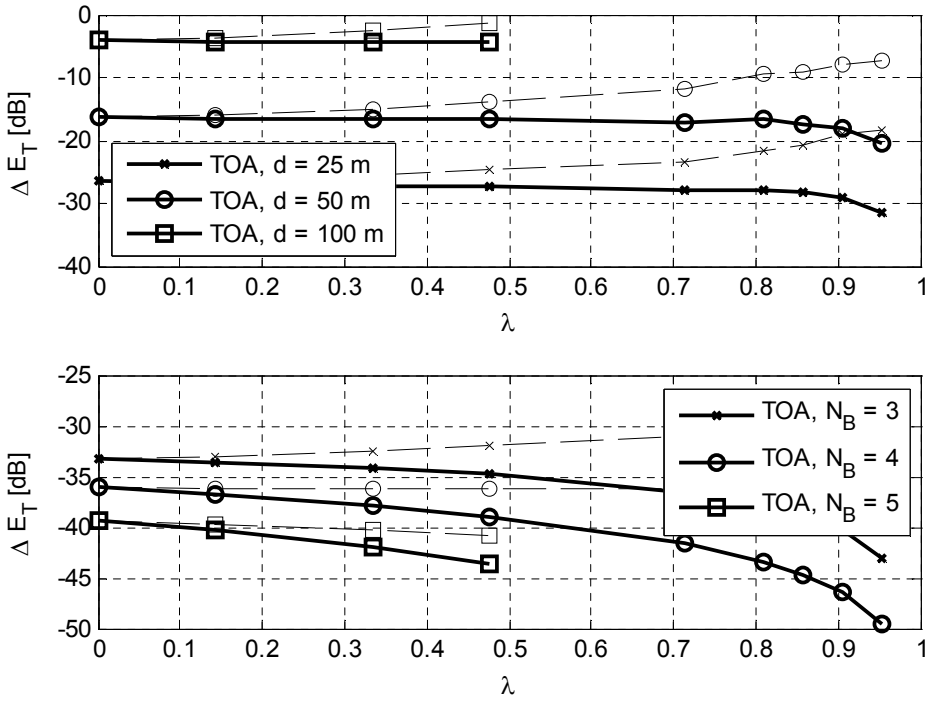

Figure 4.6: Total energy savings as a function of λ for TOA-based localization (bold lines) and different numbers of beacons (bottom) or severe path loss exponent ($\gamma = 4$, top). Dashed lines are the increase of energy in the regenerative steps for keeping the output RMSE fixed. $RMSE = 0.1$ m, $B_W = 512$ MHz, $d = 25$ m (bottom).

of beacons has an impact on the localization precision (Fig. 4.6), the propagation exponent γ affects the signal-to-noise ratio. In all the cases, the potential energy savings w.r.t. the all regenerative tracking ($\lambda = 0$) vary, when $0.5 < \lambda < 1$, from 1 to about 10 dB for low $\gamma = 1.63$ and from 0 to about $4 - 5$ dB for higher $\gamma = 4$.

4.2 A hybrid tracking algorithm composed of FP and EKF based tracking

The focus of this section is on passive signal reception exploiting scattering caused by target(s) during signal propagation. Here, a combination of fingerprinting (FP) and tracking is investigated in order to tackle conventional problems related to implementation of either tracking or fingerprinting separately. One of the common

drawbacks of FP belongs to large data size and consequent large search space as a result of either vastness of surveillance area or finer grid resolution in FP grid map which limits the application of FP to small environments or scenarios with largely spaced grid points leading to poor localization performance. By taking advantage of latest position estimate gotten from EKF, a Virtual Surveillance Area (VSA) is defined around the estimate. The dimension of this defined surveillance area is much smaller than the size of indoor environment. Consequently, there will be a possibility for FP to be applied in larger areas maintaining the possibility of adding necessary grid points in order to achieve a desired localization performance.

The second aspect of the scheme deals with the critical concern when tracking more than one passive target, i.e. to make the correct discrimination among measures as a result of occurred ambiguity in paths clusters scattered by different targets especially when targets are moving close to each other. This issue is alleviated by applying a hybrid tracking technique composed of the fusion of FP measure with the measure resulting from EKF inside the aforementioned VSA. Of course, this is also applicable for tracking one target with improved performance. In addition, in order to improve accuracy of ranging, we investigate the impact of the knowledge of a-priori information related to the clusters impulse responses and other features; the ranging algorithm for time of arrival (TOA) estimation, based on our previously presented algorithm called soft, is modified in order to take advantage of this a-priori information and to make its decision variables more accurate. Consequently, there will be more precise ranging measures passed through EKF update steps. Simulation results show a promising performance improvement via using the proposed hybrid tracking technique and applying a-priori information to soft ranging. The trade off is along a reasonable increased implementation complexity.

The main core of the applied tracking strategy is based on [25], which is realized by passive signal receptions that exploit diffused reflections caused by the target(s)

(as a passive small scattering object or by means of a backscattering process) during signal propagation. Here, we focus on indoor environments where a set of static nodes, called beacons, is used for localizing one or more targets moving in a limited area. The ranging process at each receiving beacon derive measures based on the total reflected paths between each couple of beacons. The tracking algorithm is done by means of a bank of Extended Kalman Filters (EKFs) and by managing available multiple measures in an appropriate manner. In each EKF update step, time of arrival (TOA) ranging measures resulting from soft ranging (SR) algorithm [29] is applied. *Soft* ranging outputs a vector of distances with associated likelihoods, instead of a single distance estimate and hence it is well-suited to perform multiple hypothesis testing with a multi-filter system for tracking multiple objects. In [28] and [24], a static version of the problem is considered and an algorithm based on Lagrangian relaxation is proposed to solve it.

Here the goal is to to deal with commonly addressed problem related to FP and tracking by proposing a combination of tracking and FP with a fusion mechanism between measures resulting from tracking and FP separately. One of the disadvantages related to FP online phase is the large data size depending on the size of the area under surveillance or on the large number of FP grid points for having better position estimates. This issue limits FP application to small indoor environments or larger areas with largely spaced grid points. To circumvent this drawback, the proposed algorithm defines a VSA around the latest estimate gotten from EKF which is much smaller than the original total search area. The FP part of the proposed hybrid algorithm is done over this aforementioned VSA and it is investigated and compared for different signatures, i.e. impulse response, intensity profile, power and duration.

Another contribution is the hybrid tracking method obtained by applying a measure fusion algorithm between measures from the fingerprinting procedure and measures resulting from the EKF inside the defined VSA. It is shown that the proposed

method presents a performance enhancement w.r.t the tracking algorithm proposed in [25] especially when tracking two passive targets, a task made really difficult by the ambiguity in the identification of paths clusters scattered by different targets and received overlapped.

Finally, the performance of tracking algorithm in [25] is investigated under the assumption of soft ranging measures enriched by different a-priori information (impulse response, intensity profile, power and duration like in the FP case) and, consequently, with EKF update steps improved by more accurate ranging measures. To the best of our knowledge, the combined impact of a-priori channel information in ranging and FP has not been investigated before in the literature for passive and active localization. It should be emphasized that the considered tracking scenario in this work is tracking moving devices not transmitting to the beacons, i.e. without energy consumption, since the final objective is to discuss the tracking performance of targets without energy consumption. The proposed hybrid algorithm is applicable for tracking mobile devices that can work as passive scatterers or relays with low or without signal amplification.

4.2.1 Hybrid algorithm structure

The applied scenario in the analysis is constituted by a bi-dimensional square area with $N_B = 4$ beacons in the corners, as sketched in Fig. 4.7 (d is the room side). In this sample configuration presented in Fig. 4.7, there are one or two targets moving along related trajectories. Two distinguished targets are shown with circle and square dots.

Here, targets do not participate in an active exchange of signals except in the initial connection of target(s) to WSN. They act as passive scatterers while beacons cooperate for estimating the distance of the reflected path and execute the tracking algorithm described in Sect. 4.2.2. To shed more light on this, this fact is shown

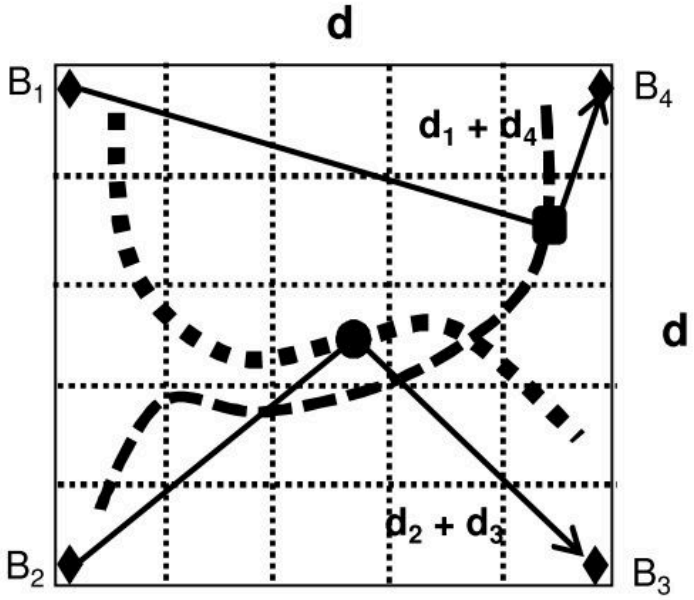

Figure 4.7: A sample presentation of system reference scenario.

in Fig. 4.1 in a way that a sample pair-wise connection among the beacon pairs $(2, 3)$ and $(1, 4)$ is presented for each of the targets shown by circle and square dot respectively.

All simulations are made at baseband and in discrete time using complex baseband-equivalent channel models adopted by the IEEE 802.15.4a working group [3]. These channels are a low-pass filtered tapped delay-line where signal components arrive at the receiver in independent clusters. Given a couple of beacons at locations B_i and B_j, the presence of a scattering device at location P is modeled by adding all the signal paths that are described by the convolution between the channel impulse response from B_i to P and that from P to B_j (ideal point scatterer or relay).

In our model, we assume that impulse responses generated by a target in two different locations are independent if the distance between these two location is greater or equal to a coherence distance d_C. From a practical point of view, the indoor environment is covered by a rectangular grid of points at distances multiple of d_C and

the impulse response of a target in a generic location P is obtained by interpolating 4 independent impulse responses at the corners of the rectangular area that includes P. The rectangular grid map is depicted in Fig. 4.1. Finally, after passing the channel, the signal is affected by additive white Gaussian noise (AWGN) with zero mean.

When a beacon does not transmit, it monitors the received signal and searches for the preambles of the other nodes in the network. When it finds one such preamble, it executes a ranging algorithm for estimating the distance. The necessity of using reflected paths between two beacons instead of directly reflected paths (e.g. between each beacon and the target) depends on the fact that each beacon is generally not able to transmit and receive simultaneously; in this application, due to the indoor short distances, the duration of a packet transmission is often much longer than the propagation time.

4.2.2 Algorithm for Zero Energy Localization

The principle exploited in the process is simple: the localization algorithm incorporates two components, ranging and tracking, which are implemented by soft ranging and a bank of N_{EKF} EKFs. Each couple of beacons, i and j, is interested in the measure of the reflected or relayed path, $d_i + d_j$ (Fig. 4.1). Sect. 4.2.3 elaborates the issue related to providing EKF update step by ranging measures with a-priori information. Sect. 4.2.4 provides a brief review of the basic structure of the tracking strategy based on [25]. Finally the proposed hybrid tracking algorithm is introduced in Sect. 4.2.5.

4.2.3 Ranging with a-priori parameter knowledge

In this work, we use soft ranging algorithm [29], whose output is composed of a discrete vector of likely distances with an associated approximation of the probability that these distances correspond to the estimates. This soft information is also used to

provide a measure of the uncertainty of the distance estimate, i.e., an estimate of the error magnitude; in fact, a large uncertainty is often associated to a NLoS measure or to a measure obtained at low Signal-to-Noise Ratio (SNR). The propagation path length between the beacons over a point scatterer at coordinates $\mathbf{s}$, is

$$d_j(\mathbf{s}) = \|\mathbf{x}_{j,1} - \mathbf{s}\| + \|\mathbf{x}_{j,2} - \mathbf{s}\|, \tag{4.13}$$

where $j = 1, \ldots, N_M$; $N_M = \begin{pmatrix} N_B \\ 2 \end{pmatrix}$. The term $\|\cdot\|$ denotes Euclidean norm, and $\mathbf{x}_{j,1}, \mathbf{x}_{j,2} \in \mathbf{R}^d$ are the transceiver coordinates of the j-th pair in $d = 2$ or $d = 3$ dimension. An estimate $\hat{d}_j(s)$ is given by a cluster time of arrival. In general, each transceiver pair will compute several multipath distance estimates.

The commonly made assumption about soft ranging assumes that nodes have no a-priori channel state information. However, due to the structure of soft ranging in the formation of decision variables for TOA estimation, it is inferred that when a-priori information about some parameters of the signal is available, ranging performance can be improved. The soft ranging is based on the computation of probabilities of presence or absence of signal in a local interval around the early arrived signal paths (P_n is the probability that no signal component is present at correlator offset n in the local interval with $n = 0, \cdots, N_w$). These probabilities are used in combination with the a-priori information for improving the cluster ranging implementation. Without a-priori information, first-path likelihood measure is given by

$$l(n) = (\prod_{j=n-N_w}^{n-1} P_j)(1 - P_n)(1 - \prod_{j=n+1}^{n+N_w} P_j), \tag{4.14}$$

where N_w is the window parameter. So an estimated cluster first-path probability vector $\hat{\mathbf{p}}$ is formed by computing likelihoods $l(n)$ for all correlator offsets in memory, and normalizing to unity for each detected cluster of paths. Soft ranging is easily

suited to the inclusion of a-priori knowledge of some channel parameters for improving the ranging output; the presence of this a-priori information can be exploited for the following cases.

CD The knowledge of the cluster duration allows to substitute in (4.14) the general window N_w with the cluster duration in that area or location N_{CD}.

CP The knowledge of the cluster power is used for improving the estimate of P_n, which is computed through the evaluation of noise and signal power. When no a-priori knowledge is available, the signal power is estimated by averaging some detected paths.

CIP The knowledge of the power associated with each path composing the cluster allows to refine further the previous point, since a probability of cluster presence is computed by exploiting jointly the signal power in each path. Notice that CIP knowledge includes previous CP and CD knowledge.

CIR Here the impulse response of the cluster allows to change the probabilistic assumptions done in [29, 25]; in fact all the received complex samples assume simply a Gaussian distribution with mean value equal to expected signal path and variance given by the noise power. The presence of the cluster is clearly given by the joint probability of these Gaussian variables.

In order to test the potential performance improvement due to ranging with a-priori knowledge of some channel parameters, the numerical results will be obtained by using the ideal knowledge of CD, CP, CIP and CIR respectively. From a practical point of view, the implementation of such a system can be achieved in two sub-optimal ways:

1. by means of the data stored in the FP grid, during the tracking procedure it is possible to recover a set of a-priori channel parameters according to the target

position predicted by the EKFs;

2. by means of an iterative procedure between the soft ranging algorithm and a conventional channel estimation process: after a first soft ranging estimate without a-priori knowledge, an estimate of the channel parameter (CD, CP, CIP or CIR) is done and it is used as a-priori knowledge for a new soft ranging call with the aim of achieving a refined identification of the cluster.

4.2.4 Tracking strategies

4.2.4.1 Track Initialization

The mobility model applied in our simulations corresponds to the EKF equations introduced in (4.1)-(4.5).

In our scenario we assume that:

- the initial position estimate and the identification of the target is performed by exchanging dedicated packets between the beacons and the target. So, the initial connection of the target to the WSN is operated with an active cooperation of the target itself. After this initial step, the target switches off and tracking is performed exploiting scattering caused by the target. This initial "active" phase has the following clear advantage in the sense that the set of beacons not only know the number of targets in the environment but also obtain a precise position estimate of the first trajectory sample.

- When the number of targets is greater than 1, they are initially divided uniformly among all the available N_{EKF} EKFs. So, each target is initially assigned to an equal number of EKFs.

4.2.4.2 Filters Update

Due to the aforementioned nature of soft ranging producing multiple ranging estimates with corresponding likelihoods, there will be a number of more or less likely first cluster-path distance estimates for each beacon pair during each measurement cycle. Consequently, each EKF must select one estimate from each beacon pair in a possibly large number of different estimates with varying likelihood values. A metric is built and updated for selecting the most likely trajectories in a hypothesis tree that is updated at each step of the tracking process. Let us define a selection $\tilde{\mathbf{Z}}_n^{(k)} = [\hat{d}_1^{(k)}, \ldots, \hat{d}_J^{(k)}]$ as a possible set of distance estimates to use for updating the n-th filter at update cycle k. In order to evaluate the merits of this selection and compare it to other different sets of estimates, we want to evaluate the probability $P(\tilde{\mathbf{Z}}_n^{(k)}|\mathbf{r}^{(k)}, \mathbf{X}_n^{(k-1)})$, i.e., the probability that distances in $\tilde{\mathbf{Z}}_n^{(k)}$, conditioned on the received signals $\mathbf{r}^{(k)}$ and the previous filter state $\mathbf{X}_n^{(k-1)}$, are estimates of multi-path distances corresponding to the object currently tracked by filter n. If we assume that the received signals and the last filter state are statistically independent and apply Bayes' rule, we can write:

$$\begin{aligned} P\left(\tilde{\mathbf{Z}}_n^{(k)}|\mathbf{r}, \mathbf{X}_n^{(k-1)}\right) =& \frac{P\left(\mathbf{r}|\tilde{\mathbf{Z}}_n^{(k)}, \mathbf{X}_n^{(k-1)}\right) P\left(\tilde{\mathbf{Z}}_n^{(k)}, \mathbf{X}_n^{(k-1)}\right)}{P(\mathbf{r})P(\mathbf{X}_n^{(k-1)})} \\ =& \frac{P\left(\mathbf{r}|\tilde{\mathbf{Z}}_n^{(k)}\right) \cdot P\left(\tilde{\mathbf{Z}}_n^{(k)}|\mathbf{X}_n^{(k-1)}\right)}{P(\mathbf{r})} \\ =& \frac{P\left(\tilde{\mathbf{Z}}_n^{(k)}|\mathbf{r}\right) \cdot P\left(\tilde{\mathbf{Z}}_n^{(k)}|\mathbf{X}_n^{(k-1)}\right)}{P(\tilde{\mathbf{Z}}_n^{(k)})}. \end{aligned} \tag{4.15}$$

Now, $P(\tilde{\mathbf{Z}}_n^{(k)}|\mathbf{r})$ can be interpreted as the probability that distance estimates in $\tilde{\mathbf{Z}}_n^{(k)}$ really correspond to first cluster-path distances (as opposed to generated by noise or located in the middle of a cluster). This factor can therefore be approxi-

mated by $P(\tilde{\mathbf{Z}}_n^{(k)}|\mathbf{r}) = \prod_{j=1}^{6} \hat{\mathbf{p}}_j^{(k)}(i_j)$ where i_j is the index in $\mathbf{p}_j^{(k)}$ corresponding to the estimate from j-th pair in $\tilde{\mathbf{Z}}_n^{(k)}$. The factor $P(\tilde{\mathbf{Z}}_n^{(k)})$ is a normalization term, while $P(\tilde{\mathbf{Z}}_n^{(k)}|\mathbf{X}_n^{(k-1)})$ can be evaluated by means of the Gaussian assumption used in the motion model of the EKF filters [23]. If we let the estimated a-priori error covariance matrix of the n-th EKF be $\mathbf{S}_n^{(k|k-1)}$, we can write

$$P\left(\tilde{\mathbf{Z}}_n^{(k)}|\mathbf{X}_n^{(k-1)}\right) = \frac{1}{\sqrt{(2\pi)^6 \left|\mathbf{S}_n^{(k|k-1)}\right|}} \cdot \tag{4.16}$$

$$\cdot \exp\left(-\frac{1}{2}(\tilde{\mathbf{Z}}_n^{(k)} - \mathbf{Z}_n^{(k|k-1)})^T \mathbf{S}_n^{(k|k-1)^{-1}} (\tilde{\mathbf{Z}}_n^{(k)} - \mathbf{Z}_n^{(k|k-1)})\right), \tag{4.17}$$

where $\mathbf{Z}_n^{(k|k-1)}$ is a vector of predicted multi-path distances at the n-th EKF. Each EKF in the filter bank has an associated figure of merit $\tilde{\lambda}_n^{(k)}$, that measures how well the n-th filter has tracked its intended target until k-th step in the hypothesis tree. By computing this metric for all possible measurement combinations $\tilde{\mathbf{Z}}_n^{(k)}$, we can select which measurements to use for filter update. The figure of merit for a given measurement combination is given by [25], i.e.

$$\lambda_n^{(k)} = \lambda_n^{(k-1)} - (\tilde{\mathbf{Z}}_n^{(k)} - \mathbf{Z}_n^{(k|k-1)})^T \cdot (\tilde{\mathbf{Z}}_n^{(k)} - \mathbf{Z}_n^{(k|k-1)}), \tag{4.18}$$

where $\lambda_n^{(k-1)}$ is the current figure of merit of the n-th EKF (at start-up all figures of merit are initialized as $\lambda_n^{(0)} = 0$). The term N_M, as previously defined, is the number of measures per target at each EKF update step; $\mathbf{Z}_n^{(k|k-1)}$ is a vector of predicted multipath distances at the n-th EKF. According to the figure of merit defined in (4.18), the following filter assignment and update strategy is applied for a bank of N_{EKF} EKFs: the N_{EKF} measurement combinations and filter states with highest merit are re-assigned to the corresponding filters. This means that an EKF can at any time be re-initialized to a new trajectory.

4.2.5 Hybrid fingerprinting and EKF based tracking

The strategies for passive tracking suffer from several problems related primarily to the low SNR levels and the large delay spread of clusters. Additionally, in case of multiple tracking, the difficulty of associating the measured distances with the correct target and hence the correct EKF is of great importance. In fact, when different targets are close to each other, the presence of multipath creates severe ambiguities since paths clusters, scattered by different targets' overlap, make the correct discrimination among measures very challenging. In order to enhance robustness of the tracking algorithms, we introduce a hybrid tracking algorithm by means of a fusion strategy between two measurements of fingerprinting and the conventional tracking.

As previously mentioned, one of the simplest mapping techniques is the selection of target coordinates based on the coordinates of FP grid point leading to minimum Euclidean distance between measured LD metric and the metric related to that specific FP grid point measured during FP offline phase. To elaborate, let us assume the number of LD measures to be N_M. For the sake of simplicity in mathematical representation, LD metric is assumed to be scalar although extension to the case, where LD parameter is a vector, is straightforward. During the offline phase of FP, the LD metric vector $\mathbf{M_{p_i}}$ $(N_M \times 1)$ is measured at each point of FP grid (p_i) and stored in a database. Consequently, target position is estimated based on minimizing the following Euclidean distance over grid points

$$\underset{\{p_i\}}{\text{Arg min}} \quad \|\mathbf{M} - \mathbf{M_{p_i}}\| \tag{4.19}$$

where $\mathbf{M}$ is the LD metric vector measured in online phase of FP. Here, applied LD metrics are the same parameters related to a-priori information in ranging and can be mentioned from the least to the most effective as

- knowledge of the cluster duration (CD);

- knowledge of the cluster power (CP);
- knowledge of the cluster intensity profile (CIP), i.e. the mean power of the resolvable paths composing the cluster;
- knowledge of the cluster impulse response (CIR), i.e. the amplitudes and phases of the resolvable paths composing the cluster.

A VSA is defined around the latest target position estimate gotten from EKF. Assuming $[\widehat{x}\ \widehat{y}]^T$ as target position estimate, the square surveillance area is defined with four vertices $[\widehat{x}\pm FP_r\ \ \widehat{y}\pm FP_r]^T$ where FP_r is the expansion of surveillance area. The vertex coordinate, exceeding room dimensions in x or y or both axis direction, will be replaced with corresponding room coordinates. Let's assume the number of FP grid points, which fall inside VSA, be $i_x \cdot i_y$ where i_x and i_y are the number of the coordinates of FP grid points along x and y axis respectively. For each of the grid points inside VSA, two Euclidean distances are independently computed. The first distance parameter is related to conventional calculated Euclidean distance (d_{FP}) between measured LD metric and that of stored in FP offline phase. The second distance parameter (d_{EKF}) is the Euclidean distance between target position estimate via EKF and coordinate of each of FP grid points in the surveillance area.

Considering two mentioned Euclidean distances to be computed for each of the grid points, there will be $N_{FP} = i_x \cdot i_y$ values for each of Euclidean distances. For each grid point p_i with the coordinate $[x_{p_i}\ y_{p_i}]^T$ and related FP metric $\mathbf{M_{p_i}}$, two Euclidean distances $d_{FP}^{(i)}$ and $d_{EKF}^{(i)}$ are defined as

$$d_{FP}^{(i)} = \|\mathbf{M} - \mathbf{M_{p_i}}\| \tag{4.20}$$

and

$$d_{EKF}^{(i)} = \left\| \begin{array}{c} \widehat{x} - x_{p_i} \\ \widehat{y} - y_{p_i} \end{array} \right\| \tag{4.21}$$

where $i = 1, \ldots, N_{FP}$.

Assuming a Gaussian distribution and considering the fact that $d_{FP}^{(i)}$ and $d_{EKF}^{(i)}$ are independent, for each grid point p_i, two independent probability metrics i.e. $P_{FP}^{(i)}$ and $P_{EKF}^{(i)}$ can be assigned which are exponential function of two distances $d_{FP}^{(i)}$ and $d_{EKF}^{(i)}$ receptively. It should be mentioned that after computation of probability metrics for all grid points, they are normalized. Afterward, final decision variable is calculated as $P_i = P_{FP}^{(i)} \cdot P_{EKF}^{(i)}$. The grid location with highest P_i will be considered as target position estimate. This estimate will be passed as a-priori estimate to the next EKF update step.

4.2.6 Performance evaluation of hybrid algorithm

The physical parameters of the transmission are taken from the UWB technology. The standard pulse has a reference bandwidth of 512 MHz and the propagation exponent is fixed to a value of $\gamma = 1.79$ according to residential Line-of-Sight UWB channel model (channel model $CM = 1$). Each receiver noise figure is fixed to 7 dB and each node respects the UWB transmission power spectral density of -41.3 dBm/MHz. In this test scenario, we exploit ranging algorithms based on the times of arrival and characterized by soft detection techniques that have demonstrated performance advantages w.r.t. other approaches. Numerical results present the effect of the proposed tracking algorithm on localization error (i.e. the distance ϵ between estimated and correct points at each algorithm step).

The reference scenario is a square room with room side $d = 30m$ and the number of beacons is fixed to $N_B = 4$ at the room corners as a typical localization environment.

Each LoS link is modeled by the IEEE 802.15.4a residential channel models ($CM = 1$). The transmitted signal experiences a channel that is obtained by the convolution between the channel realizations corresponding to the links between beacon a and the target and between the target and the beacon b that is supposed to receive the transmitted signal (in a selected beacon pair (a, b)). This approach provides the approximate impact on the propagation of a target that can be assumed as a small (point) scatterer or as a passive relay without signal amplification (e.g. exploiting backscattering mechanisms). As previously mentioned, the path loss parameters are taken according to residential LoS parameters (i.e. propagation exponents $\gamma = 1.79$ [3]). The path loss model of the overall reflected path is computed in the simulations according to [10]. The number L_{PCK} of pulses in a packet is 32 and all antenna gains are set to 0 dB. At each simulation, the set of 100 trajectories is used for averaging all the location errors. The localization algorithm is supposed to obtain distance measures corresponding to a sampling time $\Delta T = 1$ s on one (two) target(s) moving with a random walk model

$$x_k = x_{k-1} + v \cdot cos(\alpha_k)\Delta T \tag{4.22}$$

$$y_k = y_{k-1} + v \cdot sin(\alpha_k)\Delta T \tag{4.23}$$

with $\alpha_k = \alpha_{k-1} + \delta$ and δ zero mean Gaussian random variable with σ_δ^2 within an observation time equal to 45 s. We will show a set of selected, significant figures reporting the cumulative distribution function (CDF) of the localization error. For simplicity, the ranging technique is referred as $SR{+}APR$ (soft ranging) or $TR{+}APR$ (threshold ranging) with a-priori information $APR = \{CIP, CD, CP, CIR\}$; on the other hand the fingerprinting process, when present in addition to the EKFs bank, is referred as $FP[SG]$ with signature $SG = \{CIP, CD, CP, CIR\}$.

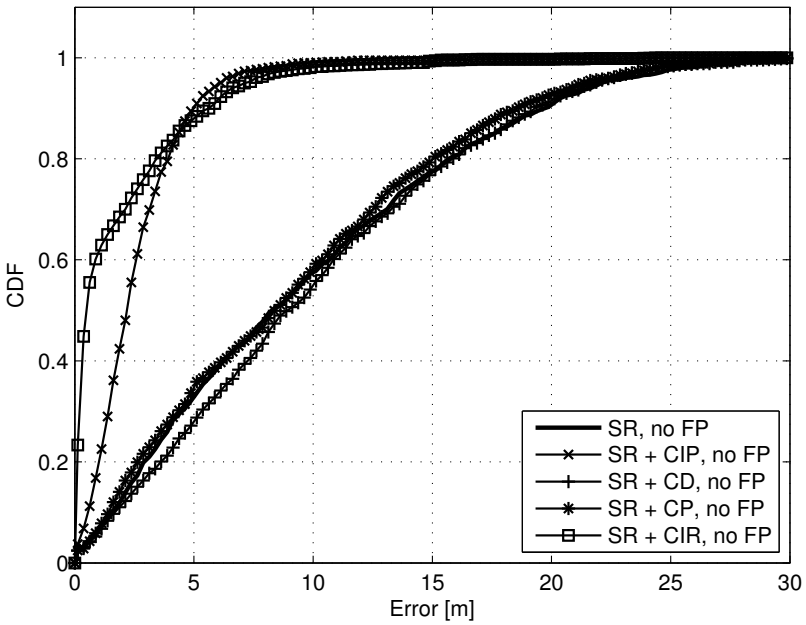

Figure 4.8: CDF of localization error when tracking a single scatterer ($\sigma_\delta = \pi/15$) using soft ranging with one EKF and no FP.

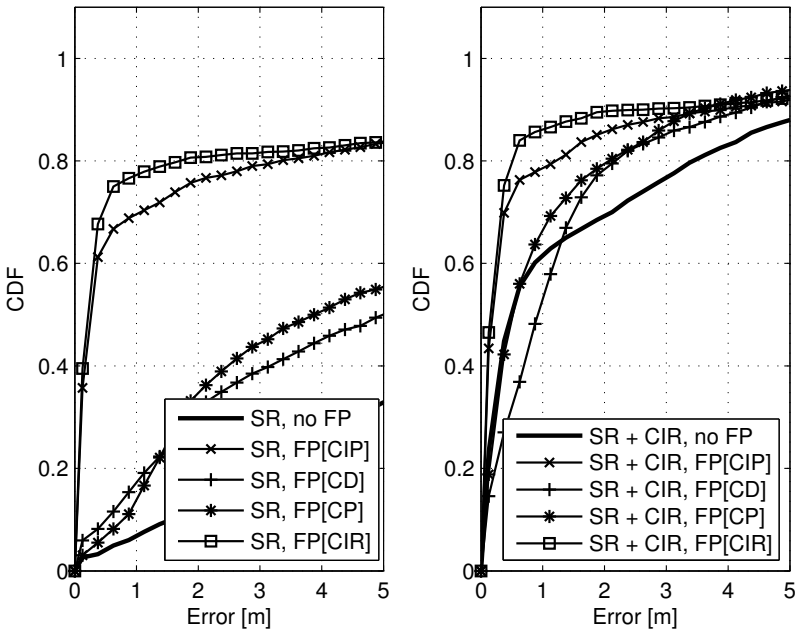

Figure 4.9: CDF plots of localization error when tracking a single scatterer ($\sigma_\delta = \pi/15$) using soft ranging SR or $SR + CIR$ with one EKF and FP.

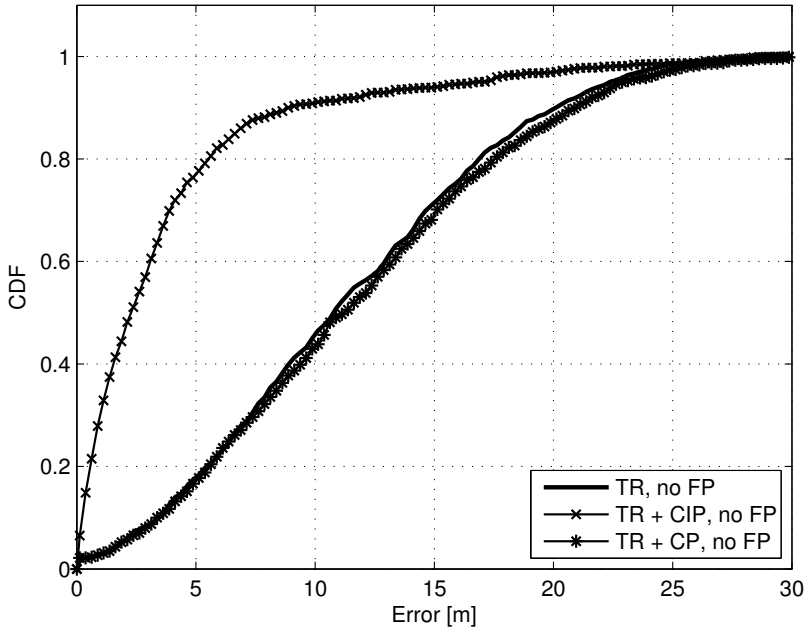

Figure 4.10: CDF of localization error when tracking a single scatterer ($\sigma_\delta = \pi/15$) using threshold ranging with one EKF and no FP.

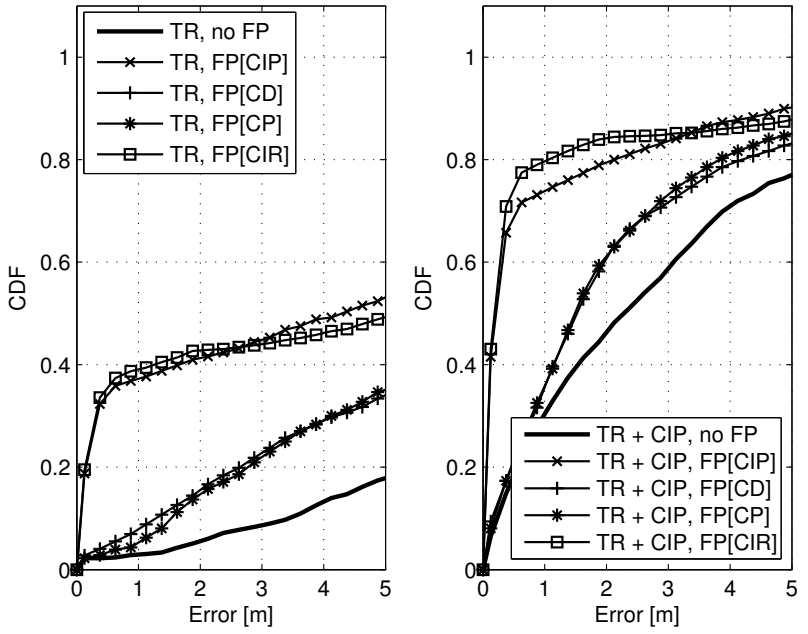

Figure 4.11: CDF plots of localization error when tracking a single scatterer ($\sigma_\delta = \pi/15$) using threshold ranging TR or $TR+CIP$ with one EKF and FP.

Fig. 4.8 depicts the CDF of the distance error for the localization with ranging enriched by a-priori information and without the FP scheme. As expected, using a-priori information related to knowledge of cluster impulse response (CIR) or cluster intensity profile (CIP) shows a relevant advantage since this knowledge allows to increase the amount of received energy available for the cluster identification; little or no advantage can be observed for $SR+CD$ and $SR+CP$ since the ranging algorithm still estimates locally these parameters for detecting its first path. Similar results are obtained for threshold ranging (TR) in which the CIR and CIP cases coincide (Fig. 4.10). On the other hand, Fig. 4.9 presents the error CDFs by using the proposed FP scheme associated to the absence (left) and to the presence (right) of the best a-priori information (CIR in Fig. 4.8). As expected, $FP[CIR]$ and $FP[CIP]$ show the best performance advantage due to taking advantage of cluster complete information i.e. impulse response even if when no a-priori information for ranging is present during tracking. In the error interval of interest, depending on the type of signature, we generally observe a performance improvement that increases with complexity; here also the cases $FP[CP]$ and $FP[CD]$ can provide a remarkable improvement since one of the main performance key factors is the inclusion of the path delay in each FP signature, which provides a windowing effect on the estimated signatures. In fact each point of the grid obviously contains also the distance and hence propagation delay information and this assists the fusion between the outputs of the EKFs and the correct positions. The synergy related to the interaction of the EKF based tracking and the FP process is observable in Fig. 4.9. Also the synergy between a-priori information in ranging and the FP process can be observed comparing the left and right figures in Fig. 4.9. Similar considerations can be derived from the threshold ranging case, reported in Fig. 4.11.

Fig. 4.12 depicts CDF of the distance error obtained from passive tracking of two scatterers without using the FP scheme. As for one target, using a-priori information

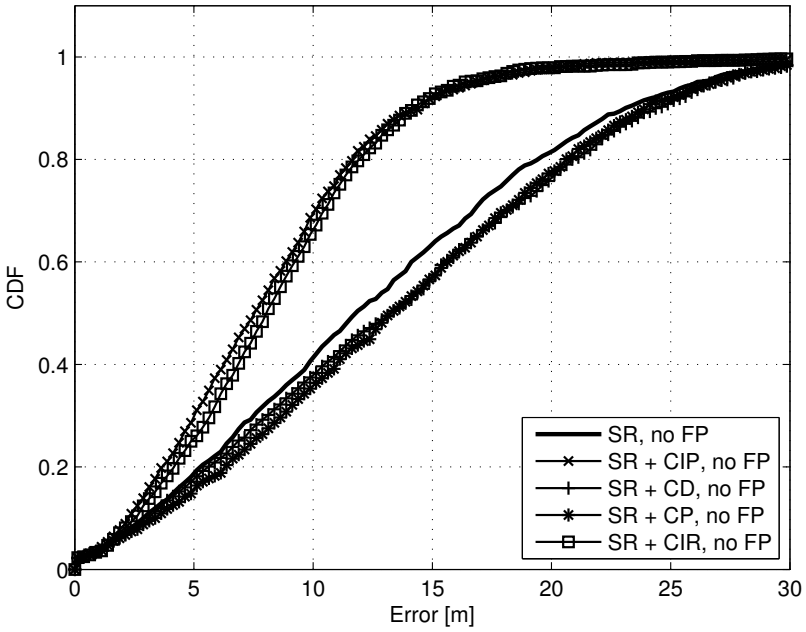

Figure 4.12: CDF plot of localization error when tracking two scatterers ($\sigma_\delta = \pi/15$) using soft ranging with two EKFs and no FP.

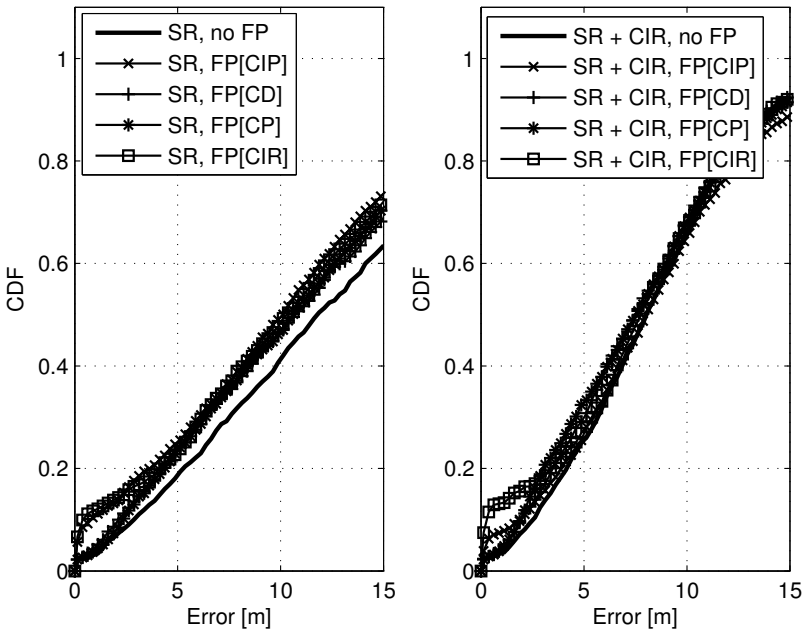

Figure 4.13: CDF plots of localization error when tracking two scatterers ($\sigma_\delta = \pi/15$) using soft ranging SR or $SR + CIR$ with two EKFs and FP.

related to knowledge of CIR and CIP provides an advantage. At the same time, it is clear that when two objects are present in the environment, the average performance is considerably decreased by phenomena of ambiguity between the overlapping cluster signals received by passive reflections by the objects (see Fig. 4.8). Fig. 4.13 presents CDFs of the distance error for two scatterers by using the proposed FP schemes without any a-priori information (left) and with the best CIR a-priori information. Here it is interesting to see that FP provides little advantage in the small error region (when localization is successful without ambiguity) either in absence (left) or presence (right) of SR with a-priori information, pointing the main issue of occurred ambiguity between multiple targets when localization is performed in a passive way. We may conclude that, in the presence of multiple targets and without specific algorithms for solving targets' ambiguity, FP does not provide a relevant advantage since, especially in a small environment, the mutual interference between targets' signals affect negatively the search and association of the signatures; on the other hand, improving the ranging algorithm by using advanced form of a-priori information concerning cluster multipath response or intensity profile gives an important performance improvement since their exact knowledge gives the possibility of distinguishing the different signals.

CHAPTER V

Power allocation algorithms for active localization scenarios

Information about the position of individual nodes, either absolute or in relation to other nodes in the network, is often crucial for a successful fulfillment of the WSN purpose. Accurate ranging and localization is considered as one the crucial applications for wireless sensor networks. This chapter consider algorithms for active localization scenarios working on the allocated powers at the beacons and possibly providing increased accuracy. In Sec 5.1, a review of power allocation techniques during a localization process is considered. Then, in Sect. 5.2, a suboptimal power allocation (PA) method based on a minimization of a parameter, called uncertainty area, is proposed. The algorithm performance evaluation leads to the fact that better localization performance is achievable via PA w.r.t localization with uniform power allocation.

In Sec 5.3, the impact of real ranging on existing PA algorithms in localization scenarios is studied. Unlike the common assumption that variance of range estimator achieves CRB, the MSE of practical ranging algorithms does not improve by increasing SNR over a certain SNR threshold. Therefore, a simple PA algorithm, which takes advantage of this phenomenon, is presented and evaluated.

5.1 Power allocation in localization

5.1.1 Literature review of optimal approaches

In [53] and [54], a lower bound for target position estimate is derived. Considering that the achieved lower bound, SPEB, is a function of the transmit power, a consequent minimization of SPEB with respect to transmit power from each beacon has been pursued in [50, 52, 55, 49]. In [50], authors consider the position error in a specific direction, called directional position error bound (DPEB), and they show that SPEB can be seen as a sum of two DPEBs in two orthogonal directions. A consequent minimization of DPEB is achieved along the direction in which the error is maximum (called maximum DPEB or mDPEB).

The main focus of [52] is on the eigenanalysis of Fisher Information Matrix (FIM) related to SPEB and both optimal power allocation (PA) and optimal beacon deployment are discussed in order to obtain the minimum SPEB. Taking into account that the parameters involved in the SPEB minimization, like angles and path losses between target and each beacon, are subject to uncertainty in practice, robust versions of the SPEB minimization are considered in [49].

All the above-mentioned formulations are for active localization where positioning is implemented geometrically by the intersection of different circles in which each beacon is in the center of the corresponding circle. In [15] a similar theoretical analysis using Cramer Rao Bound (CRB) is pursued in order to compute a lower bound for the error of target position estimate and the corresponding power allocation formulation is obtained for passive localization in which localization is implemented geometrically by the intersection of ellipses, each one characterized by a pair of beacons located in their foci.

In chapter III, a lower bound for the error of target position estimate via active localization was discussed. Equation (3.16) is a lower bound for MSE of unbiased

estimate of target position. Since this formulation deals with variance of each of distance (TOA) estimates between target and each of beacons, it is worth to elaborate variance of each range measurement using CRB for TOA estimation

$$\sigma_j^2 = E[(\hat{d}_j - d_j)^2] \geq \frac{\zeta}{p_{r_j}} = \frac{\zeta L_i}{p_{t_j}}; \zeta = \frac{c^2 \cdot p_{noise}}{8 \cdot \pi^2 \cdot B^2}. \tag{5.1}$$

In (5.1), p_{r_j} is the received power from beacons j at the target, B is a measure of bandwidth, P_{noise} is the noise power, L_j is the path loss between target and j^{th} beacon, i.e. $p_{r_j} = \frac{p_{t_j}}{L_j}$.

Assuming that variance of distance (TOA) estimator achieves CRB and replacing (5.1) in (3.16), we have

$$P = \frac{4 \cdot \zeta \cdot \sum\limits_j \frac{p_{t_j}}{L_j}}{\left(\left(\sum\limits_j \frac{p_{t_j}}{L_j} \right)^2 - \left(\sum\limits_j \frac{p_{t_j} \cdot cos(2\alpha_j)}{L_j} \right)^2 - \left(\sum\limits_j \frac{p_{t_j} \cdot sin(2\alpha_j)}{L_j} \right)^2 \right)}. \tag{5.2}$$

It is obvious that (5.2) is a function of two vital major parameters i.e. transmit power $\left\{p_{t_j}\right\}, j = 1, ..., N_b$ and signal bandwidth. Consequently, localization MSE can be changed by playing with these two parameters. However, in all of the presented formulations and, in the sequel, related to power allocation (PA), signal bandwidth is assumed to be constant.

Considering (5.2), SPEB is a convex function of $\left\{p_{t_j}\right\}, j = 1, 2, ..., N_b$ [49]. Consequently, SPEB can be minimized with respect to the major parameters $\left\{p_{t_j}\right\}, j = 1, 2, ..., N_b$. This minimization problem can be formulated as

$$\begin{aligned} \underset{\{p_{t_j}\}}{\text{minimize}} \quad & SPEB = tr\left\{\mathbf{J}^{-1}\right\} \\ \text{subject to} \quad & \sum_j p_{t_j} = P_{tot}, \end{aligned} \tag{5.3}$$

which is a minimization of SPEB with respect to a constraint of fixed total transmitted power (P_{tot}). On the other hand, there can be another formulation based on the minimization of the total transmitted power w.r.t a specific accuracy requirement (ρ):

$$\begin{aligned} \underset{\{p_{t_j}\}}{\text{minimize}} \quad & \sum_j p_{t_j} \\ \text{subject to} \quad & SPEB = tr\left\{\mathbf{J}^{-1}\right\} = \rho. \end{aligned} \tag{5.4}$$

The critical concern about these two problems is the fact that other minor parameters like the angles of target with respect to each beacon (α_j) and the path loss between target and each beacon are subject to uncertainty in practice. In [50], [52] and [55], the two above-mentioned optimization problems are considered under the assumption that an actual, ideal knowledge of minor parameters is available.

There is also another formulation for (5.3). In [50] the authors suggest to use maximum directional error bound (mDPEB) as the objective function in (5.3). Directional position error bound is defined considering the error of target position estimate in a specific direction and it is defined as [54]

$$P(\mathbf{U}) \triangleq \mathbf{U}^T \left[\mathbf{J}^{-1}\right] \mathbf{U}. \tag{5.5}$$

From (3.17) and (5.5), it is obvious that, if we set $\mathbf{U} = \begin{bmatrix} cos(\gamma) \\ sin(\gamma) \end{bmatrix}$ or $\mathbf{U} =$

$\begin{bmatrix} -sin(\gamma) \\ cos(\gamma) \end{bmatrix}$, SPEB will be equal to $\frac{1}{\mu_1}$ or $\frac{1}{\mu_2}$ respectively. Based on the assumption $\mu_1 \geq \mu_2$, the smallest eigenvalue will give a greater contribution in the position error [50]. Consequently, the minimization problem turns out to be

$$\begin{aligned} \underset{p_{t_j}}{\text{minimize}} \quad & \frac{1}{\mu_2} \\ \text{subject to} \quad & \sum_j p_{t_j} = P_{tot}. \end{aligned} \tag{5.6}$$

As previously mentioned, minor parameters are due to uncertainty in practice. Authors in [49] consider the case where there is uncertainty in the estimation of minor parameters.

All the above-mentioned formulations are for active localization where positioning is implemented by intersection of different circles in which every beacon is in the center of the related circle. In [15], similar theoretical analysis using CRB is pursued in order to compute a lower bound for the error of target position estimate and the corresponding power allocation formulation using passive localization in which localization is implemented by intersection of ellipses in which two beacons are located in the foci of each ellipse.

5.2 An algorithm for power allocation based on a likelihood area

One of the main goals in designing localization algorithms is to to provide more accurate estimates of target position. In order to achieve this objective, also power allocation among beacons can be effective for enhancing localization performance. Here, a power allocation scheme is presented which is to be applied among beacons with respect to a fixed amount of the total transmitted power. The proposed scheme is based on a power allocation procedure performed in a pair-wise way among beacons

and a successive selection strategy in order to pick the most appropriate allocated power for each beacon. Despite its suboptimal nature, simulation results confirm an improvement of localization performance via power allocation.

Here, the scenario of application is constituted by a set of fixed beacons used for static localization of one target in a limited environment. The technology considered in the simulations is the Ultra-WideBand Impulse Radio (UWB-IR). The general structure of algorithm is based on the fact that, using the well-known Cramer-Rao lower bound (CRLB) for each of the time of arrival (TOA) estimates obtainable between the target and each beacon in a selected beacon pair, a "likelihood area" is defined as a bi-dimensional area representing the level of reliability of the localization measure. The algorithm is composed by two stages. In the first, a PA scheme acts on each pair of beacons. In the second, since each beacon is participated in the pair-wise selection procedure more than once, there will be multiple allocated powers for each beacon and, therefore, an algorithm derives an overall power allocation for the whole beacons set by selecting appropriate allocated powers from the first stage outcomes. For assuring a limited computational complexity in the first part, the proposed algorithm aims to minimize the likelihood area by selecting an appropriate power allocation among beacons in a pair-wise selection procedure w.r.t. the constraint of a given total transmitted power. Finally, since each beacon is involved in more than one pair, the algorithm selects one of the allocated powers for each beacon based on a defined procedure.

The scenario used for testing the algorithm characteristics represents the simplest localization scenario and it is chosen for highlighting the algorithm properties and minimizing the impact of any other system model parameter or of the nodes layout:

- the number of beacons is 3, i.e. the minimum geometrical setup for obtaining a localization solution;
- the beacons are at the corners of a square area;

- the target locations are situated inside the perimeter of the beacons in order to focus on the best localization conditions.

The localization can be performed at the target, at the beacons or in a central processing station; here we assume that

- the beacons transmit a packet towards the target, which estimates locally the distances from the beacons (with a ranging algorithm), computes locally its position and returns it to the beacons or to a central processing station (alternatively it returns the distance estimates directly to a central processing station for the whole localization and power allocation computations);

- the algorithm for power allocation is processed at the target or at a central processing station because it needs the data of all the links between the beacons and the target;

- in order to intercept and discuss here the best potential performance of the algorithm, the algorithm is processed with perfect knowledge of the parameters that are needed for deriving the powers to be allocated (see Sect. 5.2.1).

For testing the algorithm the targets are located inside the triangular region delimitated by the 3 beacons, as sketched in the example in Fig. 5.3.

5.2.1 Structure of the proposed PA algorithm

The proposed algorithm implements power allocation among the beacons in the sense that there exists a performance advantage over localization with uniform power allocation among beacons. The proposed PA algorithm is composed by two stages: in the first, it performs PA among beacons in a pair-wise procedure in the sense that it selects two beacons as a pair and accomplishes PA for all available pairs. The important parameters in the algorithm decision process are the estimated path losses

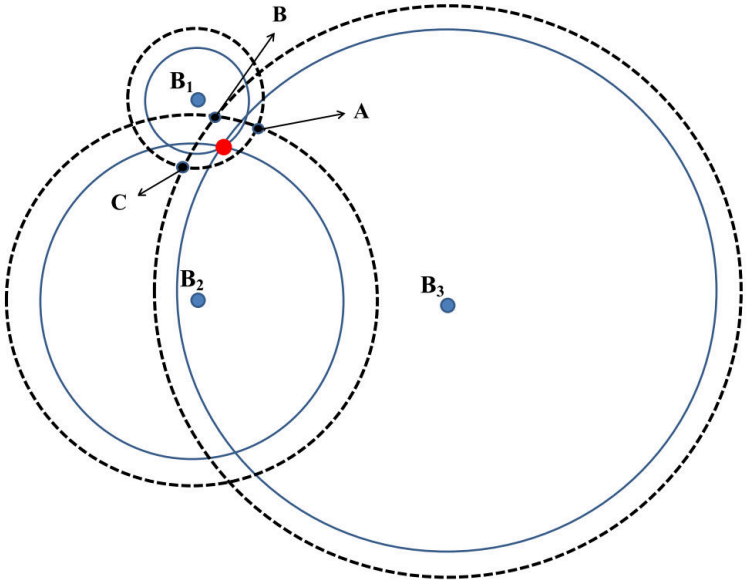

Figure 5.1: A schematic representation of the target range from each beacon. Solid circles show the real possible locations of the target around each beacon. Dashed circles depict estimated possible locations of the target around each beacon. The considered scenario is in 2D coordinates.

and the angles between target and each beacon; in a real tracking implementation, these parameters can be obtained from a previous localization step.

Based on the proposed formulation of the likelihood area (LA), the algorithm minimizes the LA by means of an appropriate power allocation among the beacons of each considered pair. As a rule thumb, the algorithm will reduce transmitted power of the beacon to which the target is closer while it increases the transmitted power of the other beacon, from which the target is farther. When the target is located in the middle of two beacons, the algorithm allocates power uniformly among the beacons of that pair.

In our test scenario, characterized by three beacons, each beacon is selected twice in the pair-wise selection procedure (3 pairs). Consequently, there will be two amounts of allocated powers for each beacon. In order to select one of these multiple (in our test scenario two) allocated powers for each beacon, the second part of the algorithm decides between these two allocated powers via a selection procedure described in

Section 5.2.3. In the following, an explanation of the two stages of the algorithm is presented.

5.2.2 Power allocation in a pair-wise selection of beacons

The first part of algorithm is based on power allocation among beacons in a pair-wise selection of the beacons. The principle, exploited in the process, is simple. Using CRLB for TOA estimates, we define a likelihood area which is dependent on the received SNR and on the angle between target and beacon. The likelihood area for the pair (i, j) is defined by an expression as

$$A = (\sin(\varphi_i) \cdot \sigma_i + \sin(\varphi_j) \cdot \sigma_j) \times (\cos(\varphi_i) \cdot \sigma_i + \cos(\varphi_j) \cdot \sigma_j) \tag{5.7}$$

where, according to CRLB, σ_i is the standard deviation for a TOA estimator related to i^{th} beacon defined in (5.1). Considering a fixed total power constraint on the transmit powers, the algorithm minimizes the likelihood area at each beacons pair. Due to implementation purposes using conventional optimization tools, we present the proof of convexity for the proposed likelihood area before proceeding with the main core of algorithm.

One way to check whether a multidimensional function is convex or not, is to check the Hessian matrix of function from definiteness point of view. If the Hessian matrix is a positive semi-definite matrix, the function is a convex function. Also, if the Hessian matrix is a positive definite matrix, the function is a strictly convex function. To this end, the Hessian matrix related to LA function (A) can be written as

$$\mathbf{H} = \begin{bmatrix} \frac{\partial^2 A}{\partial p_{t_i}^2} & \frac{\partial^2 A}{\partial p_{t_i} \partial p_{t_j}} \\ \frac{\partial^2 A}{\partial p_{t_j} \partial p_{t_i}} & \frac{\partial^2 A}{\partial p_{t_j}^2} \end{bmatrix}$$

$$= \begin{bmatrix} 2acL_i p_{t_i}^{-3} + \frac{3}{4}(ad+bc)\sqrt{L_i L_j} p_{t_i}^{-2.5} p_{t_j}^{-0.5} & \frac{1}{4}(ad+bc)\sqrt{L_i L_j} p_{t_i}^{-1.5} p_{t_j}^{-1.5} \\ \frac{1}{4}(ad+bc)\sqrt{L_i L_j} p_{t_i}^{-1.5} p_{t_j}^{-1.5} & 2bdL_j p_{t_j}^{-3} + \frac{3}{4}(ad+bc)\sqrt{L_i L_j} p_{t_i}^{-0.5} p_{t_j}^{-2.5} \end{bmatrix} \quad (5.8)$$

where $a = sin(\varphi_i), b = sin(\varphi_j), c = cos(\varphi_i)$ and $d = cos(\varphi_j)$. In order to prove convexity of A, it should be proved that $\mathbf{H}$ is a positive semidefinite or positive definite matrix. If a matrix is either positive semidefinite matrix or positive definite matrix, all of its eigenvalues should be nonnegative or positive respectively. For the Hessian matrix, we have

$$det(\mathbf{H}) = \lambda_1 \cdot \lambda_2 > 0 \quad (5.9)$$

and

$$tr\{\mathbf{H}\} = \lambda_1 + \lambda_2 > 0 \quad (5.10)$$

where λ_1 and λ_2 are eigenvalues of the Hessian matrix. Equation (5.9) and (5.10) implies that two eigenvalues are positive. Consequently Hessian matrix $\mathbf{H}$ is a positive definite matrix and it is proved that A is a strictly positive function.

As previously discussed, the proposed LA is a convex function of its variables (p_{t_i}, p_{t_j}). Consequently, if LA has a local minimum, it will be also global minimum. So, the minimization problem for the selected pair (i, j) can be written as

$$\begin{aligned} \underset{p_{t_i}, p_{t_j}}{\text{minimize}} \quad & \zeta \cdot (\sin(\varphi_i) \cdot \sqrt{\frac{L_i}{P_{t_i}}} + \sin(\varphi_j) \cdot \sqrt{\frac{L_j}{P_{t_j}}}) \times (\cos(\varphi_i) \cdot \sqrt{\frac{L_i}{P_{t_i}}} + \cos(\varphi_j) \cdot \sqrt{\frac{L_j}{P_{t_j}}}) \\ \text{subject to} \quad & p_{t_i} + p_{t_j} = P_{tot}. \end{aligned} \tag{5.11}$$

Since the objective function is a convex function and equality constraint is an affine function of optimization parameters, the formulated problem is a convex optimization problem. Consequently, the minimization problem can be solved by convex optimization solvers like CVX [27].

Fig. 5.1 shows the considered scenario in which we have three beacons $B1$, $B2$ and $B3$ and the target marked by a red point. Solid circles show the possible locations of the target around each beacon resulting from actual target distance from each beacon. Obviously, their intersection will lead to exact position of target (red point). Dashed circles represent the possible locations of the target around each beacon resulting from estimated distance of the target from each beacon obtainable via TOA estimation of received signal from beacon. Estimated position of the target will be inside this area. In fact, the algorithm goal is to minimize the uncertainty area limited by the points A, B and C as shown in Fig. 5.1. It is worth mentioning that the proposed likelihood area is an approximation of the section of above-mentioned uncertainty area related to each beacon pair. As an example, the uncertainty area in Fig. 5.1 is shown in the case of ranging overestimation. When the algorithm achieves PA among beacons of each selected pair, there will be more than one allocated power for each beacon. Consequently, one of the allocated powers should be assigned to each beacon, by means of the second part of the algorithm.

5.2.3 Selection strategy among multiple allocated powers at each beacon

The second part of the algorithm is responsible for an appropriate assignment of one of the allocated powers computed in the first part. Since each beacon is selected by the PA algorithm more than once, after finishing the pairwise selection procedure, the algorithm looks for the best amount of allocated power for each beacon according to the following approach. As it is shown in Fig. 5.2, the algorithm calculates its distances from beacons using latest predicted position information. It selects the closest beacon to the target which has the minimum computed distance. Taking into account that there are two allocated powers for the selected closest beacon being participated in two different pair-wise selection procedures, the difference of allocated powers with respect to the value of uniformly allocated power are computed. Assuming beacon i as the selected closest beacon to the target, the power differences $(j = 1, 2)$ are calculated according to

$$\Delta P_i^j = P_i^j - P_{uniform}, \tag{3}$$

where $P_i^{1,2}$ are the two allocated powers acquired from two pair-wise selection procedures for beacon i and $P_{uniform}$ is the power for uniform power allocation among beacons. If two computed differences have opposite sign, it means that two different policies should be applied to the transmitted power of considered beacon. If this condition occurs, the algorithm implements uniform power allocation on all the 3 beacons.

If the two computed differences have equal signs, it can be noticed that the allocation, imposed by twice selection of the beacon in the pair-wise selection procedure, is coherent w.r.t. the increase or decrease of the transmitted power in beacon i. Therefore the algorithm selects the allocated power which has the largest absolute value.

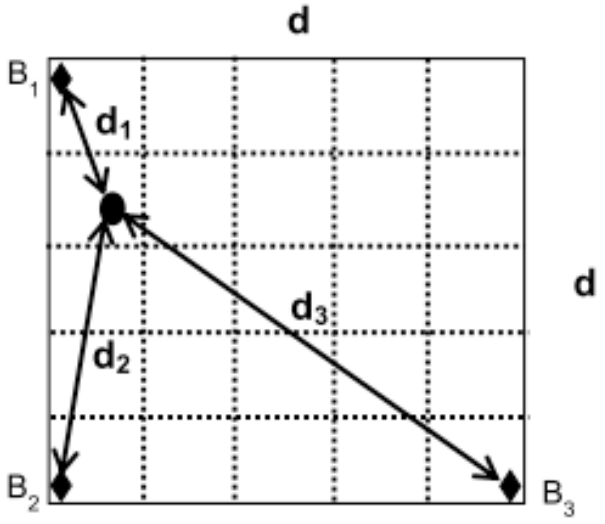

Figure 5.2: Representation of the algorithm second stage. After finding the beacon closest to the target, a decision procedure selects the allocated powers for each beacon.

The beacon participating in the pair-wise-selection procedure which determines this largest computed difference for the closest beacon, is allocated the power determined via the mentioned pairwise selection. The power at the last beacon, not participating to the pair-wise selection procedure with closest beacon and largest ΔP_i^j, is not changed.

5.2.3.1 Justification of the general selection strategy via SPEB analysis

As mentioned in Sect. 3.1.2.1, FIM can be be completely described by its two eigenvalues and the related rotation angle, i.e. $\mathbf{J} = F(\mu_1, \mu_2, \gamma)$. For a single beacon i, it can be expressed as $\lambda_i \mathbf{J}_r(\alpha_i) = F(\lambda_i, 0, \alpha_i)$. Obviously, selection of a beacon with the largest RII is the best option which is also coherent with conclusions of Sect. 3.1.2.3. Considering the fact that the considered ranging scheme is TOA based, let us elaborate RII as

$$\lambda_i = \frac{1}{\sigma_i^2}. \tag{5.12}$$

By substituting (5.1) in (5.12), we have

$$\lambda_i = \frac{8 \cdot \pi^2 \cdot B^2 SNR_i}{c^2}, \tag{5.13}$$

where SNR_i is the received SNR from i^{th} beacon, which is an inverse function of the distance between beacon and target. Consequently, the selection of closest beacon i.e. with shortest distance will lead to the strongest RII.

5.2.4 Performance evaluation

In this test scenario, numerical results are presented for two categories. In the first category, the ranging estimator MSE is assumed to achieve CRB for TOA estimator (mentioned in 5.1) while in the second category, the real ranging model mentioned in 5.14 is used which is a model for MSE of $soft$ ranging. These two categories will be referred as first category and second category in figures and related descriptions respectively. Numerical results focus on the localization error (i.e. the distance ϵ between estimated and correct locations at each algorithm step). For the sake of simplicity, localization without PA, localization with PA based on uncertainty area and localization with optimal PA based on SPEB minimization will be denoted as WPA, UCA and $SPEB\ \ based$ respectively. The simulated scenario is a square room with a side length equal to 50 m in which there are three fixed beacons in the corners (Fig. 5.3).

In order to show the advantages and the limits of the proposed scheme, simulations are done in two different conditions. Firstly, localization performance of WPA, UCA

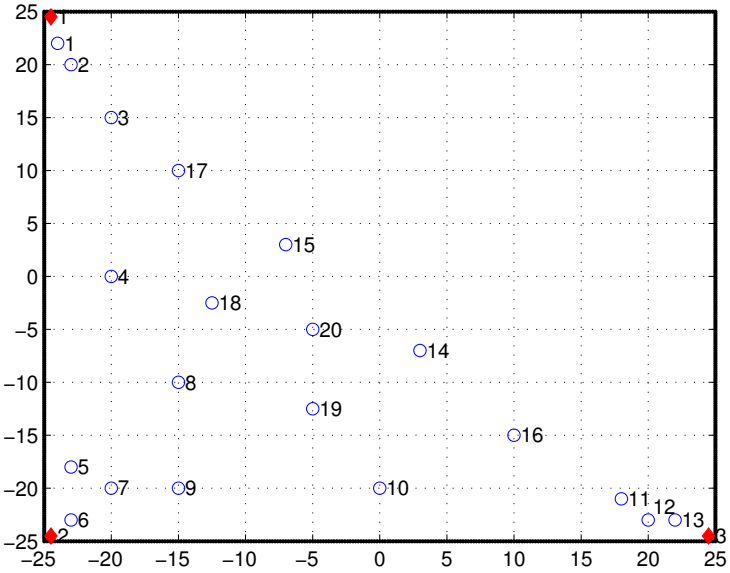

Figure 5.3: Simulation reference scenario with three beacons. Red dots show the positions of beacons. Blue circles show the point in which the algorithm with PA and without PA is evaluated.

and $SPEB$ *based* versus increasing transmission power is presented. The second set of results is related to localization performance evaluated in a number of points in the area limited by the beacons. The set of points is chosen in order to understand the different algorithm responses according to the target location; there are points which are close to the beacons and points which are approximately in a symmetric position with respect to the three beacons.

The physical parameters of the transmission are taken from the UWB technology. The standard pulse has a reference bandwidth of 512 MHz and the propagation exponent is fixed to a value of $\gamma = 1.79$ according to residential Line-of-Sight UWB channel model. Each receiver noise figure is fixed to 7 dB and each node (beacon or target) respects the UWB transmission spectral power density of -41.3 dBm/MHz.

Fig. 5.4 represents the RMSE performance comparison among WPA, UCA and $SPEB$ based versus increasing transmit power for first category evaluated in two regions, one in the proximity of one of the beacons in a circular area with radius

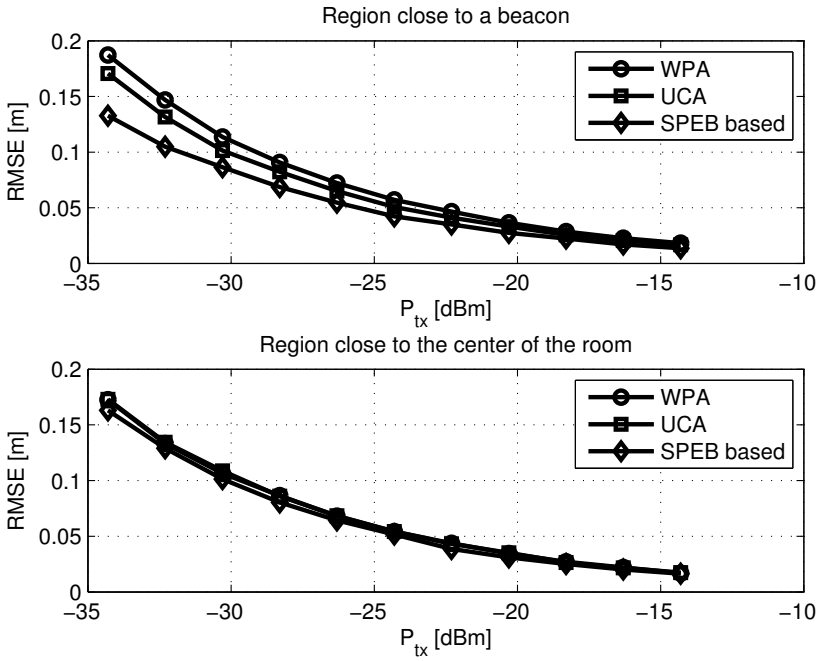

Figure 5.4: RMSE performance of WPA, UCA and $SPEB$ based power allocation (CRB based TOA estimator).

equal to 5 m and another one in the neighborhood of center of the room in a circular area with radius equal to 5 m keeping in mind that the parts of interest are within the triangle area limited by three beacons. For each value of transmit power (P_{tx}), localization performance is averaged over 300 uniformly distributed points inside the two mentioned regions. This kind of analysis gives us an insight on which areas in the room receive an effective advantage from the application of the considered localization algorithms with PA. In the region close to a beacon, due to a considerable difference in received SNR from each beacon, a considerable performance gap between localization with PA and localization without PA is observed. However, in the region close to the room center in which all of the received SNR from the beacons have similar values, there is no considerable performance gap between performance of localization with PA (either $SPEB$ *based* or UCA) and the localization without PA. Focusing on target locations in the vicinity of beacons where received SNRs have different values, it is observed that the best performance is associated with optimal

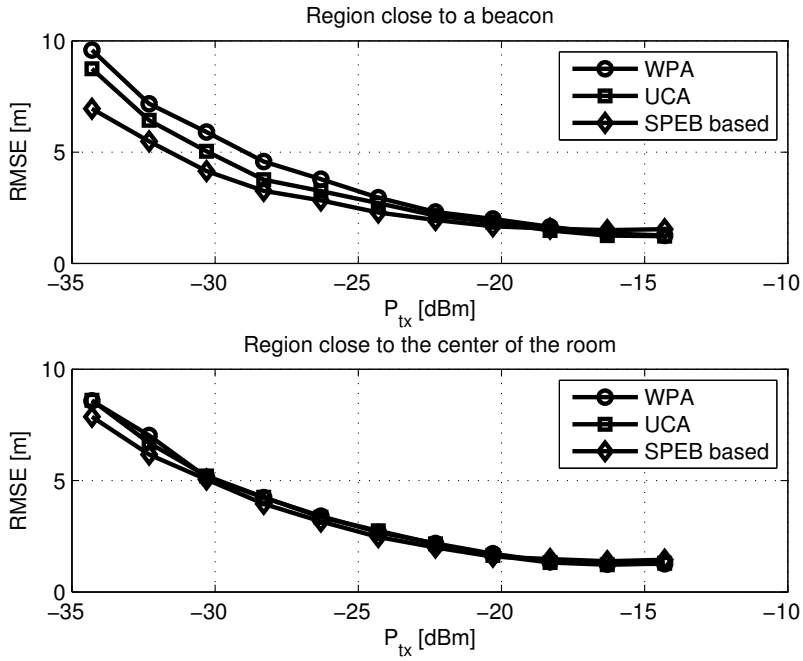

Figure 5.5: RMSE performance of WPA, UCA and $SPEB$ based (real ranging model).

PA of $SPEB$ *based*. Meanwhile, the proposed UCA performs better than the case of uniform power allocation (WPA) but not better than $SPEB$ *based*. It is observed that as the transmission power increases, performance gap gets smaller.

Fig. 5.5 presents performance comparison of WPA, UCA and $SPEB$ *based* for the second category of results, obtained with a real ranging model. The same behavior as the one observed for first category is apparent in this plot. There is one interesting observation that the optimal $SPEB$ approach does not show any advantage over a certain transmission power and this is the motivation behind the approach proposed in Sect. 5.3. Consequently, in the successive figures related to the real ranging model, localization performance related to $SPEB$ *based* is not shown.

The localization RMSE for the first category, evaluated in the points of Fig. 5.3 is shown in Fig. 5.6. The best performance is achieved by $SPEB$ based strategy, which is the optimal PA strategy in all the points. Comparing the performance of WPA and UCA, the considerable performance gap between localization appears in target

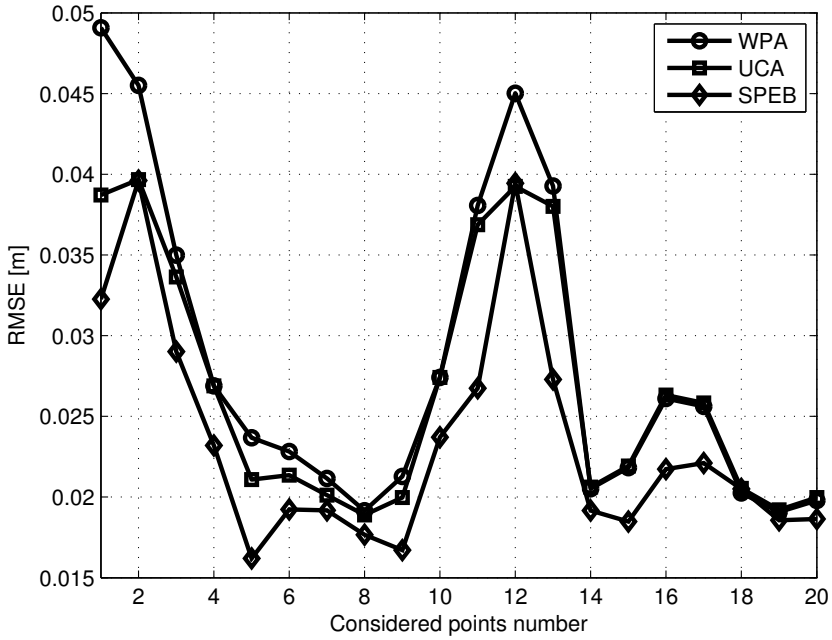

Figure 5.6: Localization performance in assumed points inside the indoor environment delimited by three beacons (CRB based TOA estimator).

locations in the vicinity of beacons like 1, 6 and 12. In other points, UCA performance is equal to that of WPA or slightly better confirming the fact that when the target approaches a beacon, UCA achieves performance better than WPA. Otherwise, the PA strategy for WPA tends to implement uniform PA leading to performance equivalent to WPA. This behavior leads to better localization performance fixed the same total transmit power at beacons or energy savings once fixed the performance level.

The same analysis for a practical ranging estimator i.e. $soft$ is presented in Fig. 5.7. All the conclusions made for Fig. 5.6 are also valid for Fig. 5.7.

Fig. 5.8 depicts in more detail some numerical results, reporting the cumulative density functions (CDFs) of the distance error for the WPA, UCA and $SPEB$ based for first category results. The plots reveal the CDFs of distance error at two points, 1 (Fig. 5.8.a) and 19 (Fig. 5.8.b), one close to the beacon located at the top corner of the room and one located almost in the middle of the room. As it is expected,

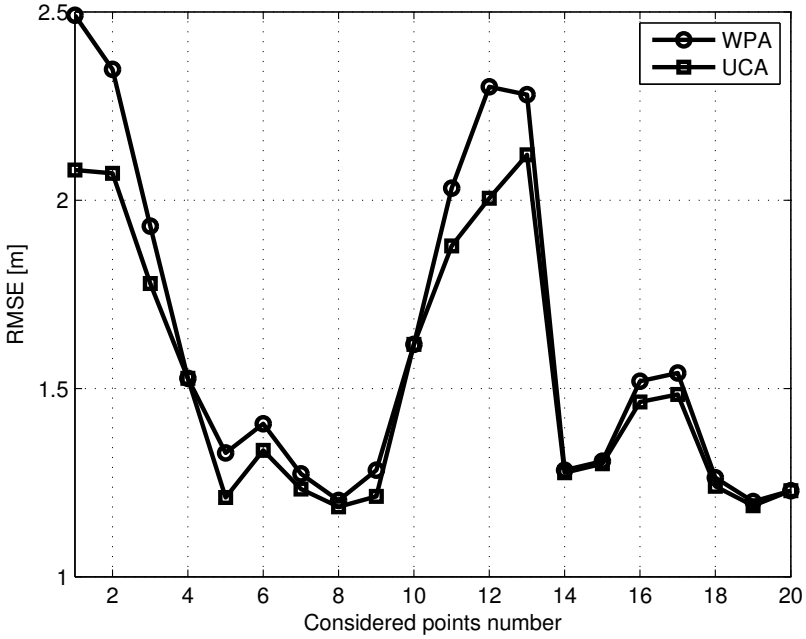

Figure 5.7: Localization performance in the points inside the indoor environment delimited by three beacons and related to the real ranging model.

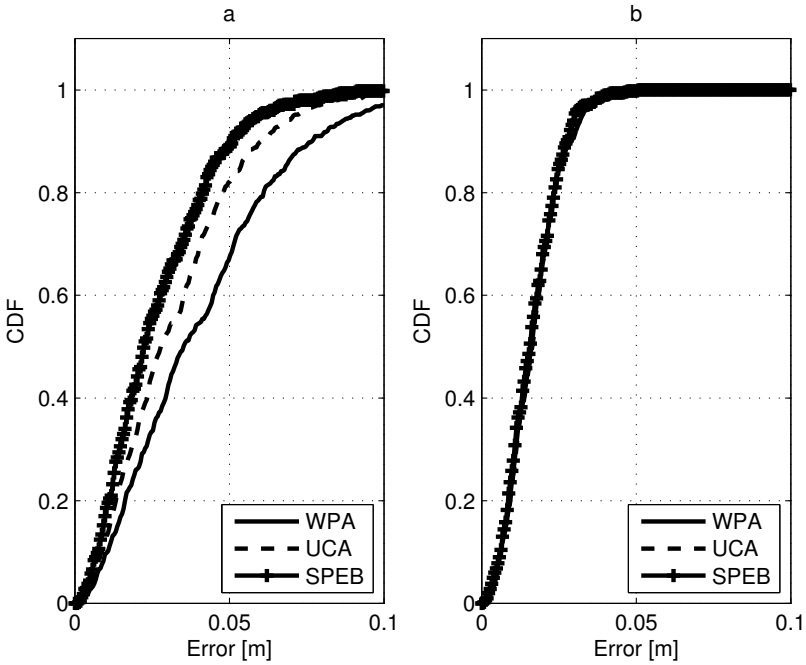

Figure 5.8: CDF plots of localization error related to CRB based TOA estimator in two points.

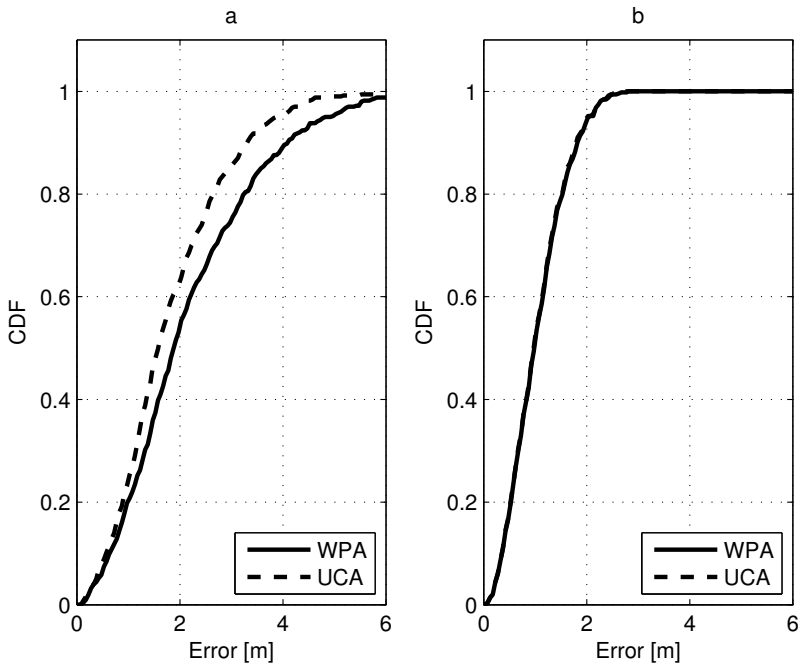

Figure 5.9: CDF plots of localization error related to second category results in two points.

the localization advantage, with the proposed PA algorithm, is present only at the point closer to the beacon while it is absent in the other point, where the best power allocation is just the uniform one (this is obvious also by using simple geometrical considerations). This is also correct for the second category results, reported in Fig. 5.9.

5.3 Impact of real ranging on algorithms for power allocation

As presented in (5.3)-(5.4), optimal PA is achieved by considering ranging measures as necessary inputs of the localization algorithm. In the literature, on one hand the common assumption about ranging measures is that their ideal values are equal to their corresponding Cramer-Rao bounds but, on the other hand, at high signal-to-noise ratios, real ranging estimators are characterized by different lower limits on their performance mainly as a result of maximum sampling rate and computational

load available in the sensors. This section considers the impact of a real ranging method on PA procedure in localization processes and a computationally efficient simplification is proposed.

In this work, we use a model of a realistic ranging algorithm, based on the division into two regions: in the first region, the performance worsens as SNR increases (similar to the CRB formulation for TOA ranging estimates) while the second region is characterized by a floor in which ranging performance is not improved with increasing SNR anymore. On the other hand, as a practical example for ranging estimator with this kind of behavior we use soft ranging, which outputs a discrete vector of likely distances with an associated approximation of the probability that these distances correspond to the estimates [29, 28].

The principles mentioned in Sec. 5.2 are also valid in this section i.e. the scenario used for testing the algorithm characteristics represents the simplest localization scenario and it is chosen for highlighting the algorithm properties and minimizing the impact of any other system model parameter or of the nodes layout:

- the number of beacons is 3, i.e. the minimum geometrical setup for obtaining a localization solution;
- the beacons are at the corners of a square area;
- the target locations are situated inside the perimeter of the beacons in order to focus on the best localization conditions.

The beacons cooperatively estimate the unknown positions of the target and they can update their transmit powers according to the target position estimate. The localization can be performed at the target, at the beacons or in a central processing station; here we assume that

- the beacons transmit a packet towards the target, which estimates locally the distances from the beacons (with a ranging algorithm), computes locally its

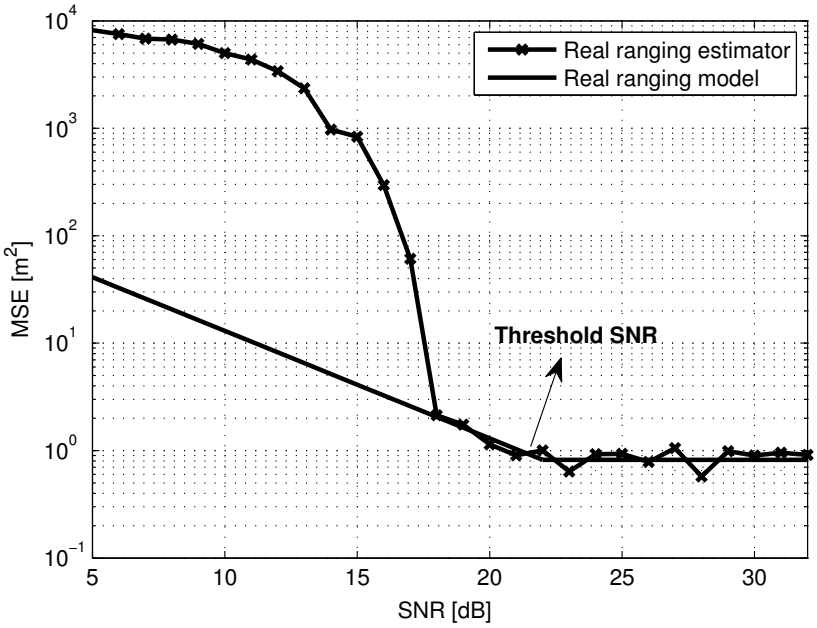

Figure 5.10: MSE performance of a practical ranging estimator.

position and returns it to the beacons or to a central processing station (alternatively it returns the distance estimates directly to a central processing station for the whole localization and power allocation computations);

- the algorithm for power allocation is processed at the target or at a central processing station because it needs the data of all the links between the beacons and the target;

- in order to intercept and discuss here the best potential performance of the algorithm, the algorithm is processed with perfect knowledge of the parameters that are needed for deriving the powers to be allocated.

5.3.1 Proposed PA algorithm for real ranging estimators

There is one common assumption in the formulations reviewed in Sect. 5.1.1, i.e. estimator variance achieves the CRB. In other words, ranging accuracy is proportional to the inverse of SNR and the more SNR increases, the better ranging precision is. In

this Section, we discuss the impact of real ranging estimators, in which there is a floor in MSE performance, i.e. MSE remains approximately constant while SNR grows over a certain threshold. This behavior is due primarily to maximum sampling rate and computational load achievable in sensors. Fig. 5.10 shows MSE performance of soft ranging estimator [29, 28] evaluated at several SNR in a fixed link for residential LoS channel; SNR is here defined as the ratio between the total received signal energy and the noise spectral density N_0 (corresponding to the SNR that can be measured at the output of an ideal RAKE receiver).

It is clear that there are two performance regions: in the first region, estimation accuracy is improved as SNR is increased till a threshold SNR (SNR_{dB}^{thr}) and, in the second region, a floor is observed in the way that estimation accuracy remains almost fixed while SNR exceeds the threshold SNR. Equivalently, in this context increasing transmit power of a beacon with an SNR above SNR_{dB}^{thr} will not provide better accuracy on the corresponding ranging measure and consequently on its contribution to the target localization; so the basic idea is based on distributing transmit power of beacons with SNR above SNR_{dB}^{thr} to beacons with SNR below SNR_{dB}^{thr} realizing a type of adaptive power allocation (APA) based directly on measured SNRs.

The following notations are used in the sequel: x_{dB} and x_{lin} are variable x in logarithmic and linear scale respectively. For the sake of simplicity, beacons with SNR above SNR_{dB}^{thr} are titled $high$ beacons and the beacons with SNR below SNR_{dB}^{thr} are titled low beacons. The transmit power of each beacon (in dBm) for uniform power allocation (UPA) is denoted as P_{dBm}^{U}.

The APA algorithm structure is as follows: firstly, difference of SNR related to each beacon with respect to the threshold SNR is calculated. Then, based on the sign of each element of the vector $\delta\mathbf{SNR}_{dB}$, it can be determined which SNR is above or below SNR_{dB}^{thr}. Before proceeding to the main core of algorithm, it is worth elaborating the cases where UPA is assumed as a solution of this algorithm. The first

case is the one in which all elements of $\delta\mathbf{SNR}_{dB}$ are positive. In other words, all beacons' SNR are above the SNR_{dB}^{thr} and hence there is no beacon with SNR under which estimation accuracy is improved by increasing the transmit power. The second case occurs when all elements of $\delta\mathbf{SNR}_{dB}$ are negative; as a result, there is no beacon with SNR above SNR_{dB}^{thr} for reducing its transmit power leading to an SNR equal to SNR_{dB}^{thr}. Excluding these cases, the algorithm really works in a scenario with one group of beacons *high* and another *low*.

When one group of $\delta\mathbf{SNR}_{dB}$ elements has positive sign while another group contains negative values, the first phase is dedicated to decreasing transmit power of beacons with positive δSNR_{dB}^{i} in a way that the resulting SNR after power cutting is equal to SNR_{dB}^{thr} (lines 8-12). After the equalization of transmit power of *high* beacons, the second phase corresponds to distribution of total cut power (P_{cut}^{tot}) over *low* beacons. The priority is with *low* beacons having lowest SNR. Simultaneously with this prior selection, one condition is checked confirming the fact that the amount of power required for the SNR of selected *low* beacon to reach SNR_{dB}^{thr} is smaller than total cut power. In fact it is infeasible to distribute an amount of power greater than P_{cut}^{tot} in order to respect the constraint of fixed total transmit power (line 18). Each of the *low* beacons, satisfying the aforementioned condition, will be allocated the power so that the related SNR reaches SNR_{dB}^{thr}, keeping in mind that the selection of *low* beacons starts from the one with lowest SNR. After completion of PA for qualified *low* beacons, if there is any remaining P_{cut}^{tot}, it is allocated to the beacon with lowest SNR. The main core of algorithm is iterated to ensure that SNRs related to newly allocated powers does not pass SNR_{dB}^{thr}.

5.3.2 Performance evaluation

The physical parameters of the transmission are taken from the UWB technology. The standard pulse has a reference bandwidth of 512 MHz and the propagation

Algorithm 1 Pseudocode for the APA algorithm structure (x_{dB} and x_{lin} refer to variable x in logarithmic and linear scale respectively).

Calculate $\delta SNR^i_{dB} = SNR^i_{dB} - SNR^{thr}_{dB}$
if $max(\delta SNR^i_{dB}) < 0$ **then**
  do UPA
else
  if $min(\delta SNR^i_{dB}) > 0$ **then**
    do UPA
  else
    for each beacon B_i
    if $\delta SNR^i_{dB} > 0$ **then**
      $P^{N_i}_{dBm} = P^U_{dBm} - \delta SNR^i_{dB}$
      $P^{N_i}_{lin} = 10^{P^{N_i}_{dBm}/10}$
      $P^{tot}_{cut} = \sum_i P^U_{lin} - P^{N_i}_{lin}$
    end if
  end if
end if
Allocate the cut power from beacons with SNR above threshold to the beacons with SNR lower than threshold giving priority to beacons with worst situation i.e. with lowest SNR below SNR^{thr}_{dB}
if $\delta SNR^i_{dB} < 0$ **then**
  compute $P^{check}_{dBm} = P^U_{dBm} - \delta SNR^i_{dB}$
  if $P^{check}_{lin} < P^{tot}_{cut}$ **then**
    $P^{N_i}_{dBm} = P^{check}_{dBm}$
    $P^{tot}_{cut} = P^{tot}_{cut} - P^{N_i}_{lin}$
  end if
end if
Decision about possible remaining power
if $P^{tot}_{cut} > 0$ **then**
  Allocate it to remaining links with SNR below SNR^{thr}_{dB}
end if

exponent is fixed to a value of $\gamma = 1.79$ according to residential Line-of-Sight UWB channel model (channel model $CM = 1$). Each receiver noise figure is fixed to 7 dB and each node (beacon or target) respects the UWB transmission spectral power density of -41.3 dBm/MHz. In this test scenario, we exploit ranging algorithms based on the times of arrival and characterized by soft detection techniques that have demonstrated performance advantages w.r.t. other approaches. Numerical results focus on the localization error. The reference scenario is a square room with side $d = 50m$. The number of beacons is fixed to $N_B = 3$ at 3 adjacent corners of the room and SNR_{dB}^{thr} is set to be 21 dB. In order to give an additional reference on the signal-to-noise level in the system, when the transmit power P_{tx} of a beacon is -14.3 dBm the average SNR inside the room, measured as in Sect. 5.3.1 and Fig. 5.10, turns out to be about 34 dB.

We remark that the crucial parameters for considered PA algorithms are the path loss and the angles between the target and each of the beacons; optimal knowledge of these parameters is assumed in our simulations [55, 41]. The proposed PA scheme, the PA based on SEPB minimization and localization without PA will be referred as APA, $SPEB\ based$ and WPA respectively.

The MSE of practical ranging scheme contains two performance regions. In the former region, MSE is decreased by increasing SNR with an inversely proportional relation as in the CRB (5.1), excluding very low SNRs with very high MSE but with no interest for practical applications. In the latter performance region, MSE is not improved significantly by increasing SNR and remains almost constant (Fig. 5.10). Therefore, we use a simple model to describe the behavior corresponding to variance of practical ranging required to compute SPEB. The model is defined as

$$\sigma_j^2 = \begin{cases} \frac{c}{SNR_{lin}^j} & \text{if } SNR_{lin}^j < SNR_{lin}^{thr} \\ \frac{c}{SNR_{lin}^{thr}} & \text{if } SNR_{lin}^j \geq SNR_{lin}^{thr} \end{cases}, \tag{5.14}$$

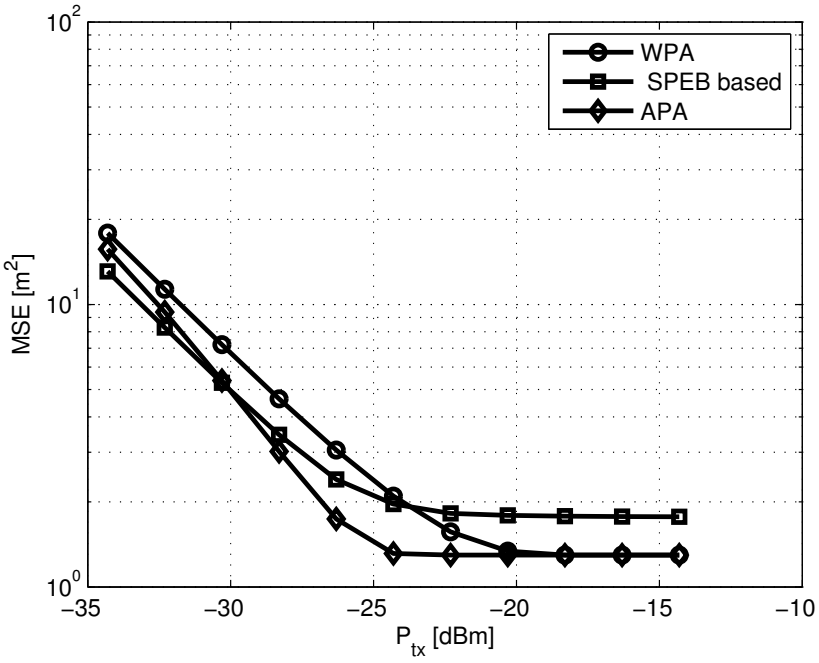

Figure 5.11: MSE performance of APA, $SPEB$ based and WPA. The mentioned model for soft ranging MSE is applied for computing the SPEB.

where, considering the particular case of Fig. 5.10, c has been evaluated equal to 130 according to a simple curve fitting procedure.

Fig. 5.11 represents the MSE performance comparison among APA, $SPEB$ based and WPA versus increasing transmit power. For each value of transmit power (P_{tx}), localization performance is averaged over 400 uniformly distributed points inside the triangle area limited by three beacons. It is evident that for small values of transmit power (low SNR regime with SNR_{dB}^{thr} equal to 21 dB) where SNR is in the first performance region of the range estimator, $SPEB$ based performs better than APA. In addition, it is worth mentioning that APA shows an advantage w.r.t localization without PA. By increasing transmit power, the performance gap between $SPEB$ based and APA decreases and the two performance curves intersect at $P_{int} = -30.3$ dBm. This behavior is due to the fact that SNR approaches the threshold SNR and consequently ranging MSE achieves the floor. By increasing P_{tx} over P_{int}, the performance gap changes in favor of the proposed algorithm.

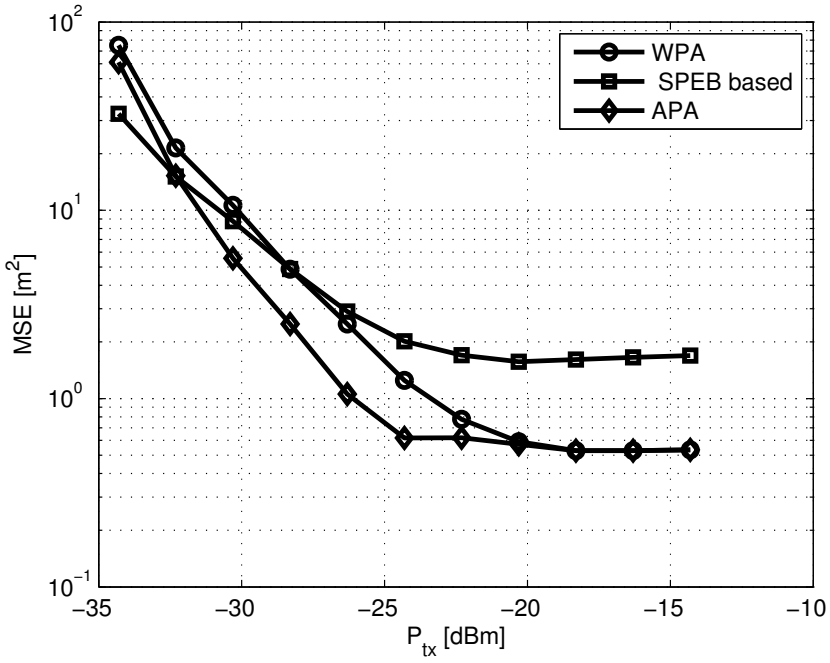

Figure 5.12: MSE performance of APA, $SPEB$ based and WPA. Direct evaluation of soft ranging algorithm is applied for computing the SPEB.

It is interesting that by increasing further transmit power or, equivalently, moving into the second performance region of the ranging estimator, there is no performance advantage by means of PA. Fig. 5.12 depicts the performance comparison among $SPEB$ *based*, APA and WPA when soft ranging is directly evaluated to compute SPEB, instead of the model (5.14). Note that the same behavior commented for Fig. 5.11 is also apparent here. Fig. 5.13 depicts MSE performance of considered localization schemes evaluated in two regions, one in the proximity of one of the beacons in a circular area with radius equal to 5 m and another one in the neighborhood of center of the room in a circular area with radius equal to 5 m keeping in mind that the parts of interest are within the triangle area limited by three beacons. For each value of transmit power (P_{tx}), localization performance is averaged over 100 uniformly distributed points inside the two mentioned regions. Soft ranging is directly evaluated to compute SPEB, instead of the model (5.14). This kind of analysis gives us an insight on which areas in the room receive an effective advantage from the application of the

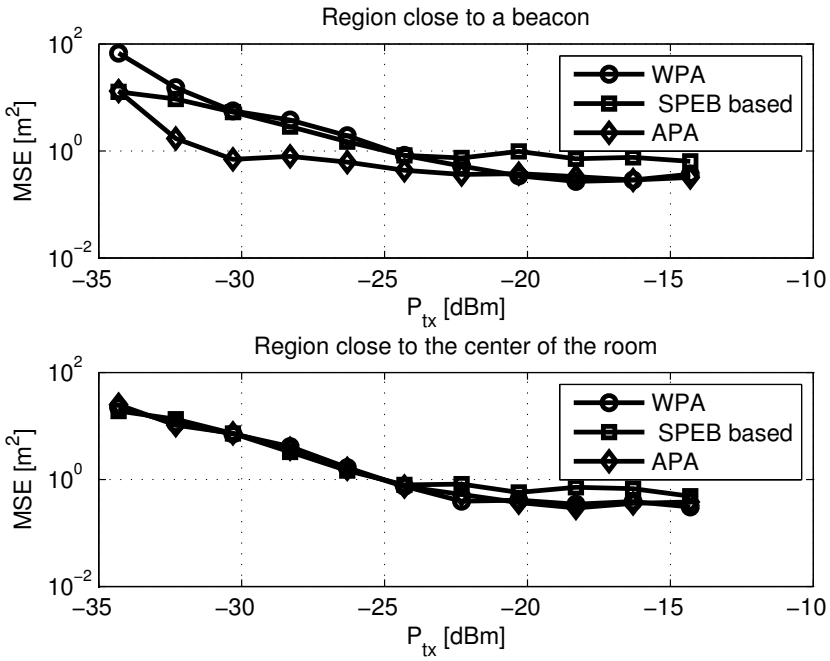

Figure 5.13: MSE performance of APA, $SPEB$ based and WPA evaluated in two regions one close to the room center and another one close to a beacon.

considered localization algorithms with PA. In the region close to a beacon, due to a considerable difference in received SNR from each beacon, a considerable performance gap between localization with PA and localization without PA is observed. However, in the region close to room center in which all of the received SNR from the beacons have similar values, there is no considerable performance gap between performance of localization with PA and localization without PA.

Fig. 5.14 shows MSE performance comparison of APA, $SPEB$ based and WPA versus path loss exponent evaluated for two different values of transmit power -29.3 dBm and -14.3 dBm. Soft ranging is directly evaluated to compute SPEB, instead of the model (5.14). For transmit power of -29.3 dBm, since the ranging MSE lies in the second region for small values of the path loss exponent (till 2), on one hand optimal $SPEB$ based does not provide any advantage over WPA. On the other hand, APA performs better taking advantage of the impact of real ranging. By increasing path loss exponent over 2 or, equivalently, moving towards the first region of ranging

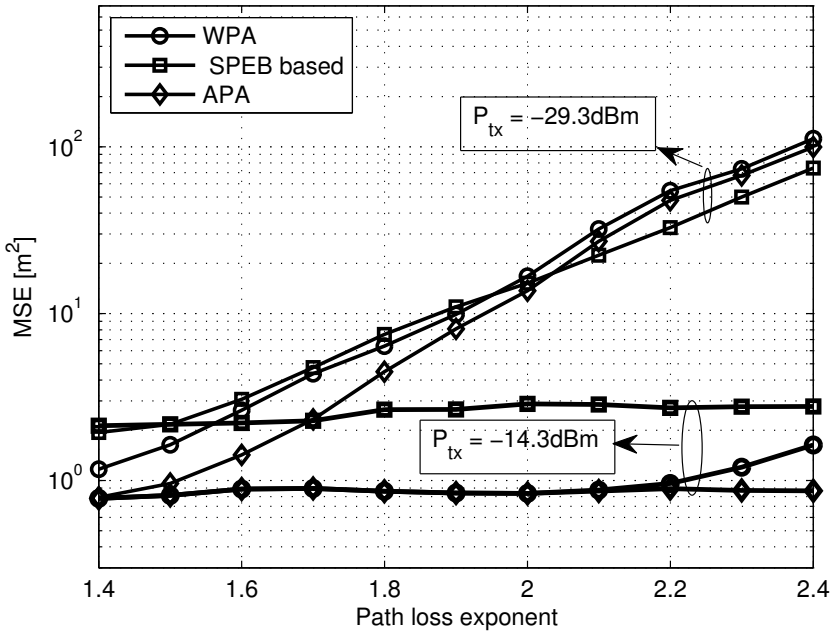

Figure 5.14: MSE performance of APA, $SPEB$ based and WPA versus path loss exponent.

MSE, the MSE curve of optimal $SPEB$ based intersects that of APA and it starts to show a performance advantage w.r.t APA and WPA as expected. For transmit power of -14.3 dBm, since ranging MSE lies in the second region despite increasing path loss exponent, optimal $SPEB$ based does not show advantage. In the high SNR context, APA does not improve UPA, so realizing a localization performance very close to WPA. By increasing path loss exponent over 2.2 or correspondingly sliding gradually toward first performance region of soft ranging MSE, proposed APA shows an advantge over $SPEB$ based and WPA.

BIBLIOGRAPHY

BIBLIOGRAPHY

[1] 02-48, F. (2002), Revision of part 15 of the commissions rules regarding ultra-wideband transmission systems, *Tech. rep.*, FCC.

[2] A. BharathidasanJ, V. A. S., and Pondura (2008), Sensor Networks: An Overview, *Tech. rep.*, Department of ECE, University of California, Davis, Technical Report, www.csif.cs.ucdavis.edu/ bharathi/sensor/survey.pdf.

[3] A.F. Molisch , et al. (2005), Ieee 802.15.4a channel model - final report, *IEEE P802.15 WPAN*.

[4] Alan Bensky (2008), *Wireless Positioning Technologies and Applications*, Artech House.

[5] C. Nerguizian, C. Despins, and S. Affes (2006), Geolocation in mines with an impulse response fingerprinting technique and neural networks, *IEEE Trans. Wireless Commun.*, *5*, 603–611.

[6] C. Steiner, F. Althaus, F. Troesch, and A. Wittneben (2007), Ultra Wideband Geo-Regioning: A novel clustering and localization technique, *EURASIP J. Adv. Signal Process., Special Issue on Signal Processing for Location Estimation and Tracking in Wireless Environ.*

[7] Chen Liang, Wu Lenan, and R. Piche (2009), Posterior cramer-rao bound for mobile tracking in mixed los/nlos conditions, in *17th European Signal Processing Conference (EUSIPCO 2009)*.

[8] Cheng Chang, and Anant Sahai (2004), Estimation Bounds for Localization, *IEEE Conference on Sensor and Ad Hoc Communications and Networks*, pp. 415–424.

[9] D. Dardari, A. Conti, U. J. Ferner, A. Giorgetti, and M. Z. Win (2009), Ranging with ultrawide bandwidth signals in multipath environments, *Proc. IEEE*, *97*, 404–426.

[10] D. Kim, M. A. Ingram, and W. W. Smith (2003), Measurements of small scale fading and path loss for long range rf tags, *IEEE Transactions on Antennas and Propagation*, *51*, 1740–1749.

[11] F. Althaus, F. Troesch, and A. Wittneben (2005), UWB geo regioning in rich multipath environment, *IEEE Vehicular Technology Conference*.

[12] G. Mao, and B. Fidan (2009), *Localization Algorithms and Strategies for Wireless Sensor Networks*, Information Science Reference, New York: Hershey.

[13] Gelb, A. (1974), *Applied Optimal Estimation*, M.I.T. Press, Cambridge (MA).

[14] H. Arslan, Z. N. Chen, and M. G. D. Benedetto (2006), *Ultra Wideband Wireless Communication*, Wiley.

[15] H. Godrich, A. Petropulu, and H. V. Poor (2011), Power allocation strategies for target localization in distributed multiple-radar architectures, *IEEE Trans. Signal Process.*, *59*, 3226–3240.

[16] H. Hashemi (1993), The indoor radio propagation channels, *Proc. IEEE*, *81*, 943968.

[17] H. Liu, H. Darabi, P. Banerjee, and J. Liu (2007), Survey of wireless indoor positioning techniques and systems, *EEE Trans. Syst., Man, Cybern. C: Applications and Reviews*, *37*, 10671080.

[18] I. Akyildiz, W. Su, Y. Sankarasubramniam, and E. Cayirci (2002), A survey on sensor networks, *IEEE Commun. Mag.*, *40*(8), 102–114.

[19] J. Reed (2005), *An Introduction to Ultra Wideband Communication Systems*, Prentice Hall Press, Upper SaddleRiver, NJ, USA.

[20] J. Y. Lee, and R. A. Scholtz (2002), Problems in modeling UWB channels, *Asilomar Conference on Systems and Computers*, *1*, 706–711.

[21] J. Yick, B. Mukherjee, and D. Ghosal (2008), Wireless sensor network survey, *Computer Networks*, *52*, 2292–2330.

[22] JY. Lee, and R. A. Scholtz (2002), Ranging in a dense multipath environment using an UWB radio link, *IEEE Trans. Select. Areas Commun.*, *20*, 1677–1683.

[23] Kay, S. (1993), *Fundementals of Statistical Signal Processing: Estimation Theory*, Prentice Hall, New Jersey.

[24] L. Reggiani, M. Rydström, E. G. Ström, and A. Svensson (2008), An algorithm for mapping the positions of point scatterers, *Sensor array and multi-channel signal processing workshop*, p. 6367.

[25] L. Reggiani, M. Rydström, G. Tiberi, and E. G. Ström (2009), Ultra-wide band sensor networks for tracking point scatterers or relays, *International Symposium on Wireless Communication Systems*, p. 15.

[26] Liuqing Yang, and G. B. Giannakis (2004), Ultra-wideband communications: an idea whose time has come, *IEEE Signal Process. Mag.*, *21*, 26–54.

[27] M. Grant, and S. Boyd (2014), Cvx: Matlab software for disciplined convex programming, *IEEE Trans. Signal Process.*

[28] M. Rydstrom, E. G. Strom, A. Svensson, and L. Reggiani (2008), An algorithm for positioning relays and point scatterers in wireless systems, *IEEE Signal Processing Letters*, *15*, 381–384.

[29] M. Rydstrom, L. Reggiani, E.G. Strom, and A. Svensson (2008), Suboptimal soft range estimators with applications in UWB sensor networks, *IEEE Trans. Signal Process.*, *56*, 4856–4866.

[30] Mustapha Boushaba, Abdelhakim Hafid, and Abderrahim Benslimane (2009), High accuracy localization method using AoA in sensor networks, *Computer Networks*, *53*, 3076–3088.

[31] N. Patwari, J. Ash, S. Kyperountas, A. O. Hero, R. M. Moses, and N. S. Correal (2005), Locating the nodes: Cooperative localization in wireless sensor networks, *IEEE Signal Process. Mag.*, *22*, 54–69.

[32] P. Tichavsky, C. Muravchik, and A. Nehorai (1998), Posterior cramer-rao bounds for discrete-time nonlinear filtering, *IEEE Transactions on Signal Processing*, *46*(5).

[33] Proakis, J. G. (2001), *Digital Communications*, McGraw Hill, New York.

[34] Qi, Y. (2003), Wireless geolocation in a non-line-of-sight environment, Ph.D. thesis, Princeton University.

[35] R. Peng, and M. L. Sichitiu (2006), Angle of Arrival Localization for Wireless Sensor Networks, *IEEE Communications Society, Conf. on Sensor, Mesh and Ad Hoc Communications and Networks*.

[36] R. Zekavat, and R. M. Buehrer (2011), *Handbook of Position Location*, Wiley, Hoboken, NJ, USA.

[37] Reggiani, L., and R. Morichetti (2010), Hybrid active and passive localization for small targets, in *Proc. 2010 International Conference on Indoor Positioning and Indoor Navigation (IPIN 2010)*.

[38] R.M. Taylor, B.P. Flanagan, and J.A. Uber (2003), Computing the recursive posterior cramer-rao bound for a nonlinear nonstationary system, in *2003 IEEE International Conference on Acoustics, Speech, and Signal Processing (ICASSP '03)*, vol. 6.

[39] R.M. Taylor, B.P. Flanagan, and J.A. Uber (2005), Computing the recursive posterior cramr-rao bound for a radar tracking system, *The MITRE Co.*

[40] Rudolph Emil Kalman (1960), A New Approach to Linear Filtering and Prediction Problems, *Transactions of the ASMEJournal of Basic Engineering*, *82*, 3545.

[41] S. Bybordi, and L. Reggiani (2013), Algorithm for power allocation in localization processes, *International Symposium on Wireless Communication Systems (ISWCS)*.

[42] S. Gezici, Z. Tian, G. B. Giannakis, H. Kobayashi, A. F. Molisch, H. V. Poor, and Z. Sahinoglu (2005), Localization via ultra-wideband radios: a look at positioning aspects for future sensor networks, *IEEE Signal Process. Mag.*, *22*, 70–84.

[43] S. Gezici, Z. Tian, G.B. Giannakis, H. Kobayashi, A.F. Molisch, A.F. Molisch, and Z. Sahinoglu (2005), Localization via ultra-wideband radios, *IEEE Signal Processing Mag.*, *22*, 7084.

[44] S. Haykin (2001), *Kalman Filtering and Neural Networks*, Wiley.

[45] Taylor, J. (1979), The cramer-rao estimation error lower bound computation for deterministic nonlinear systems, *IEEE Transactions on Automatic Control*, *24*, 343 –344.

[46] Trees, H. L. V. (1968), *Detection, Estimation, and Modulation Theory*, John Wiley and Sons.

[47] V. Heiries, K. Belmkaddem, F. Dehmas, B. Denis, L. Ouvry, and R. D'Errico (2011), Uwb backscattering system for passive rfid tag ranging and tracking, in *2011 IEEE International Conference on Ultra-Wideband (ICUWB).*

[48] W. Q. Malik, and B. Allen (2007), Wireless sensor positioning with ultra wideband fingerprinting, *Proc. Eur. Conf. Antennas Propagat.*

[49] W. W.-L, Y. Shen, Y. J. Zhang, and M. Z. Win (2005), Robust power allocation for energy-efficient location-aware networks, *Proc. IEEE Global Telecomm. Conf.*

[50] W. W.-L. Li, Y. amd Y. J. Zhang, and M. Z. Win (2011), effcient anchor power allocation for location-aware networks, *IEEE Int. Conf. Commun*, pp. 1–6.

[51] Y. Bar-Shalom, and X. R. Li. (1995), *Multitarget-Multisensor Tracking: Principles and Techniques*, YBS Publishing.

[52] Y. Shen, and M. Z. Win (2008), energy efficient location-aware networks, *IEEE Int. Conf. Commun.*, pp. 2995–3001.

[53] Y. Shen, and M. Z. Win (2010), Fundamental limits of wideband localization Part I: A general framework, *IEEE Trans. Inf. Theory*, *56*, 4956–4980.

[54] Y. Shen, H. Wymeersch, and M. Z. Win (2010), Fundamental limits of wideband localization Part II: Cooperative networks, *IEEE Trans. Inf. Theory*, *56*, 4981–5000.

[55] Y. Shen, W. Dai, and M. Z. Win (2012), Optimal power allocation for active and passive localization, *Proc. IEEE Global Telecomm. Conf.*

[56] Yuan Zhou, Choi Look Law, Yong Liang Guan, and F. Chin (2009), Localization of passive target based on uwb backscattering range measurement, in *IEEE International Conference on Ultra-Wideband (ICUWB 2009).*

[57] Z. Sahinoglu, S. Gezici, and I. Guvenc (2008), *Ultra-Wideband Positioning Systems: Theoretical Limits, Ranging Algorithms, and Protocols*, Cambridge University Press.

[58] Z. Yang, Z. Zhou, and Y. Liu (2014), From RSSI to CSI: Indoor Localization via Channel Response, *ACM Computing Surveys*, *46*.